# INVESTIGATING THE EFFECTS OF SELENIUM AND THIOUREA CONCENTRATION ON COPPER ELECTROWINNING

by

**Franklin Ngandu**

Thesis presented in partial fulfillment
of the requirements for the Degree

*of*

Master of Engineering

(Extractive Metallurgical Engineering)


in the Faculty of Engineering
at Stellenbosch University

*Supervisor*

Prof. Christie Dorfling

*Co-Supervisor*

Prof. Steven Bradshaw

**December 2016**

# DECLARATION

By submitting this thesis electronically, I declare that the entirety of the work contained therein is my own, original work, that I am the sole author thereof (save to the extent explicitly otherwise stated), that reproduction and publication thereof by Stellenbosch University will not infringe any third party rights and that I have not previously in its entirety or in part submitted it for obtaining any qualification.

Date: December 2016

# ABSTRACT

Recent studies have investigated different process routes for selenium and tellurium removal and recovery of platinum group metals (PGM) from copper sulphate leach solutions. The aforementioned studies have found that a substantial improvement in PGM recovery is achievable using excess thiourea as a precipitation agent instead of sulphurous acid, which is widely used at present.

The current study was necessitated by the need to fully elucidate the effects that excess thiourea amounts as well as variations in selenium concentration may have on copper electrowinning efficiency and cathode quality.

The experimental work was divided into electrochemical and electrowinning tests. The electrochemical tests were performed utilising a cyclic voltammetry technique to gain initial information on the possible interaction between selenium and thiourea and the copper ions during deposition. The effects of varying selenium and thiourea concentration on cathode quality and electrowinning efficiency were effectively studied by performing electrowinning tests.

Both the electrowinning and electrochemical tests were conducted using a 3 electrode system consisting of a rotating disk platinum working electrode, a saturated calomel reference electrode and a graphite counter electrode. A synthetic copper sulphate electrolyte containing about 63 g/ℓ copper, 33 g/ℓ nickel, 1.2 g/ℓ iron and 35 g/ℓ sulphuric acid into which varying concentrations of selenium and thiourea had been added was used. Thiourea was investigated at levels of 10 mg/ℓ, 100 %, 200 % and 320 % excess while selenium was investigated at concentrations of 20, 57 and 150 mg/ℓ.

It was observed through cyclic voltammetry that thiourea inhibited the cathodic reduction of copper ions. In the presence of excess thiourea the area under the cupric ion reduction peak decreased and shifted towards more negative values. This, coupled with a reduction in the size of the oxidation peak, indicated that thiourea polarised the working electrode and thus reduced the efficiency of the cupric ion reduction reaction.

In the presence of selenium a second cathodic peak was observed. This peak was ascribed to the simultaneous reduction of copper and selenium leading to the formation of a copper selenide compound.

The electrowinning tests performed in the presence of excess thiourea showed a decrease in the cathodic current and a subsequent reduction in the current density. The electrodeposits obtained in the presence of thiourea showed varying characteristics. At 10 mg/ℓ a smooth, fine grained and coherent electrodeposit was obtained. At 100 % excess thiourea a coherent but rough electrodeposit was obtained. At higher concentrations of 200 % and 320 % excess thiourea, brittle and flaky deposits were obtained. The electrodeposits were also contaminated with carbon, sulphur and nitrogen which are the constituent elements of thiourea. In the absence of thiourea a current efficiency of 96.06 % was obtained. The introduction of 10 mg/ℓ thiourea resulted into a current efficiency of 96.01 %. In the presence of excess thiourea, the current efficiencies dropped to 93.88 %, 92.87 % and 87.46 % for 100 %, 200 % and 320 % excess thiourea, respectively.

The electrodeposits obtained from selenium containing electrolytes formed nodules on the surface. These deposits were also contaminated with selenium and were covered by a black mass on the surface. This black mass was ascribed to a copper selenide compound formed through the simultaneous reduction of copper and selenium. The intensity of this black mass increased with increasing selenium concentration. The presence of selenium in the electrolyte also affected the electrowinning efficiency negatively. At 20 mg/ℓ the current efficiency obtained was 95.96 % compared to 96.06 % in the absence of selenium. The current efficiency was observed to drop further to 94.78 % and 85.35 % at concentrations of 57 and 150 mg/ℓ, respectively. Based on these results, it can be concluded that precipitation of PGM from the copper sulphate solution with excess thiourea prior to electrowinning is not a feasible process option.

# OPSOMMING

Onlangse studies het verskillende prosesroetes vir die verwydering van selenium en tellurium en die herwinning van platinum groep metale (PGM) uit kopersulfaat logingsoplossings ondersoek. Hierdie studies het bevind dat 'n beduidende verbetering in PGM herwinning haalbaar is indien oormaat hoeveelhede tio-ureum as presipitasiemiddel gebruik word in plaas van swaweligsuur, wat tans algemeen gebruik word. Die huidige studie was belangrik om die effek van oormaat hoeveelhede tio-ureum sowel as variasie in die selenium konsentrasie op die koper elektrowinning effektiwiteit en katode kwaliteit te verduidelik.

Die eksperimentele werk is verdeel in elektrochemiese en elektrowinning toetse. Die elektrochemiese toetse is uitgevoer deur gebruik te maak van 'n sikliese voltammetrie tegniek om inligting te bekom oor moontlike interaksies tussen selenium en tio-ureum en die koper ione tydens deposisie. Die effek van variërende selenium en tio-ureum konsentrasie op katode kwaliteit en elektrowinning effektiwiteit is ondersoek deur elektrowinning toetse uit te voer.

Beide die elektrowinning en die elektrochemiese toetse is uitgevoer deur gebruik te maak van 'n 3-elektrode sisteem bestaande uit 'n roterende skyf platinum werkende elektrode, 'n versadigde kalomel verwysingselektrode en 'n grafiet teenelektrode. 'n Sintetiese kopersulfaat elektroliet wat 63 g/ℓ Cu, 33 g/ℓ nikkel, 1.2 g/ℓ yster en 35 g/ℓ swawelsuur sowel as variërende konsentrasies selenium en tio-ureum bevat het, is gebruik. Tio-ureum is ondersoek by vlakke van 10 dele per miljoen (dpm), 100 %, 200 % en 320 % oormaat, terwyl selenium ondersoek is by konsentrasies van 20, 57 en 150 dpm.

Sikliese voltammetrie het aangetoon dat tio-ureum die katodiese reduksie van koper ione onderdruk. In die teenwoordigheid van oormaat hoeveelhede tio-ureum het die area onder die koper(II) ioon reduksie piek afgeneem en in die rigting van meer negatiewe waardes geskuif. Hierdie waarnemings, tesame met die afname in die grootte van die oksidasie piek, het aangedui dat tio-ureum die werkende elektrode gepolariseer het en dus die effektiwiteit van die koper(II) ioon

reduksie reaksie verlaag het. In die teenwoordigheid van selenium is 'n tweede katodiese piek waargeneem. Hierdie piek is toegeskryf aan die gelyktydige reduksie van koper en selenium wat aanleiding gegee het tot die vorming van 'n koperselenied verbinding.

Die elektrowinning toetse wat in die teenwoordigheid van oormaat tio-ureum uitgevoer is het 'n afname in die katodiese stroom en 'n gevolglike afname in die stroomdigtheid getoon. Die neerslae wat in die teenwoordigheid van tio-ureum verkry is het variërende eienskappe getoon. 'n Gladde, koherente neerslag met 'n fyn grein is by 10 dpm tio-ureum verkry. By 100 % oormaat tio-ureum is 'n koherente maar rowwe neerslag verkry. Bros en skilferige neerslae is by hoër konsentrasies van 200 % en 320 % oormaat tio-ureum verkry. Die neerslae was ook besmet met koolstof, swawel en stikstof, wat die samestellende elemente van tio-ureum is. In die afwesigheid van tio-ureum is 'n stroom effektiwiteit van 96.06 % behaal. Die byvoeging van 10 dpm tio-ureum het tot 'n stroom effektiwiteit van 96.01 % aanleiding gegee. In die teenwoordigheid van 'n oormaat tio-ureum het die stroom effektiwiteite tot 93.88 %, 92.87 % en 87.46 % vir 100 %, 200 % en 320 % oormaat tio-ureum, onderskeidelik, geval.

Die neerslae wat verkry is vanaf selenium bevattende elektroliete het knoppies op die oppervlak gevorm. Hierdie neerslae was ook besmet met selenium en was bedek met 'n swart massa op die oppervlak. Die swart massa is toegeskryf aan 'n koperselenied verbinding wat gevorm het deur die gelyktydige reduksie van koper en selenium. Die intensiteit van die swart massa het toegeneem met toenemende selenium konsentrasie. Die teenwoordigheid van selenium in die elektroliet het ook die elektrowinning effektiwiteit negatief beïnvloed. 'n Stroom effektiwiteit van 95.96 % is behaal by 20 dpm in vergelyking met 96.06 % in die afwesigheid van selenium. Die stroom effektiwiteit het verder afgeneem na 94.78 % en 85.35 % by konsentrasies van 57 en 150 dpm, onderskeidelik. Gebaseer op hierdie resultate kan die gevolgtrekking gemaak word dat dit nie lewensvatbaar is om PGM met oormaat tio-ureum vanuit die kopersulfaat oplossing te presipiteer voor koper elektrowinning nie.

# ACKNOWLEDGEMENTS

I wish to thank God Almighty for giving me the strength and will to pursue this research project.

I also wish to give my sincere gratitude and thanks to the following individuals and institutions:

- My project supervisors, Professor Christie Dorfling and Professor Steven Bradshaw, for affording me the opportunity to pursue these studies and for their technical guidance.
- The South African Minerals to Metals Research Institute, the Department of Science and Technology and the Department of Process Engineering Stellenbosch University, for the financial and material support.
- My parents for their words of encouragement and support.
- My wife and children (Sampa and Mwalula) for their patience, understanding and support.

# TABLE OF CONTENTS

DECLARATION ..... i

ABSTRACT ..... ii

OPSOMMING ..... iv

ACKNOWLEDGEMENTS ..... vi

TABLE OF CONTENTS ..... vii

LIST OF FIGURES ..... xii

LIST OF TABLES ..... xviii

NOMENCLATURE ..... xx

1. INTRODUCTION ..... 1

1.1. Background ..... 1

1.2. Problem statement ..... 4

1.3. Research aim and objectives ..... 4

1.4. Research limitations ..... 5

1.5. Thesis structure ..... 5

2. LITERATURE REVIEW ..... 7

2.1. Fundamentals of metal electrodeposition ..... 7

2.1.1. Nucleation and crystal growth during metal deposition ..... 8

2.1.2. Electrode potential ..... 10

2.1.3. Electrochemical polarisation ..... 13

2.2. Copper electrowinning ..... 14

2.2.1. An overview of industrial copper electrowinning ..... 14

2.2.2. Effects of operating parameters on electrowinning ..... 18

2.2.2.1. Temperature ..... 18
2.2.2.2. Metal ion concentration ..... 18
2.2.2.3. pH ..... 18
2.2.2.4. Current density ..... 19
2.2.2.5. Current efficiency ..... 19
2.2.2.6. Additives in copper electrowinning ..... 20
2.2.2.7. Cathodes ..... 20
2.2.2.8. Anodes ..... 21
2.3. Electrochemical techniques ..... 21
2.3.1. Cyclic voltammetry ..... 21
2.3.2. Rotating disk electrodes ..... 23
2.4. The chemistry of selenium and thiourea ..... 24
2.4.1. Physical and chemical properties of selenium ..... 24
2.4.1.1. Reduction chemistry of selenium ..... 25
2.4.1.2. Selenium water system ..... 27
2.4.2. Physical and chemical properties of thiourea ..... 29
2.4.2.1. The chemistry of thiourea in $CuSO_4$ and $H_2SO_4$ system ..... 29
2.4.2.2. Oxidation of thiourea ..... 30
2.4.3. Current practices in selenium precipitation from leach solutions ..... 32
2.4.3.1. Selenium precipitation using cuprous ions ..... 32
2.4.3.2. Selenium precipitation using sulphur dioxide ..... 33
2.4.3.3. Selenium precipitation using thiourea ..... 34
2.4.4. Effects of organic additives on copper electrowinning ..... 35
2.4.4.1. Classification of organic additives ..... 35

2.4.4.2. Action mechanism of organic additives ..... 36
2.4.4.3. Adsorption of additives during deposition ..... 39
2.4.4.4. Effect of organic additives on the cathode overpotential ..... 42
2.4.4.5. Key findings from previous investigations on the effects of thiourea on copper deposition ..... 44
2.4.5. Effects of selenium and other dissolved impurities on electrowinning ..... 49
2.5. Summary ..... 55
3. Experimental ..... 56
3.1. Electrochemical tests ..... 56
3.1.1. Materials ..... 56
3.1.2. Methodology ..... 56
3.1.2.1. Experimental design ..... 57
3.1.2.2. Experimental setup ..... 58
3.1.2.3. Electrode cleaning ..... 59
3.1.2.4. Experimental procedure ..... 60
3.2. Electrowinning tests ..... 61
3.2.1. Materials ..... 61
3.2.2. Methodology ..... 61
3.2.2.1. Experimental design ..... 62
3.2.2.2. Experimental setup ..... 62
3.2.2.3. Experimental procedure ..... 62
3.2.2.4. Analytical methods ..... 63
4. Results and discussion ..... 64
4.1. Electrochemical tests ..... 64

4.1.1. Cyclic voltammogram for copper ..... 64
4.1.2. Cyclic voltammogram for selenium ..... 65
4.1.3. Cyclic voltammogram for thiourea ..... 67
4.1.4. Effects of thiourea ..... 70
4.1.5. Effects of selenium ..... 73
4.1.6. Combined effect of thiourea and selenium ..... 76
4.2. Electrowinning tests ..... 78
4.2.1. Electrowinning in the absence of thiourea ..... 78
4.2.2. Electrowinning in the presence of thiourea ..... 81
4.2.2.1. Effects of low thiourea concentrations on cathode morphology ..... 81
4.2.2.2. Effects of excess thiourea amounts on cathode quality ..... 85
4.2.2.3. Effects of excess thiourea on electrowinning efficiency ..... 93
4.2.2.4. Electrowinning at higher potential ..... 95
4.2.3. Electrowinning in the presence of selenium ..... 97
4.2.3.1. Effects of selenium on cathode morphology ..... 97
4.2.3.2. Effects of selenium on electrowinning efficiency ..... 104
5. Conclusions and Recommendations ..... 107
5.1. Effects of excess thiourea on copper electroreduction ..... 107
5.2. Effects of excess thiourea on cathode quality and electrowinning efficiency .. 107
5.3. Effects of selenium on copper electroreduction ..... 108
5.4. Effects of selenium on cathode quality and electrowinning efficiency ..... 109
5.5. Suitability of thiourea as a Se/Te precipitating agent ..... 109
5.6. Recommendations ..... 110
6. References ..... 111

APPENDIX A: SYNTHETIC SOLUTION PREPARATION ..... 120

APPENDIX B: CYCLIC VOTAMMETRY REPEATABILITY ..... 121

APPENDIX C: EXPERIMENTAL DATA ..... 125

# LIST OF FIGURES

*Figure 1.1.A typical simplified process flow diagram for a base metal refinery (after Bircumshaw, 2008).* 3

*Figure 2.1. Electrocrystallisation steps during metal deposition (Pasa and Munford 2006)* 7

*Figure 2.2. Electric double layer at the substrate-electrolyte interface (after Deni, 1994)* 16

*Figure 2.3. Power requirements and losses in copper electrowinning (After Schlesinger et al., 2011)* 17

*Figure 2.4. Diagram showing the variation of potential during a standard cyclic voltammetry test* 22

*Figure 2.5. Electrolyte flow pattern at a rotating disk electrode (after Nikolic et al., 2000)* 24

*Figure 2.6. Eh-pH diagram for the selenium water system at 25˚C ( Using HSC chemistry 7.1)* 27

*Figure 2.7. Eh-pH diagram for the copper-sulphur-selenium-water system at 25˚C (using HSC chemistry 7.1)* 28

*Figure 2.8.A current-potential profile for additive adsorption on the electrode (after Bockris et al., 1998)* 41

*Figure 2.9. Grain size variation as a function thiourea concentration (after Kao et al., 2004)* 46

*Figure 3.1. Schematic diagram of the experimental setup* 59

*Figure 4.1.Cyclic voltammogram for copper in 0.01 M $Cu^{2+}$ ions and 1 M sulphuric acid at 25˚C* 65

*Figure 4.2. Cyclic voltammogram for 600 mg/ℓ selenium and 1 M sulphuric acid at 25˚C* 66

*Figure 4.3. Cyclic voltammogram for thiourea in 0.05 mM thiourea and 1 M sulphuric acid at 25°C with potential scan range of -0.25 V to 1.3 V* 69

*Figure 4.4. Cyclic voltammogram for thiourea in 0.05 mM thiourea and 1 M sulphuric acid at 25°C with potential scan range of -0.5 V to 0.5 V* 69

*Figure 4.5.Cyclic voltammogram for copper ($Cu^{2+}$ 0.01 M) with varying concentrations of thiourea, 100 %, 200 % and 320 % excess in 1 M sulphuric acid at 25°C* 70

*Figure 4.6.Cyclic voltammogram for copper in 0.01 M $Cu^{2+}$ and 1 M sulphuric acid in the presence of 320 % excess thiourea at 25°C* 72

*Figure 4.7.Cyclic voltammogram for copper in 0.01 M $Cu^{2+}$ and 1M sulphuric acid in the presence of 200 % excess thiourea at 25°C* 72

*Figure 4.8. Cyclic voltammogram for copper in 0.01 M $Cu^{2+}$ and 1 M sulphuric acid in the presence of 100 % excess thiourea at 25°C* 73

*Figure 4.9. Cyclic voltammogram for copper in 0.01 M $Cu^{2+}$ and 1 M sulphuric acid in the presence of 20 mg/ℓ selenium at 25°C* 74

*Figure 4.10. Cyclic voltammogram for copper in 0.01 M $Cu^{2+}$ and 1 M sulphuric acid in the presence of 57 mg/ℓ selenium at 25°C* 75

*Figure 4.11. Cyclic voltammogram for copper in 0.01 M $Cu^{2+}$ and 1 M sulphuric acid in the presence of 150 mg/ℓ selenium at 25°C* 75

*Figure 4.12. Image showing the appearance of the working electrode after a cyclic voltammetry test in 0.01 M $Cu^{2+}$ and 1 M sulphuric acid in the presence of 150 mg/ℓ selenium* 76

*Figure 4.13. Cyclic voltammogram for the combined effect of thiourea and selenium in 0.01 M $Cu^{2+}$ and 1 M sulphuric acid at 25°C* 77

*Figure 4.14. Scanning electron microscopy (SEM) image of a copper electrodeposit obtained in a standard electrolyte solution at constant potential.* 79

*Figure 4.15. Scanning electron microscopy (SEM) image showing the grain structure of a copper electrodeposit obtained from a standard electrolyte* 80

*Figure 4.16. Scanning electron microscopy (SEM) image of a copper electrodeposit obtained from a standard electrolyte containing 10 mg/ℓ thiourea at a constant potential* 83

*Figure 4.17. Scanning electron microscopy (SEM) image showing the grain structure of a copper electrodeposit obtained from standard electrolyte containing 10 mg/ℓ thiourea at a constant potential* 83

*Figure 4.18. Digital images of electrodeposits obtained in the presence of varying concentrations of thiourea [A] 100 %, [B] 200 % and [C] 320 % excess thiourea* 87

*Figure 4.19. Scanning electron microscopy (SEM) image of an electrodeposit obtained from a solution containing 100 % excess thiourea at constant potential and 25˚C.* 88

*Figure 4.20. Impurity levels detected from electrodeposits obtained the presence of varying concentrations of thiourea.* 90

*Figure 4.21. Scanning electron image of an electrodeposit obtained from an electrolyte containing 200 % excess thiourea showing incorporated impurities carbon and sulphur* 90

*Figure 4.22. Elemental maps showing the distribution of elements in an electrodeposit obtained from an electrolyte containing 200 % excess thiourea, [A]-copper, [B]-carbon, [C]-oxygen and [D]-sulphur* 91

*Figure 4.23. Scanning electron image of an electrodeposit obtained from an electrolyte containing 200 % excess thiourea showing some specific sites sampled.* 92

*Figure 4.24. Current transients showing the effect of varying thiourea concentration on the cathodic current during cupric ion reduction* 94

*Figure 4.25. Current efficiencies obtained from electrowinning tests done in the presence of varying thiourea concentrations.* 95

*Figure 4.26. Digital image of electrodeposit produced at 600 mV in the presence of 320 % excess thiourea.* 96

*Figure 4.27. Current transients showing cathodic current at two different potentials in the presence of 320 % excess thiourea.* 96

*Figure 4.28. Comparison of impurity levels, carbon, sulphur and nitrogen in electrodeposits produced at different potentials in the presence of 320 % excess thiourea.* 97

*Figure 4.29. Digital images of electrodeposits obtained in the presence of varying concentrations of selenium [A] 20 mg/ℓ, [B] 50 mg/ℓ and [C] 150 mg/ℓ* 98

*Figure 4.30 . Scanning electron microscopy (SEM) image of an electrodeposit obtained from an electrolyte containing 20 mg/ℓ Se at constant potential and 25˚C.* 99

*Figure 4.31. Scanning electron microscopy (SEM) image of an electrodeposit obtained from an electrolyte containing 57 mg/ℓ Se at constant potential and 25˚C* 100

*Figure 4.32. Scanning electron microscopy (SEM) image of an electrodeposit obtained from an electrolyte containing 150 mg/ℓ Se at constant potential and 25˚C* 100

*Figure 4.33. Scanning electron microscopy image of an electrodeposit obtained from an electrolyte containing 150 mg/ℓ Se at constant potential and 25˚C* 101

*Figure 4.34. Elemental maps showing the distribution of elements on an electrodeposit obtained from an electrolyte containing 150 mg/ℓ Se, [A]-copper, [B]-oxygen, [C]-selenium, [D]-iron, [E]-nickel and [F]-carbon* 102

*Figure 4.35. Scanning electron microscopy (SEM) image of a nodule formed on the surface of an electrodeposit obtained from an electrolyte containing 150 mg/ℓ Se* 103

*Figure 4.36. Current transients showing the effects of varying selenium concentration on the cathodic current during cupric ion reduction* 105

*Figure 4.37. Current efficiencies obtained in the absence and presence of varying selenium concentration* 106

*Figure B.1. Cyclic voltammograms obtained for 0.01 M $Cu^{2+}$ and 1 M sulphuric acid at 25˚C.* 121

*Figure B.2. Cyclic voltammograms obtained for 0.05 mM and 1 M sulphuric acid at 25˚C.* 121

*Figure B.3 Cyclic voltammograms obtained for 600 ppm Se and 1 M sulphuric acid at 25˚C* 122

*Figure B.4. Cyclic voltammograms obtained for 0.01 M $Cu^{2+}$, 320 % excess thiourea and 1 M sulphuric acid at 25˚C.* 122

*Figure B.5. Cyclic voltammograms obtained for 0.1 M Cu2+, 200 % excess thiourea and 1 M sulphuric acid at 25˚C.* 123

*Figure B.6. Cyclic voltammograms obtained for 0.01 M $Cu^{2+}$ , 20 mg/ℓ selenium and 1M sulphuric acid at 25˚C.* 123

*Figure B.7. Cyclic voltammograms obtained for 0.01 M $Cu^{2+}$, 57 mg/ℓ selenium and 1 M sulphuric acid at 25 ˚C.* 124

*Figure B.8. Cyclic voltammograms obtained for 0.01 M Cu2+, 150 mg/ℓ selenium and 1 M sulphuric acid at 25˚C.* 124

*Figure C.1 SEM image and elemental maps showing distribution of elements in an electrodeposit obtained from a standard electrolyte* 130

*Figure C.2 SEM image and elemental maps showing grain structure and distribution of elements in an electrodeposit obtained from a standard electrolyte* 131

*Figure C.3 SEM image and elemental maps showing the distribution of elements in an electrodeposit obtained in the presence of 100 ppm thiourea* 132

*Figure C.4 SEM image and elemental maps showing grain structure distribution of elements in an electrodeposit obtained in the presence of 10 ppm thiourea* 133

*Figure C.5.SEM image and elemental maps showing the distribution of elements in an electrodeposit obtained in the presence of 100% excess thiourea* 134

# LIST OF TABLES

*Table 1.1. Typical industrial electrolyte composition (source, Global Cu EW survey copper, 2013)* 2

*Table 1.2.Typical impurity levels in base metal refinery copper cathodes (source, Global Cu EW survey copper, 2013)* 2

*Table 2.1. Copper electrowinning cell voltage distribution (Davenport et al., 2002)* 17

*Table 2.2: Results obtained from Se removal study (Weir et al., 1982)* 34

*Table 3.1. List of chemicals used in the electrochemical experiments.* 56

*Table 3.2. Summary of variable factors and factor values used in the electrochemical tests* 58

*Table 3.3. Summary of fixed factors and factor values used in the electrochemical tests* 58

*Table 3.4. List of chemicals used in the electrowinning tests.* 61

*Table 4.1. Spot elemental composition of certain sites from the deposit obtained in a standard electrolyte* 81

*Table 4.2. Spot elemental composition of specific sites from an electrodeposit obtained from an electrolyte containing 10 mg/ℓ thiourea* 85

*Table 4.3. Spot elemental composition of specific sites from an electrodeposit obtained from an electrolyte containing 200 % excess thiourea.* 92

*Table 4.4. Spot elemental composition of specific sites from a surface nodule observed on an electrodeposit obtained from an electrolyte containing 150 mg/ℓ Se* 103

*Table C.1. ICP results for test performed in the presence of thiourea* 125

*Table C.2. ICP results for tests performed in the presence of selenium* 125

*Table C.3. ICP results for tests performed using standard electrolyte* 126

*Table C.4. Actual and assay electrodeposit weights obtained in the electrowinning tests* 126

*Table C.5. Sample of cathodic current data during deposition in the presence of thiourea* 127

*Table C.6. Sample of cathodic current data during deposition in the presence of selenium* 128

*Table C.7. Current efficiencies obtained during the electrowinning tests* 129

# NOMENCLATURE

| Symbol | Unit | Meaning |
|---|---|---|
| $C^b$ | Mole/ℓ | Bulk concentration of additive |
| d | m | Molecular diameter of solute species |
| D | $m^2/s$ | Diffusivity |
| E | V | Electrode potential |
| $E^0$ | V | Standard electrode potential |
| F | C/mol | Faradays Constant |
| $\Delta G$ | J/mol | Gibbs free energy change |
| $\Delta G_{max}$ | J/mol | Maximum activation Gibbs free energy barrier |
| $\Delta G_{bulk}$ | J/mol | Gibbs free energy-bulk |
| $\Delta G_r$ | J/mol | Gibbs free energy change of a reaction |
| $\Delta G_{surf}$ | J/mol | Gibbs free energy-surface |
| $\Delta G_{ss}$ | J/mol | Molar free energy of super saturation |
| $i_a$ | A | Anodic current |
| $i_c$ | A | Cathodic current |
| I | A | Electric current |
| $j_o$ | $A/m^2$ | Exchange current density |
| J | $m^3$ | Number of nuclei per unit volume |
| $k_B$ | J/K | Boltzman constant |
| M | mol/ℓ | Molarity |
| n | mol | Number of moles |
| $M_r$ | g/mol | Molecular weight |
| $pK_a$ | | Acid dissociation constant |
| $r_{crit}$ | μm | Critical nucleus radius |
| R | J/mol k | Ideal gas constant |
| t | min ,hr or S | Time |
| T | °C or K | Temperature |
| $V_m$ | $m^3$ | Volume of one mole of metal |
| η | V | Total overpotential |

| | | |
|---|---|---|
| $\eta_a$ | V | Anodic overpotential |
| $\eta_c$ | V | Cathodic overpotential |
| $\Theta$ | | Additive surface coverage |
| $\beta_a$ | Volt/decade | Anodic tafel constant |
| $\beta_c$ | Volt/decade | Cathodic tafel constant |
| $\Delta\emptyset$ | V | Potential difference |
| $\emptyset_M$ | V | Potential of the metal phase |
| $\emptyset_s$ | V | Potential of the solution phase |
| $\alpha$ | | Charge transfer coefficient |
| $\delta$ | $J/m^2$ | Surface free energy |

| **Acronym** | **Meaning** |
|---|---|
| CE | Counter electrode |
| EDX | Energy dispersive x-ray spectroscopy |
| ICP-OES | Inductively coupled plasma optical emission spectroscopy |
| ppm | Parts per million |
| rpm | Revolutions per minute |
| RE | Reference electrode |
| RDE | Rotating disk electrode |
| SCE | Saturated calomel electrode |
| SEM | Scanning electron microscopy |
| WE | Working electrode |
| XRD | X-ray diffraction |

# 1. INTRODUCTION

## 1.1. Background

Recovery of copper by leach-solvent extraction (SX)-electrowinning (EW) is a widely practiced technology in the mining and metallurgical industries. Leaching involves the dissolution of metal values followed by solid liquid separation. The leach solution then undergoes purification processes such as solvent extraction before passing to electrowinning for the production of cathode copper.

The initial steps in the preparation of the electrolyte that finally passes to a typical base metal refinery (BMR) involves ore dressing operations such as crushing, grinding and milling at the concentrator. The run of mine ore undergoes size reduction stages until a size suitable for flotation is attained. A platinum group metal (PGM) rich concentrate is produced by flotation and treated through the smelter to produce a molten sulphide matte. This sulphide matte is further treated in a Peirce Smith converter where iron and sulphur are oxidised producing a converter matte that is amenable to refining. The converter matte is milled and subjected to atmospheric leaching followed by solid-liquid separation in a thickener (refer to Figure 1.1). The thickener overflow passes to the nickel crystalliser for the production of nickel sulphate crystals while the residue is subjected to a $2^{nd}$ and $3^{rd}$ pressure leach using autoclaves. The product from the autoclaves undergoes solid-liquid separation producing a copper sulphate leach solution and a PGM-rich solid residue. The pregnant copper sulphate leach solution contains impurities such as selenium and tellurium together with an appreciable amount of PGMs dissolved during the high pressure oxidative leach stage. Selenium and tellurium removal using sulphur dioxide precedes copper electrowinning. The dissolved PGMs are recycled back to the head of the circuit. This recycle stream means that a lot of PGM inventory is locked in the system and these may potentially be lost if strict operating procedures are not put in place. This study focuses on the copper recovery process through electrowinning.

A typical composition of the electrolyte sent for electrowinning is shown in Table 1.1.

*Table 1.1. Typical industrial electrolyte composition (source, Global Cu EW survey copper, 2013)*

| | Copper | Nickel | Iron | Sulphuric acid | Selenium |
|---|---|---|---|---|---|
| Composition (g/ℓ) | 60-70 | 30-40 | 0.7 | 35 | 57 mg/ℓ |

The copper is plated out on stainless steel permanent starting sheets after a typical cycle time of about 7-10 days. Lead-antimony (92 % Pb and 8 % Sb) rolled metal sheets are used as anodes. Guar gum and thiourea are employed as smoothening agents at 250 g and 150 g per tonne of copper produced, respectively (Global Cu EW survey, 2013). Table 1.2 shows a typical elemental composition of the impurities in the copper cathodes produced.

*Table 1.2.Typical impurity levels in base metal refinery copper (source, Global Cu EW survey copper, 2013)*

| Element | Lead | Nickel | Iron | Sulphur | Selenium | Tellurium | Cobalt |
|---|---|---|---|---|---|---|---|
| Composition (ppm) | <5 | <60 | <10 | <20 | <20 | <40 | <5 |

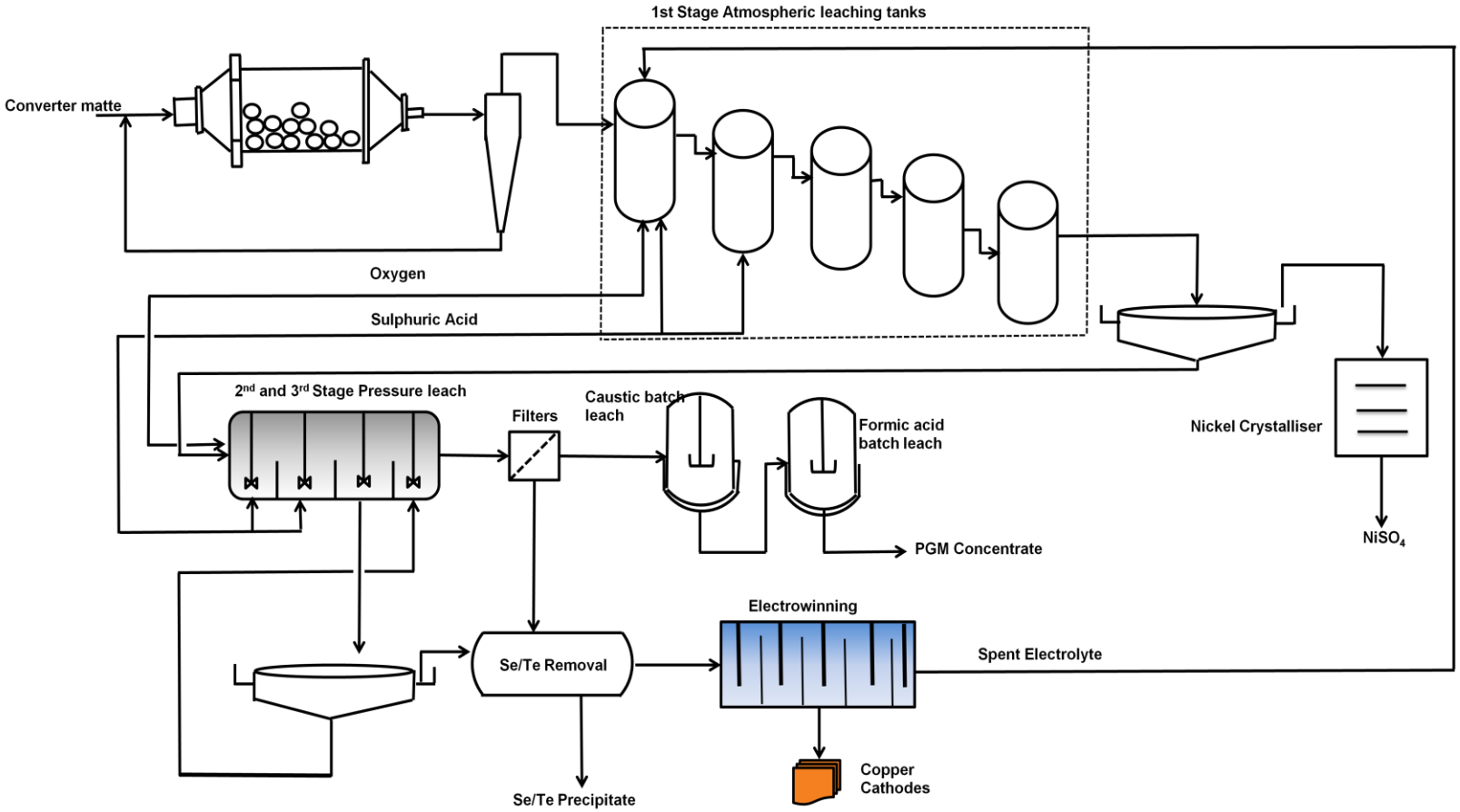


*Figure 1.1.A typical simplified process flow diagram for a base metal refinery (after Bircumshaw, 2008).*

## 1.2. Problem statement

The copper electrowinning process is known to be sensitive to the chemistry of the electrolyte. The presence of impurities in the electrolyte might have detrimental effects on electrowinning parameters such as current efficiency and the quality of the deposits produced. It is therefore imperative that any impurities present in the electrolyte are removed to acceptable levels were the efficiency of the electrowinning process is not negatively affected.

Currently the precipitation of impurities (selenium and tellurium) from copper electrolytes is widely done using sulphurous acid. However, recent studies have proposed the use of excess amounts of thiourea in place of sulphurous acid as a precipitating agent in the removal of the said impurities (Mulwanda, 2014; Lottering et al., 2011).

The use of excess thiourea in selenium and tellurium precipitation has the advantage that high recovery of dissolved PGMs is also achievable which could potentially result in reduced PGM losses as the dissolved PGMs are in some cases recycled to the head of the circuit as part of the tank house spent electrolyte. However, the effects that the use of excess amounts of thiourea will have on the electrowinning process are not well understood. Selenium and tellurium present in the electrolyte may also have adverse effects on electrowinning efficiency and cathode quality.

## 1.3. Research aim and objectives

The aim of this study was to establish the effects that excess thiourea and variations in selenium concentration may have on the production of copper cathodes through the electrowinning process. In order to achieve this, the following objectives were set:

- Perform electrochemical tests to investigate how excess amounts of thiourea, as well as variations in selenium concentration, interact with the cathodic copper deposition reaction.

- Carry out electrowinning tests to investigate the effects that excess amounts of thiourea, as well as variations in selenium concentration, may have on the morphology of the copper deposits, their chemical composition and the electrowinning current efficiency.

## 1.4. Research limitations

In order to ensure that a reasonable focus is maintained, the following were the limitations:

- Although nickel was one of the elements in the electrolyte used its behaviour and effects on the electrowinning process were not explored.
- Tests using an electrolyte from which selenium and tellurium have been removed in the manner proposed in the work that provided impetus to this study were not done.
- The effects of tellurium were not explored fully. In an attempt to investigate the effects of tellurium, an air bubble was observed to cover the electrode surface; as a result, electrochemical processes taking place could not be observed. This bubble was attributed to a possible formation of hydrogen or hydrogen telluride (Bouroushian, 2010). Some sections of literature have reported that tellurium may be investigated using polarography.

## 1.5. Thesis structure

A theoretical background covering some steps involved in the initial stages of metal deposition, nucleation and growth are presented in chapter 2. Some fundamental aspects of electrode kinetics as well as a brief overview of industrial copper electrowinning are also discussed within chapter 2. Relevant literature to the chemistry of selenium and thiourea is reviewed in chapter 2, as well as related applied research on the effects of thiourea and selenium on the electrowinning of copper from acidified sulphate solutions.

The experimental materials, methodologies and equipment are discussed in chapter 3; thereafter the experimental results are presented and discussed in

chapter 4. The conclusions drawn from this study as well as recommendations are outlined in chapter 5.

# 2. LITERATURE REVIEW

## 2.1. Fundamentals of metal electrodeposition

The electrodeposition process essentially entails the formation of new nuclei in the presence of an electric field. Nucleation or nuclei formation is the first step in metal deposition. Fabian (2005) proposed that metal deposition progresses by three surface processes, charge transfer, surface diffusion and movement from adatom position after electron transfer into kink or step position. According to Pasa and Munford (2006), the charge transfer step is relatively fast and therefore the growth rate of the nucleus is governed by mass transfer of cations onto the growing sites. The electrodeposition process as illustrated in Figure 2.1 involves the diffusion of a solvated ion from the bulk solution to the electrode surface, transfer of electrons between ion and electrode and adsorption (Pasa & Munford, 2006). The adatom then moves into a deposition or nucleation site by surface diffusion. The electrode surface usually has some surface defects which act as deposition (nucleation) sites (Pasa & Munford, 2006). The nuclei are formed from the adatoms which diffuse into these sites and eventually grain formation occurs followed by deposit formation or growth.

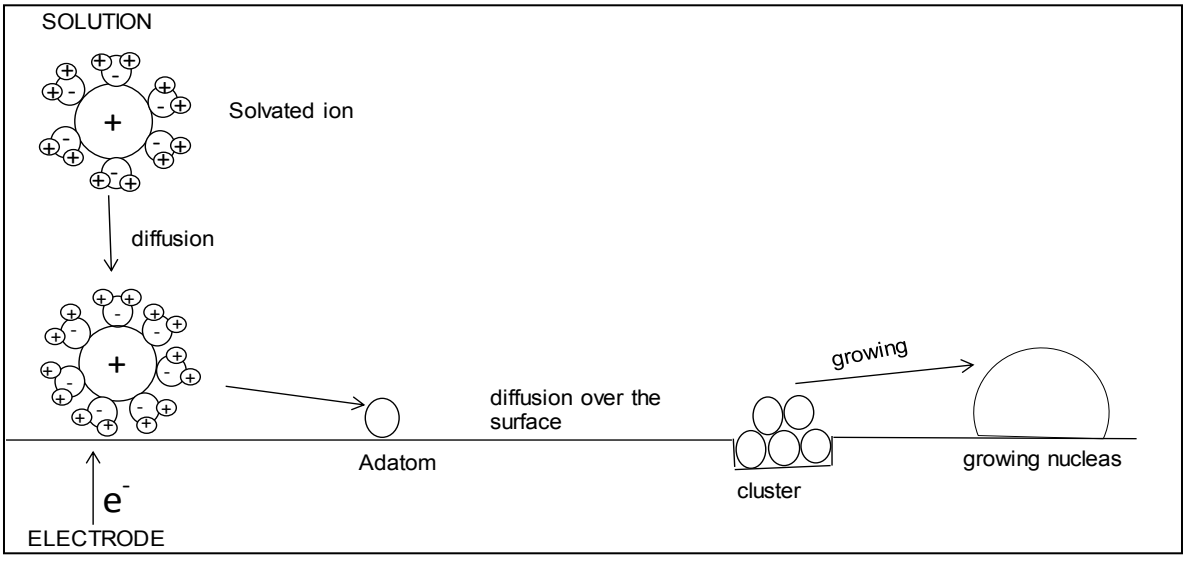


*Figure 2.1 Electrocrystallisation steps during metal deposition (Pasa and Munford, 2006)*

The growth of a new phase starts with nuclei formation. For electrochemical processes such as electrodeposition phase formation occurs on the surface of a foreign particle or native substrate. The relative rates of nucleation and growth determines the structure of the deposit, fine crystallite sizes are obtained when nucleation (new nuclei formation) is favored over crystal growth. The structure and smoothness of the deposit is to a large extent determined by the kinetics of nucleation and growth as they influence the overall deposition kinetics.

### 2.1.1. Nucleation and crystal growth during metal deposition

As mentioned in Section 2.1, nucleation occurs on a foreign or native substrate. It has been reported in some sections of literature that only a few atoms constitute the nucleus of a growing deposit. Depending on how nucleation proceeds it may be termed as either homogeneous or heterogeneous. Homogeneous nucleation proceeds when all the available nucleation sites are identical (ideal crystal surface). Electrode surfaces contain defects which act as growth sites or nucleation sites (Täubert, 2006). When atoms accumulate at these sites and form nuclei, heterogeneous nucleation is said to occur. Two processes are fundamental in the formation and growth of nuclei during metal deposition;

- Diffusion and subsequent adsorption of the ions (atoms) at the electrode surface.
- Movement of adatoms or adions across the electrode surface.

The Gibbs free energy associated with the formation of nuclei on a substrate surface by a cluster of atoms is given by the sum of the bulk free energy and the surface free energy as shown in Equation 2.1

$$\Delta G_{max} = \Delta G_{bulk} + \Delta G_{surf} \qquad 2.1$$

The critical nucleus radius ($r_{crit}$) and the critical Gibbs free energy of nucleation determine nucleus instability or stable growth. Equation 2.2 gives $r_{crit}$ for a semi spherical nucleus. It must be noted that at the critical radius, a certain amount of energy, the activation energy or nucleus free energy, must be overcome for the

growth of the nuclei to be initiated. It follows therefore that the maximum free energy will be obtained at the critical nucleus radius.

$$r_{crit} = \frac{2\delta}{\Delta G_{ss}} V_m \qquad 2.2$$

Volmer and Weber (1926) showed that the rate of nucleation takes the form of the Arrhenius equation as shown by Equation 2.3

$$J = A\exp\left(\frac{-\Delta G_{crit}}{k_B T}\right) \qquad 2.3$$

and A is given as;

$$\left(\frac{2D}{d^5}\right)$$

Where;

J is the number of nuclei per unit volume ($m^3$)

D is diffusivity of the solute ($m^2/s$)

d is the molecular diameter of solute species (m)

$k_B$ is the Boltzmann constant 1.38 X $10^{-23}$ $JK^{-1}$

The nucleation process can either be instantaneous or progressive where nuclei are formed instantaneously or progressively based on the availability of nucleation sites on the electrode surface. Instantaneous nucleation occurs when a fixed number of defects are present at the electrode as the deposition potential is reached. Paunovic and Schlesinger (2006) proposed that at or near the standard deposition potential, a fixed number of defects are already present at the electrode surface and nucleation takes place instantaneously.

For instantaneous nucleation all the existing nucleation sites on the electrode surface are instantaneously converted to nuclei. The presence of foreign molecules (such as organic additives) may influence the nucleation process by promoting progressive nucleation.

### 2.1.2. Electrode potential

Electrochemical reactions involving a metal-solution interface are known to occur at the metal surface. According to Paunovic and Schlesinger (2006) when a metal electrode is immersed in an aqueous electrolyte containing metal ions, $M^{z+}$, an exchange of metal ions between the two phases (metal and solution) takes place. It must be realised that at the inception, the exchange of these ions between the two phases will be faster in one direction than the other. If the movement of $M^{z+}$ ions from the metal crystal lattice is faster than the rate at which $M^{z+}$ ions enter the crystal lattice, the metal will possess an excess of electrons and assume a negative charge, $q_M^-$ (Paunovic et al., 2010). The researchers further reported that the now negatively charged metal phase begins to attract $M^{z+}$ ions from the solution. As a consequence, there will be an excess of positive $M^{z+}$ ions in the solution in the vicinity of metal and the solution phase within that vicinity assumes an equal and opposite positive charge, $q_S^+$. It was reported that with time a dynamic equilibrium between the metal and the ions in solution is established as shown by Equation 2.4.

$$M^{Z+} + ze \leftrightarrow M \qquad 2.4$$

At the dynamic equilibrium, the metal-solution interface region is also in neutral equilibrium as shown by Equation 2.5

$$q_M = -q_s \qquad 2.5$$

As a consequence of the charging of the metal-solution interface, a potential difference (electrode potential), $\Delta\emptyset$, between the potential of the metal phase, $\emptyset_M$ and that of the solution phase, $\emptyset_S$, is established and is given as shown by Equation 2.6;

$$\Delta\emptyset\,(M,S) = \emptyset_M - \emptyset_S \qquad 2.6$$

The anodic and cathodic reactions in an electrochemical system are kept in balance by the potential of the metal.

At non-standard conditions, the electrode potential can be calculated using the Nernst equation. For a redox reaction as shown by Equation 2.7, energy is required to initiate either the forward or backward reaction.

$$M^{n+} + ne \leftrightarrow M \quad 2.7$$

Depending on the free energy either the forward or backward reaction will be favoured. According to Brookins (2012) the free energy of the reaction is given by Equation 2.8

$$\Delta G_{298} = \Delta G^{0}_{298} + RTlnK \quad 2.8$$

Where $\Delta G^{0}_{298}$ is the standard free energy (J/mol)

T is the temperature (K)

R is the ideal gas constant (J/ K mol)

K is the equilibrium constant

The standard half-cell potential $E^0$ is related to the standard free energy as shown by Equation 2.9

$$\Delta G^{0} = -nFE^{0} \quad 2.9$$

Where n is the number of electrons transferred during the reaction and F is the Faraday constant

At non-standard conditions the free energy change is given by Equation 2.10

$$\Delta G = -nFE \quad 2.10$$

Inserting Equation 2.9 and Equation 2.10 into Equation 2.8 gives Equation 2.11 the Nernst equation;

$$E = E^{0} + \frac{RT}{nF} ln|M^{n+}| \quad 2.11$$

where

E is the reduction potential

$E^0$ is the standard electrode potential

n is the number of moles of electrons involved

R is the universal gas constant (8.314 J/k mol)

T is the absolute temperature

$M^{n+}$ is the reaction quotient

Hibbert (1993) reported that the complexation of metal ions and ligands (as is the case in the presence of thiourea and other organic additives) results in a change in the concentration of the metal ions and thus altering the electrode potential. Considering a half cell metal ion-metal reaction, Equation 2.12

$$M^{n+} + e^- \leftrightarrow M \qquad 2.12$$

Addition of a complexing ligand L having constant of formation $K_f$ Equation 2.12 takes the form of Equation 2.13

$$M^{n+} + e^- \leftrightarrow \left[ML_q\right]^{(n-qz)+} \qquad 2.13$$

And the formation constant is given by Equation 2.14

$$K_f = \frac{a_{complex}}{a_{metal}\, a_{ligand}^{q}} \qquad 2.14$$

From the Nernst equation, Equation 2.11, for $M^{n+}$ incorporating the activities of the ligand and complex, and of the formation constant

$$E = E^0 - \frac{RT}{nF}\ln\left(K_f a_{ligand}^{q}\right) + \frac{RT}{nF}\ln\left(a_{complex}\right) \qquad 2.15$$

After simplification Equation 2.15 then becomes Equation 2.16;

$$E = E^{0}_{complex} + \frac{RT}{nF}\ln(a_{complex}) \quad 2.16$$

According to Hibbert (1993) the electrode potential can shift by as much as 1 volt in either direction as a result of complex formation.

### 2.1.3. Electrochemical polarisation

The deviation of the electrode potential from its equilibrium value is known as electrode polarisation. Polarisation has an effect on the electrochemical processes taking place at the electrode. When an electrode is polarised, the efficiency of the electrochemical reactions is lowered. During electrowinning, electrode polarisation may result in increased cell voltages and reduction in the current. The mechanisms of polarisation may include the formation of compounds or metal-ligand complexes that passivate the electrode and the depletion of metal ions resulting in concentration gradients. The degree of electrode polarisation is measured by the overpotential, which is defined mathematically as shown by Equation 2.17

$$\eta = E - E_{eq} \quad 2.17$$

A positive overpotential results when the electrode is polarised to a potential higher than its equilibrium potential resulting in an oxidation reaction (anodic overpotential). Reduction of the electrochemical species occurs at negative overpotentials when the electrode potential is less than its equilibrium potential (cathodic overpotential) (Hibbert, 1993).

The anodic and cathodic overpotentials can be expressed mathematically as shown by Equation 2.18 and Equation 2.19 respectively

$$\eta_a = \beta_a \log i_a - \beta_a \log j_o \quad 2.18$$

For the cathodic process

$$\eta_c = \beta_c \log i_c - \beta_c \log j_o \quad 2.19$$

Where

$$\beta_a = \frac{2.303RT}{\alpha nF} \quad \text{and} \quad \beta_c = \frac{2.303RT}{(1-\alpha)nF}$$

But from Equation 2.17 the respective anodic and cathodic overpotentials are given by Equation 2.20 and Equation 2.21 below

$$\eta_a = E_a - E_{oc} \quad 2.20$$

For the cathodic overpotential;

$$\eta_c = E_c - E_{oc} \quad 2.21$$

The total overpotential is said to be a complex parameter that can be divided into five additive terms: charge transfer overpotential, diffusion overpotential, crystallisation overpotential and resistance overpotential. The use of organic additives may result in polarisation of the cathode affecting the deposition overpotential as discussed in Section 2.4.4.4.

## 2.2. Copper electrowinning

### 2.2.1. An overview of industrial copper electrowinning

Two principle reactions are known to occur during the electrowinning of copper from sulphate leach solutions, the cathodic and anodic reactions as shown by Equation 2.22 and Equation 2.23

$$Cu^{2+} + 2e^- \rightarrow Cu^0 \quad 2.22$$

An inert anode is used in electrowinning therefore there is no copper deposition at the anode and the following reaction takes place;

$$H_2O \rightarrow H^+ + (OH)^- \rightarrow \frac{1}{2}O_2 + 2H^+ + 2e^- \quad 2.23$$

The overall electrowinning reaction is therefore a combination of the two electrode half reactions (in the presence of sulphate ions) and is represented as shown in Equation 2.24

$$Cu^{2+} + SO_4^{2-} + H_2O \rightarrow Cu^0 + \frac{1}{2}O_2 + 2H^+ + SO_4^{2-} \quad 2.24$$

Equation 2.24 shows that the products are metallic copper, oxygen gas and some acid. The acid may be recycled back to the leaching circuit.

The heterogeneous copper reduction reaction as shown in Equation 2.22 takes place at the electrode-electrolyte interface known as the electrical double layer, shown in Figure 2.2 below.

The hydrated copper ions go through a series of steps before they are incorporated into the metal lattice as illustrated in Figure 2.1. The ions first move by convective diffusion to the electrode surface, then undergo electronation, surface diffusion, dehydration, nucleation and growth. The overall process in shown by Equation 2.25 and Equation 2.26

$$Cu^{2+}_{(bulk)} \rightarrow Cu^{2+}_{surf} \quad 2.25$$

$$Cu^{2+} + 2e^- \rightarrow Cu^0_{(surf)} \quad 2.26$$

The electrode potential normally exerts some control over some of the processes mentioned above (Deni, 1994). The presence of ions or molecules other than the copper ions on the electrode surface or in the double layer may to a large extent influence the quality of copper deposited (Deni, 1994).

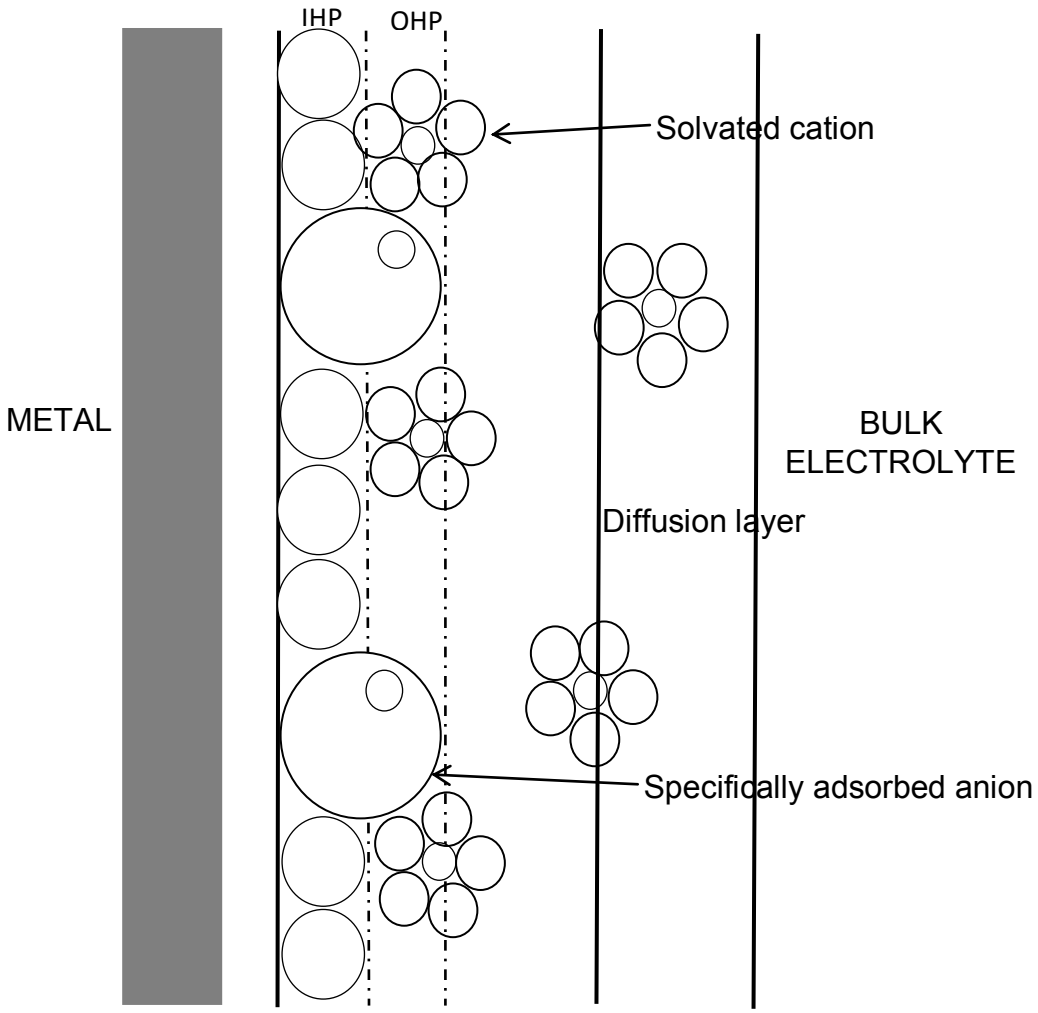


*Figure 2.2. Electric double layer at the substrate-electrolyte interface (after Deni, 1994)*

The copper electrowinning cell is considered to be an electrolytic cell as it requires work for the reactions to occur, i.e. the Gibbs free energy for an electrolytic cell is positive ($\Delta G>0$). Electrical energy is therefore required to drive electrodeposition reactions in electrowinning. The equilibrium thermodynamic energy required for electrochemical processes is given by the Nernst equation, Equation 2.11. However, the actual energy requirement is higher than that predicted by the Nernst equation. The average voltage (cell voltage) requirement for the initiation of copper electrowinning has been reported by several researchers to be approximately 2.0 Volts. This constitutes the voltage requirement for the reaction in Equation 2.24, the oxygen overvoltage, and

copper deposition overvoltage, electrical resistance due to hardware and electrical resistance in the electrolyte as shown in Table 2.1.

*Table 2.1. Copper electrowinning cell voltage distribution (Davenport et al., 2002)*

| | |
|---|---|
| Electrowinning reaction | ~0.90 V |
| Copper deposition overvoltage | ~0.05 V |
| Oxygen evolution overvoltage | ~0.50 V |
| Electrolyte resistance | ~0.25 V |
| Resistance due to hardware | ~0.25 V |

The overall power requirement for electrowinning can be represented diagrammatically as shown in Figure 2.3

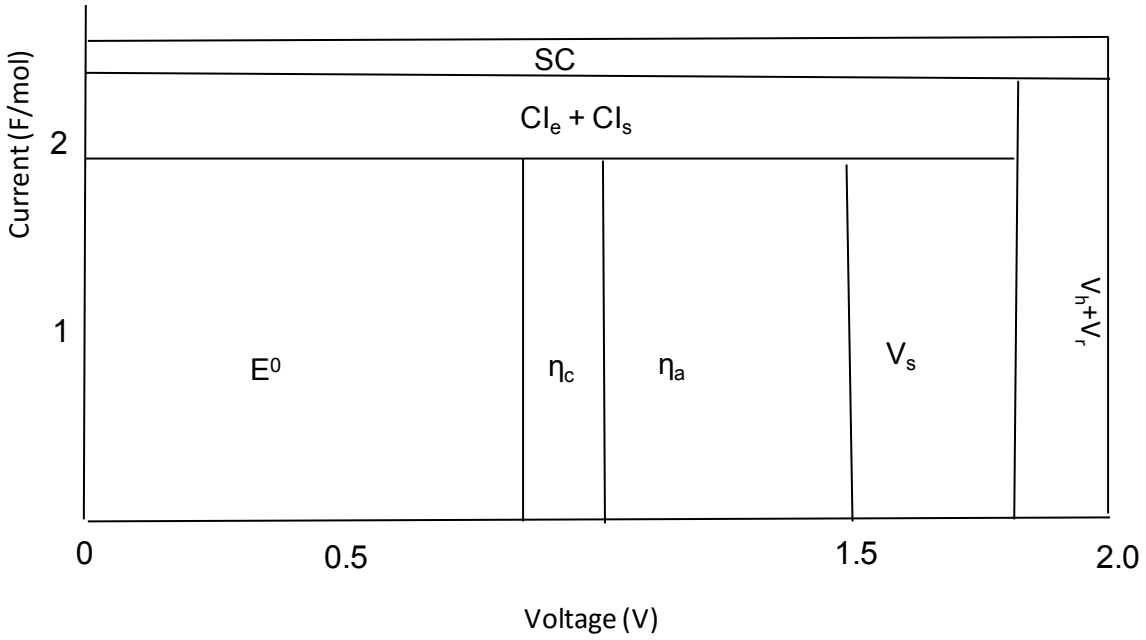


*Figure 2.3. Power requirements and losses in copper electrowinning (After Schlesinger et al., 2011)*

Where,

$E^0$ Voltage requirement for electrowinning

$\eta_c$ Cathodic overpotential

$\eta_a$ Anodic overpotential

$V_s$ Voltage drop in the electrolyte

$V_h+V_r$ Voltage across hardware and rectifier

SC Stray currents

$CI_e$ Current loss due to side reactions

$CI_s$ Current loss due to shorts

The total energy requirement for electrowinning is approximately 2000 kWh/ton of copper cathode; however, only about 30 % of this requirement is utilised directly for actual copper deposition, the remaining 70 % is lost or used up in side reactions as illustrated in Figure 2.3 (Schlesinger et al., 2011).

### 2.2.2. Effects of operating parameters on electrowinning

#### 2.2.2.1. Temperature

Temperature is an important parameter in electrowinning. Most electrowinning operations are performed within the temperature range of 30˚C to 55˚C. At high temperatures, solubility and electrical conductivity of the electrolyte are known to be enhanced through increased ion mobility. Elevated temperatures are however also reported to suppress additive adsorption rendering them ineffective. At low temperatures the electrolytic bath diffusion kinetics are negatively affected.

#### 2.2.2.2. Metal ion concentration

The concentration of the metal ions in the electrolytic bath should be kept high as low bath concentrations will easily lead to cathode polarization. High bath concentrations can also favour electrowinning operations at high current densities thus resulting in improved production rates.

#### 2.2.2.3. pH

The pH of the electrolyte during electrowinning has a significant role to play in as far as current efficiency, hydrogen evolution and precipitation of hydroxides is concerned. A very low concentration of $H^+$ ions would result into the build-up of hydroxides in the region close to the cathode. These hydroxides may get occluded in the cathode deposit and distort its properties.

### 2.2.2.4. Current density

According to Faraday's Law of electrolysis, the extent of metal deposition has a direct relationship with the rate or number of electron flow (current). The amount of current that is passed through an electrochemical cell will determine the degree to which electrochemical reactions will occur.

According to Woollacott and Eric (1994) the ohmic drop across the cell (cell resistance) is directly proportional to the electrode inter spacing and inversely proportional to the electrode surface area. For this reason most electrowinning operations involve the use of cathodes with a large surface area. The performance of an electrochemical cell is therefore mostly assessed using the current density, which is the current flowing per unit area of electrode active area. Operating at high current densities results in increased plant throughput, however care must be taken, as too high a current density will result in poor deposits as result of induced concentration polarization and enhanced hydrogen evolution. Most plants have to strike a balance between high production and high quality deposits. Brown (1975) suggested that the capability index could be used to determine the current density based on the electrolyte concentration. The researcher suggested that a factor of 0.5 to 0.7 of the electrolyte concentration (g/ℓ) could be used to give current density in amp/ft$^2$. The distribution of current on the electrode surface is of paramount importance as poor current distribution may result in variations in the surface thickness of deposit thus, rendering the quality of the deposit poor.

### 2.2.2.5. Current efficiency

Current efficiency (CE) in electrowinning is the ratio of actual copper deposited to the expected theoretical deposition based on the applied current; it is the actual current used to drive the deposition reaction. Lower than theoretical copper production means low current efficiency. In most electrowinning plants the CE is not equal to the theoretical value of 100 % as some of the applied current is consumed by side reactions such as the decomposition of water at the anode

(Beukes and Badenhorst, 2009). Iron is the single most current consuming impurity because of its cyclic oxidation and reduction behaviour. Current efficiency is also affected by the electrolyte composition and other electrolyte properties as well as electrode type; the electrode should not get polarised as result of the electrochemical reactions taking place. A linear relationship exists between current efficiency and current density (CD). An increase in CD results in increased CE, however there is a limiting value of CD at which CE begins to drop due to the production of a loose cathode deposit with poor adherence. In practice electrowinning is done below this limiting value so at to produce good quality and compact deposits.

#### 2.2.2.6. Additives in copper electrowinning

Electrodeposit crystal growth requires the use of certain electrolyte additives. This is so because of the differences in the substrate and depositing metal crystallographic characteristics (Fabian, 2005). Commonly, chloride ions and organic compounds are added to the electrolyte in order to produce smooth, compact and void free copper cathodes. Chloride ions have been reported to influence cathodic processes through the formation of CuCl and a complex $CuCl_2^-$ (Ilgar and O'Keefe, 1997). Knuutila et al. (1987) reported that chloride ions are added to the electrolyte to act as grain refiners. According to Ettel and Tilak (1981) chloride ions are typically added in concentrations of between 20-30 mg/ℓ. The role of organic additives in electrodeposition is discussed in Section 2.4.4.

#### 2.2.2.7. Cathodes

The cathode is the negative terminal of the electrowinning cell; reduction and metal deposition takes place at the cathode. The copper cations in the electrolyte migrate to the cathode where they gain electrons and form metallic copper. Traditionally copper starting sheets have been used as cathode material; however development in electrometallurgy has seen the advent of reusable stainless steel blanks. Apart from being reusable, the permanent blanks are less labour intensive and allow for up to 10 % increase in current efficiency by

tolerating operations at high current densities while producing high purity copper. The size of the active surface area of the electrode is an important parameter in electrowinning as it has a bearing on the rates of metal deposition.

#### 2.2.2.8. Anodes

The use of lead anodes as positive terminals in the electrowinning of copper from acidified sulphate solutions has been in practice for decades and still remains the number one choice. Lead is preferred because it is inert and it has the capacity to form a stable and insoluble oxide ($PbO_2$) protective layer which regenerates when damaged and halts continued corrosion (Prengaman et al., 2010).

Lead is usually alloyed with other elements to improve its mechanical and structural properties so as to increase its life expectancy. Common alloying elements include tin, calcium and antimony. Cobalt is normally added to the electrolyte as cobalt sulphate which inhibits the corrosion of anodes by decreasing the oxygen evolution overpotential. The lead anode is inert and therefore there is no copper deposition at the anode, the only reaction taking place is the evolution of oxygen as shown by Equation 2.23.

## 2.3. Electrochemical techniques

A number of techniques exist which can be used to study electrochemical reactions. In this study cyclic voltammetry was used and as such the basic principles of voltammetry are discussed below as well as the technique of rotating disk electrodes.

### 2.3.1. Cyclic voltammetry

Cyclic voltammetry may be employed in investigating a number of electrochemical processes with little limitation. With this technique it is feasible to obtain information about the type of reaction taking place at the electrode and at what potentials they occur.

A three electrode system is mostly used employing a working electrode, a reference electrode and an auxiliary electrode (also known as counter or secondary electrode). In a standard cyclic voltammetry test, the current flowing through the working electrode is measured during a triangular potential sweep. The potential of the working electrode is initially held at a potential $E_i$ were no electrode reaction is likely to occur. The potential is then swept linearly between potentials $E_1$ and $E_2$ as shown in Figure 2.4 and the resultant current-potential graph is recorded. As the potential is swept in the negative direction towards the standard electrode potential, a cathodic current is observed as electrons begin to flow from the electrode into the solution effecting the reduction of any oxidised species at the surface of the electrode.

.

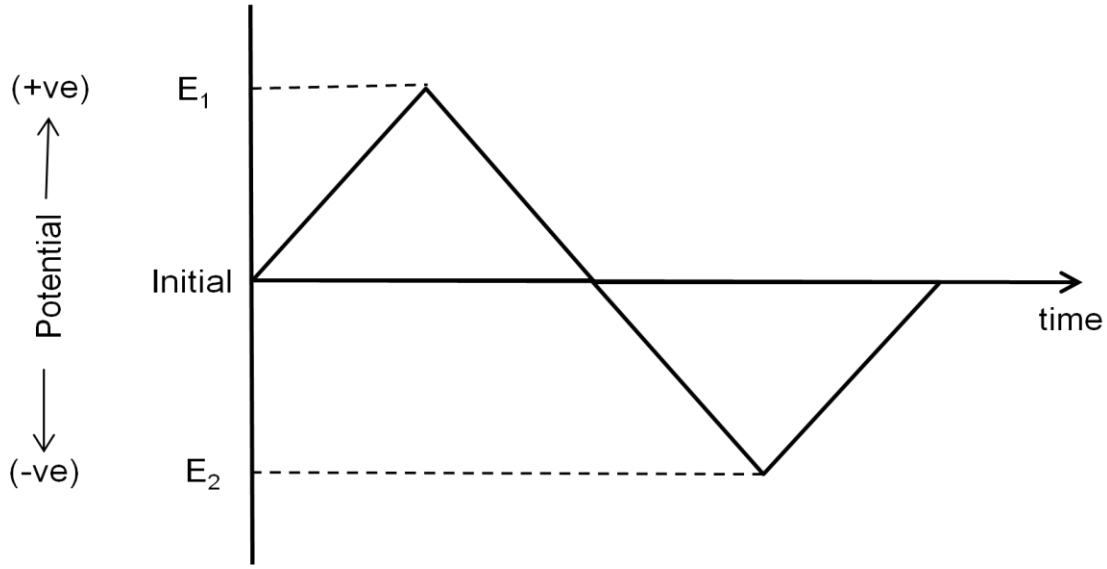


*Figure 2.4. Diagram showing the variation of potential during a standard cyclic voltammetry test*

During the cathodic sweep (towards negative potentials) the current is assigned a negative value while during the anodic sweep (increasing potential), the current is assigned a positive value. Cyclic voltammetry has been used by several researchers to study the electrochemical behaviour of copper at the working electrode during deposition in the presence and absence of thiourea (Muresan et

al., 2000; Fabricius et al., 1994; Gomez et al., 2009; Grujicic and Pesic, 2002; Safizadeh et al., 2011).

### 2.3.2. Rotating disk electrodes

The convective mass transport of electrochemical species in an electrochemical cell can be achieved through two different approaches. In the first approach solid electrodes are used and the electrolyte is allowed to flow on the surface of the electrode by means of an applied force. In the second approach the electrode is rotated and the rotating action of the electrode introduces convective currents in the electrolyte.

The rotating disk electrode assembly consists of a rotator and an electrode disk embedded in a shaft made out of non-conducting materials such as Polytetrafluoroethylene (PTFE). The rotator, together with the shaft, is coupled to a motor which drives the assembly by the application of an external electrical potential. The frequency of rotation $f$ in revolutions per second is known and is used in determining the angular velocity ($\omega$) as $\omega = 2\pi f$.

As the electrode rotates it drags the solution upwards and as a result of the centrifugal force created the solution is thrown radially outward as shown in the Figure 2.5 below (Nikolic et al., 2000). The rotation action of the RDE drags fresh electrolyte from the bulk solution to the electrode surface where it can react.

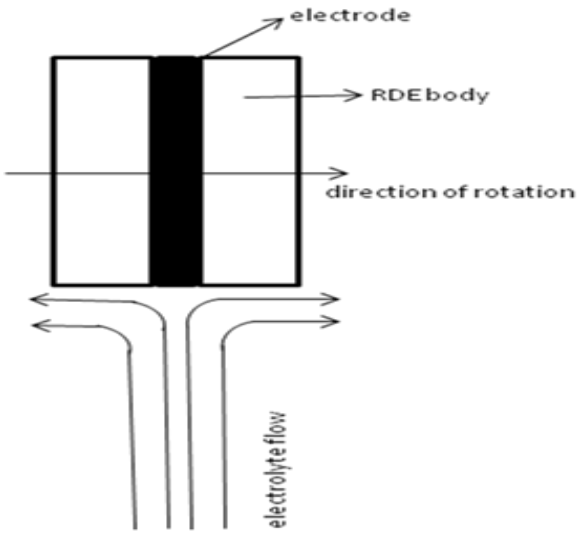


*Figure 2.5. Electrolyte flow pattern at a rotating disk electrode (after Nikolic et al., 2000)*

## 2.4. The chemistry of selenium and thiourea

### 2.4.1. Physical and chemical properties of selenium

Selenium (Se) with atomic number 34 is found in group 16 (Chalcogens) of the periodic table of elements. The properties of selenium are similar to those of Sulphur (S) and tellurium (Te) which are also in the same group on the periodic table. Tellurium is however known to be not as reactive as either selenium or sulphur but is more basic, more metallic and shows improved amphoteric inclination than selenium and sulphur. Elemental state selenium is allotropic and is insoluble in water.

The element selenium is known to exhibit variable oxidation states i.e. (-2), (+2), (+4) and (+6). The variable oxidation state of selenium is the main property that influences its solubility (Martens, 2003). The solution pH, temperature and redox conditions of the aqueous media in which its species are dissolved influences the valence state in which it will occur. It has been shown thermodynamically that $Se^{2-}$ (selenide) will most likely be found in strongly reducing environments and may exist as either an insoluble selenide of a metal or as $H_2Se$ gas, $Se^{+4}$(selenite) species in fairly oxidising environments and $Se^{6+}$(selenate) is mostly found in oxidising environments (Martens, 2003). The selenite ion is

known to be electro active than the selenate ion which shows less adsorption and precipitation capacities. Selenium is reduced by metals to yield ionic compounds with the $Se^{2-}$ ion present; it forms covalent bonds with other materials.

#### 2.4.1.1. Reduction chemistry of selenium

The existence of selenium in multiple oxidation states allows it to take part in various self-exchange reactions such as Se (+6)/Se (+4), Se (+4)/Se (0) Se (+4)/Se (-2) and Se (0)/Se (-2) (Saji and Lee, 2013). As already stated, the electrolyte conditions such as acidity and temperature will influence the type of species in which selenium will occur. Equation 2.27 to Equation 2.36 shows some of the important reactions with their standard electrode potentials (vs. SHE) for the electrochemistry of selenium (Saji and Lee, 2013).

$$H_2SeO_3 + 4H^+ + 4e^- \leftrightarrow Se + 3H_2O \qquad 0.740\ V \qquad (2.27)$$

$$HSeO_3^- + 5H^+ + 4e^- \leftrightarrow Se + 3H_2O \qquad 0.778V \qquad (2.28)$$

$$H_2SeO_3 + 6H^+ + 6e^- \leftrightarrow H_2Se + 3H_2O \qquad 0.360V \qquad (2.29)$$

$$HSeO_3^- + 6e^- + 7H^+ \leftrightarrow H_2Se + 3H_2O \qquad 0.386V \qquad (2.30)$$

$$SeO_4^{2-} + 4H^+ + 2e^- \leftrightarrow H_2SeO_3 + H_2O \qquad 1.150V \qquad (2.31)$$

$$SeO_4^{2-} + H_2O + 2e^- \leftrightarrow SeO_3^{2-} + 2OH^- \qquad -0.050V \qquad (2.32)$$

$$SeO_3^{2-} + 3H_2O + 4e^- \leftrightarrow Se + 6OH^- \qquad -0.366V \qquad (2.33)$$

$$SeO_3^{2-} + 6H^+ + 6e^- \leftrightarrow Se^{2-} + 3H_2O \qquad 0.276V \qquad (2.34)$$

$$Se + 2H^+ + 2e^- \leftrightarrow H_2Se \qquad -0.369V \qquad (2.35)$$

$$Se + 2e^- \leftrightarrow Se^{2-} \qquad -0.920V \qquad (2.36)$$

Various voltammetric investigations have shown that the reduction of selenium follows a two-step sequence, Se (+4) → Se (0) Se → (-2), with the reduction of Se (0) occurring at more negative potentials (Saji and Lee, 2013; Kowalik, 2014; Buffle and Haerdi, 1979; Lai et al., 2009). The reduction of selenite (+4) can either proceed by a 4 electron reaction, Equation 2.27 or a six electron reaction Equation 2.29 (Saji and Lee, 2013). The formation of $H_2Se$ gas has been reported to result into complex voltammograms during cyclic voltammetry tests. $H_2Se$ gas undergoes a chemical reaction with selenium according to Equation 2.37 .

$$H_2SeO_3 + 2H_2Se \leftrightarrow 3Se + 3H_2O \qquad 2.37$$

It has been reported that with relatively high concentrations of selenium Equation 2.37 is reported to exhibit fast reaction kinetics, and the overall selenium reduction process takes place according to Equation 2.27. Selenium is further reported to interact with metal electrodes as shown by Equation 2.38 (Saji and Lee, 2013).

$$nM + H_2SeO_3 + 4H^+ + 4e^- \leftrightarrow M_nSe + 3H_2O \qquad 2.38$$

Zuman and Somer (1999) further reported that metals such as nickel and copper can reduce selenium (IV) to yield $Se^{2-}$.

Lai et al., (2013) investigated the electrochemical behaviour of selenite using cyclic voltammetry. Three voltammetric peaks were observed, two cathodic and one anodic peak. The first cathodic peak was attributed to the 4 electron reduction of selenium according to Equation 2.27. The second cathodic peak was attributed to the six electron reduction of selenite to selenide according to Equation 2.29. The anodic peak observed was attributed to the oxidation of selenite to elemental selenium.

### 2.4.1.2. Selenium water system

Figure 2.6 shows the selenium water system at 25˚C. From the figure it can be deduced that selenium is thermodynamically stable in an aqueous environment throughout the entire pH range, this however only holds in the absence of any reducing or oxidising agent.

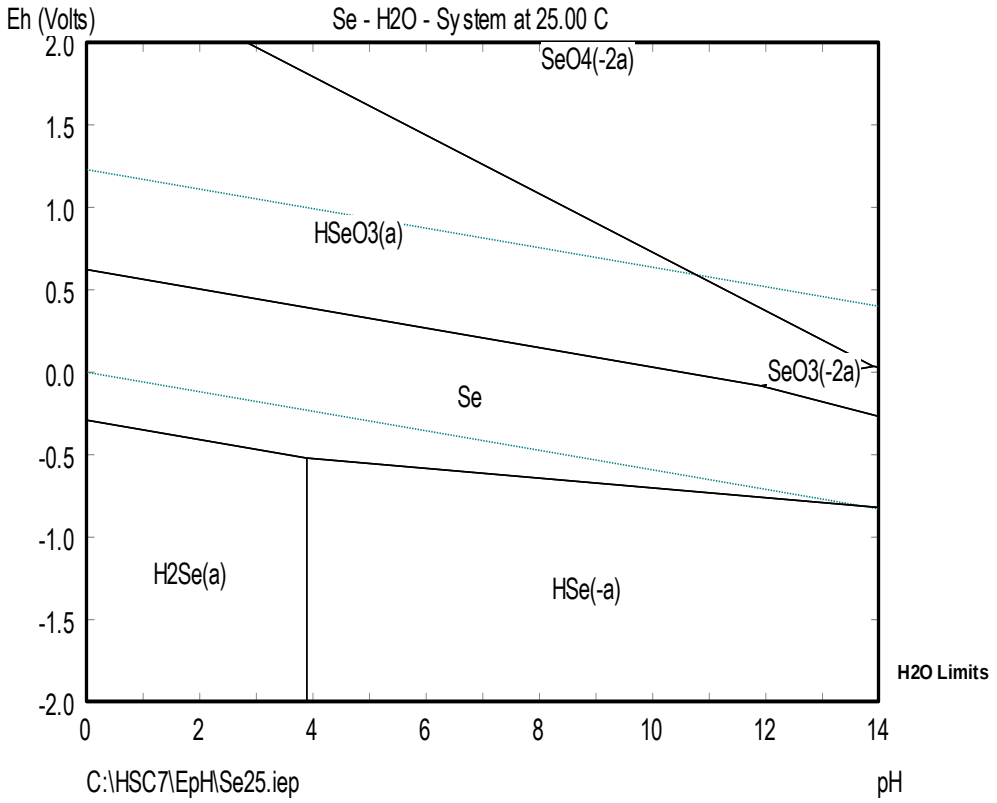


*Figure 2.6. Eh-pH diagram for the selenium water system at 25˚C (Using HSC chemistry 7.1)*

Selenium can be reduced to hydrogen selenide or other metal selenides as shown by Figure 2.6. These selenides are generally not stable in water and aqueous systems.Figure 2.6 further shows that selenium electrochemically oxidises to Selenous acid and other selenites in water and aqueous environments.

Saji and Lee (2013) reported that the solution acidity and the temperature influence the nature of dissolved selenium. They reported that in the presence of $SeO_2$ and $H^+$ in an aqueous solution, the following acid-base equilibria are established at 25°C;

$$H_2SeO_3 \leftrightarrow HSeO_3^- + H^+ \quad (pK_a = 2.72) \qquad 2.39$$

$$HSeO_3^- \leftrightarrow SeO_3^- + H^+ \quad (pK_a = 8.32) \qquad 2.40$$

In an aqueous solution containing cupric and cuprous ions, selenium forms copper selenide compounds (CuSe and $Cu_2Se$) which are stable over the entire pH range as is shown in Figure 2.7 below.`

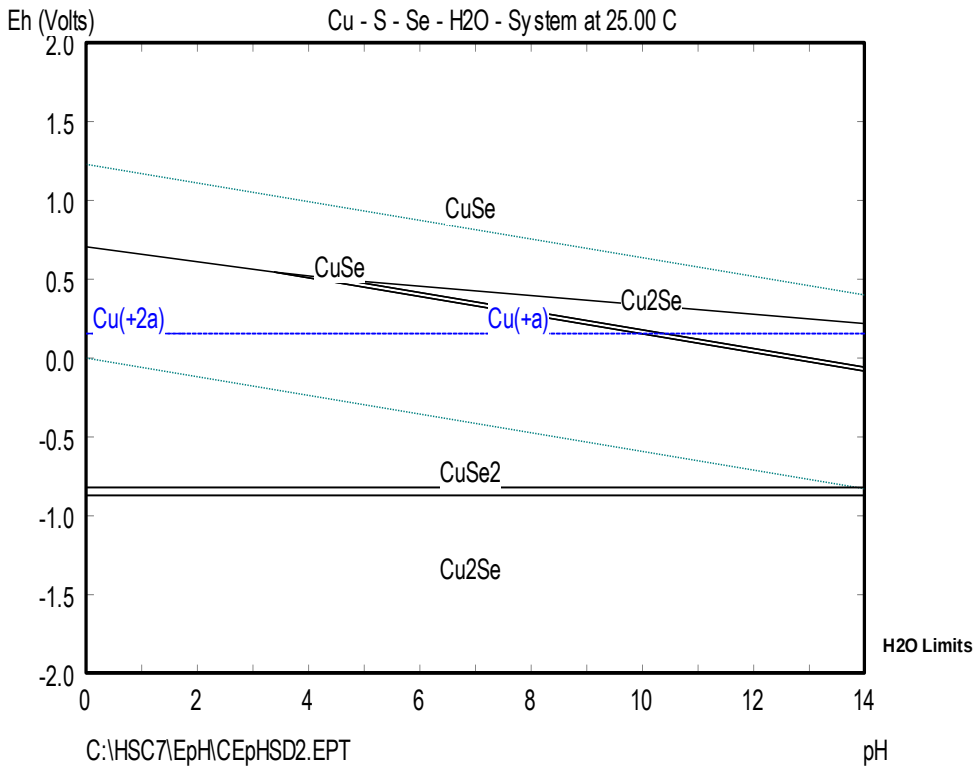


*Figure 2.7. Eh-pH diagram for the copper-sulphur-selenium-water system at 25°C (using HSC chemistry 7.1)*

## 2.4.2. Physical and chemical properties of thiourea

Thiourea or thiocarbamide is a white odourless organosulphur compound whose molecular formula is $CH_4N_2S$. It is soluble in water and exists in two tautomeric structures, the thione structure and the thiol structure.

The symmetric position that the two nitrogen atoms occupy in the thiourea molecule gives the hydrogen atom freedom to occupy three different positions. It is this property that allows thiourea to act as an electron donor and thus allowing it to form complexes with metals such as copper and nickel (Jin et al., 2002).

### 2.4.2.1. The chemistry of thiourea in $CuSO_4$ and $H_2SO_4$ system

In an acidic sulphate solution containing cuprous ions ($Cu^+$), three distinct cuprous-thiourea complexes are known to form. The concentration of cuprous ions and thiourea (Tu) in the copper sulphate solution determines the ratio of $Cu^+$ to Tu in these complexes. Piro et al. (1985) carried out a study on cuprous-thiourea complexes using X-ray diffraction methods, the three complexes identified were $[Cu_2(Tu)_6](SO_4)\cdot H_2O$, $[Cu_2(Tu)_5](SO_4)\cdot 3H_2O$ and $[Cu_4(Tu)_7](SO4)_2\cdot H_2O$. Piro et al. (1985) reported that the $Cu^+$—Tu complex exists in the form of a $Cu^+$ tetranuclear ion, $[Cu_4(Tu)_{12}]^{4+}$ located on a crystallographic inversion axis. The copper ions were observed to be in tetrahedral coordination with thiourea ligands.

Javet and Hintermann (1967) reported that at high concentrations of sulphuric acid thiourea forms a complex with cuprous ions according to Equation 2.41, this complex was reported to decompose gradually with time.

$$Cu^+ + Tu \overset{K_1}{\rightarrow} (CuTu) \overset{K_2}{\rightarrow} \text{degradation products} \qquad 2.41$$

Where, $K_1$ and $K_2$ are kinetic constants.

In an acidic copper sulphate solution with a pH range of between 1.5 and 3.8, Baub and Schiffner (1971) reported that a cuprous-thiourea complex is formed according to Equation 2.42

$$2(NH_2)_2CS + 2Cu^{2+} = {}^{NH_2}_{NH}\rangle C - S - S - C\langle {}^{NH_2}_{NH} + 2Cu^{+} + 2H^{+} \quad 2.42$$

According to Krzewska et al. (1980), cupric ions also react with thiourea as shown by Equation 2.43.

$$Cu^{2+} + (n+1)Tu \rightarrow [Cu(Tu)_n]^{+} + \frac{1}{2}[(NH_2)_2CSSC(NH_2)]^{2+} \quad 2.43$$

The researchers further reported that in the in the presence of cuprous ions, a relatively more stable complex is formed according to Equation 2.44.

$$Cu^{+} + nTu \rightarrow [Cu(Tu)_n]^{+}\ ;\ \beta_n = \frac{[Cu(Tu)_n]^{+}}{[Cu]^{+}[Tu]^{n}} \quad 2.44$$

With formation constants given as $\log\beta_1$ =10.2; $\log\beta_2$ = 13; $\log\beta_3$ = 15.9; $\log\beta_4$ =18.1 respectively for $Cu(Tu)_1^{+}$, $Cu(Tu)_2^{+}$, $Cu(Tu)_3^{+}$, $Cu(Tu)_4^{+}$. Ratajczak (1975) proposed that at high amounts of excess free thiourea, complexes from $[Cu_2(Tu)CSSC]^{2+}$ up to $Cu(Tu)_n^{+}$ are formed in a copper sulphate solution.

### 2.4.2.2. Oxidation of thiourea

According to Wang and O'Keefe (1984) cupric ions can oxidise thiourea to form formamidine disulfide (FDS) according to Equation 2.45.

$$2Cu^{2+} + 2(NH_2)_2CS \rightarrow 2Cu^{+} + (NH_2)_2(NH)_2C_2S_2 + 2H^{+} \quad 2.45$$

A reduction-oxidation couple is then established between thiourea and formamidine disulphide as shown in Equation 2.46.

$$2(NH_2)CS \leftrightarrow (NH_2)(NH_2)C_2S_2 + 2H^{+} + 2e^{-} \quad 2.46$$

The researchers also noted that formamidine disulphide can complex with cuprous ions to form [Cu (FDS)]$^{+}$, the formation of this complex is said to occur at low concentrations of thiourea. It was reported by the researchers that at high concentrations of thiourea [Cu (Tu)]$^{+}$ is formed with thiourea displacing the

formamidine disulphide. The formation of formamidine disulfide through the oxidation of thiourea has been reported by several other researchers (Gupta, 1963; Krzewska et al., 1980; Kuzeci and Kammel., 1989; Bolzan et al., 1999).

Kirchnerova and Purdy (1981) reported that in both acidic and neutral systems, thiourea is oxidised following a relatively slow, one electron reaction leading to the formation of a radical, $[(H_2N)_2CS^{\bullet}]^+$. The formation of this radical ion was also reported by Bolzan et al. (1999). The researchers stated that this radical ion reacts with similar ions in solution leading to the formation of formamidine disulphide in its cationic form, $[(NH_2)_2(NH_2)C_2S_2]^{2+}$.

Kuzeci and Kammel (1989) studied the behaviour of 0.1 M thiourea on a carbon paste electrode and reported that two oxidation peaks were observed, the first peak was attributed to the oxidation of thiourea to formamidine disulfide according to Equation 2.47. The second peak was attributed to the formation of thiourea oxides.

$$2CS(NH_2)_2 \rightarrow (NH)(NH_2)C - S - S - C(NH_2)(NH) + 2H^+ + 2e^- \qquad 2.47$$

Shevtsova et al. (2005) reported that at potentials higher than 0.9 V both thiourea and formamidine disulfide undergo complete oxidation forming carbon dioxide, cyanide containing ions, sulphate and sulphide ions. The researchers further stated that the sulphide ion is also generated during the steady decomposition of both thiourea and formamidine disulphide.

Quinet et al. (2009) reported the formation of cupric/cuprous-thiourea complexes according to the following reactions, Equation 2.48 to Equation 2.50 based on the concentrations of thiourea and formamidine disulfide (FDS);

$$Cu^+ + nTu \rightarrow [Cu(Tu)_n]^+ \qquad 2.48$$

$$Cu^+ + nFDS \rightarrow [Cu\,(FDS)_n]^+ \qquad 2.49$$

$$Cu^{2+} + nTu \rightarrow [Cu(Tu)_n]^{2+} \qquad 2.50$$

The three complexes are further reported to be reduced at the negative electrode as shown in Equation 2.51 to Equation 2.53.

$$[Cu(Tu)_n]^+ + e^- \rightarrow Cu^0 + nTu \quad 2.51$$

$$[Cu(FDS)_n]^+ + e^- \rightarrow Cu^0 + nFDS \quad 2.52$$

$$[Cu(Tu)_n]^{2+} + 2e^- \rightarrow Cu^0 + nTu \quad 2.53$$

### 2.4.3. Current practices in selenium precipitation from leach solutions

Selenium may pass readily into solution during the oxidative high pressure leaching of copper-nickel containing residues in base metal and platinum group metal (PGM) processing circuits. Because of its detrimental effects on electrowinning, the dissolved impurity must be sufficiently removed from the copper sulphate electrolyte before copper can be electrowon.

A number of reducing and precipitating agents have been studied, among them, cuprous ions, sulphur dioxide, titanium sulphate and thiourea. Thermodynamically, metals whose reduction potentials are lower than those of $Se^{4+}/Se^{6+}$ have the capability of reducing selenate/selenite to $Se^0$ or selenide (Martens, 2003).

#### 2.4.3.1. Selenium precipitation using cuprous ions

Cuprous ion is a well-known reducing agent and is applied in the precipitation of selenium as metallic selenides from copper sulphate solutions in acidic media. Industrially, plants that are known to use cuprous ion or copper powder in selenium removal from their electrolytes include Luili in the Democratic Republic of Congo (Charles et al., 1970), Vale in Sandbury Canada (Stewart et al., 1985), Naoshima's smelter and refinery in Kagawa Japan (Shibasaki et al., 1991) and Freeport's refinery in El Paso USA (Wang et al., 2003) .

The use of copper powder or cuprous ions is favoured over other reducing agents because copper does no introduce impurities into the copper electrowinning electrolyte and it is environmentally friendly as opposed to other reducing reagents such as sulphur dioxide and other metals cations. Charles et al. (1970) suggested that the reduction of selenious acid was not a direct reaction with copper metal but rather selenious acid was reduced by cuprous ions formed in the presence of cupric ions. The reduction rate of selenite to the lower oxidation states is significantly different from biselenate reduction rate to selenite using copper metal (Qin, 2007).

Bello (2014) identified two process routes as being available for the precipitation of selenium and tellurium from sulphate leach solutions. Bello (2014) suggested that Se and Te could be removed by use of sulphur dioxide alone or use of both sulphur dioxide and metallic copper. The researcher noted that the addition of copper powder improved the precipitation kinetics of tellurium.

#### 2.4.3.2. Selenium precipitation using sulphur dioxide

Sulphur dioxide is another reducing agent used in precipitating dissolved selenium and tellurium from acidic sulphide solutions. Weir et al. (1982) investigated the process of $Se^{4+}$ and $Se^{6+}$ removal using sulphur dioxide by injecting it into a pipe reactor through which a copper sulphate solution was being passed. The researchers suggested that for a solution containing both $Se^{4+}$ and $Se^{6+}$ ions, a 3:1 ratio ($Se^{4+}$:$Se^{6+}$) is required for successful reduction of $Se^{6+}$ ions to acceptably low levels. A test was carried out using a copper sulphate solution at pH 4, 60 g/ℓ cuprous ions, 33.3 mg/ℓ $Se^{4+}$ and 9 mg/ℓ $Se^{6+}$.Table 2.2 shows the results obtained at varying temperatures.

*Table 2.2: Results obtained from Se removal study (Weir et al., 1982)*

| Head Solution (mg/ℓ) | | Solution Temperature $^0$C | Final Solution (mg/ℓ) | | Precipitation Efficiency (%) | |
|---|---|---|---|---|---|---|
| $Se^{4+}$ | $Se^{6+}$ | | $Se^{4+}$ | $Se^{6+}$ | $Se^{4+}$ | $Se^{6+}$ |
| 33.3 | 9.0 | 25 | 0.25 | 0.26 | 99.2 | 97.1 |
| 33.3 | 9.0 | 50 | 0.30 | 0.46 | 99.0 | 94.8 |
| 33.3 | 9.0 | 100 | 0.30 | 0.75 | 99.0 | 91.7 |
| 33.3 | 9.0 | 125 | 0.30 | 1.34 | 99.0 | 85.4 |
| 33.3 | 9.0 | 150 | 0.35 | 2.10 | 98.9 | 76.4 |

From the results obtained, it was evident that both $Se^{4+}$ and $Se^{6+}$ were sufficiently removed from the solution by the use of sulphur dioxide. The researchers ascribed the achievement of these results to the absence of a discrete gaseous phase while the copper-bearing solution and selenium-reducing compound were passing through the tubular member.

### 2.4.3.3. Selenium precipitation using thiourea

Lottering et al. (2011) investigated the use of a number of reagents in selenium and tellurium removal, among them, thiourea, sulphur dioxide, formaldehyde, formic acid and sodium thiosulphate. The researchers showed that thiourea and sulphur dioxide were capable of removing a significant amount of dissolved selenium, up to 90 % selenium precipitation was achieved. Sulphur dioxide was however found to precipitate more tellurium than thiourea which exhibited poor tellurium precipitation characteristics.

Mulwanda (2014) also investigated the use of thiourea and sulphurous acid in the precipitation of dissolved PGMs (ruthenium, iridium and rhodium) from a sulphide leach solution which also contained dissolved selenium and tellurium. Thiourea was found to give better PGM recovery as compared to sulphurous acid. Thiourea was noted to give good reaction kinetics in the precipitation of ruthenium; approximately 100 % ruthenium precipitation was achievable within 20 minutes. Thiourea was also observed to precipitate out all the selenium from solution at all the temperature levels investigated. The researcher noted that

thiourea formed some sulphur containing species which exhibit fast reaction kinetics in metal precipitation. The concentrations of thiourea that gave promising results according the researcher were 200 % and 320 % excess taking into account the reaction of thiourea with ferric ions present in the electrolyte.

### 2.4.4. Effects of organic additives on copper electrowinning

The use of organic additives is an essential step in the copper electrowinning process as these additives are known to influence nucleation and crystal growth during the initial stages of electro-crystallisation. Organic additives are also known to influence electrode kinetics, this results in controlled physical and mechanical properties of the deposits. In the absence organic additives, the nucleation process is often said to be instantaneous resulting in rough and granular deposits. This is so because nucleation occurs relatively fast on a small number of nucleation centres formed instantaneously. Organic additives on the other hand promote progressive nucleation taking place on a large nuclear number density resulting in smooth deposits (Fabricius et al., 1994). The additives are able to alter the electrode kinetics and in turn the deposition characteristics when added in small amounts (mg/ℓ).

#### 2.4.4.1. Classification of organic additives

Additives in electrodeposition may be categorised based on the effect that a particular type of additive will have on the deposit. The categories of additives are known, namely levellers, brighteners and carriers.

##### 2.4.4.1.1. Levelers

Levelling is the controlled surface diminution in the surface roughness as metal electrodeposition proceeds. Metal deposition in the micro recesses is favoured over deposition on the peaks. Levelling can be categorised as either geometric levelling or electrochemical levelling also known as true levelling. Electrochemical levelling is known to proceed in the presence of additives as there is increased current density in the micro recesses as opposed to the peaks.

This is so because additive adsorption on the micro peaks takes effect. Geometric levelling occurs as a result of a uniform current density on the electrode surface. According to Täubert (2006) organic additives which contain the thiocarbamide group [-C(S)-NH-] like thiourea and its derivatives are known to act as levelling agents in acidified copper sulphate solutions.

#### 2.4.4.1.2. Brighteners

The brightness of a deposit surface can be defined as its optical reflecting power. Brightening occurs in fine grained deposits with wave length of less 0.4 µm (less the wave length of visible light). The three mechanisms which promote the formation of bright deposits are, diffusion controlled levelling, grain refining and random progression of crystal growth. Compounds that act as brighteners include organic sulphides, disulphides and thiocarbamates.

#### 2.4.4.1.3. Carriers

These are compounds containing oxygen with molecular weights of between 1000 and 20000 g/mol (high molecular weight compounds). Carriers enhance the performance of other additives present in the electrolyte. However, carriers are also known to produce fine grained and bright deposits when used on their own.

### 2.4.4.2. Action mechanism of organic additives

The mechanisms by which organic additives influence the nucleation process include the capability to adsorb on the cathodic substrate and even get trapped in the deposit. The use of organic additives has found wide spread application in copper electrowinning chiefly because of their ability to act as levelling and brightening agents. More often than not most of these additives will act as either a levelling agent or a brightening agent or can perform both functions as in the case of thiourea. The levelling action is said to be governed by two theories; (i) the adsorption theory and (ii) the diffusion theory (Gale, 1972). The adsorption theory suggests that the electrode will favour the adsorption of the additive on micro peaks of a rough electrode, such that inhibition of cation deposition on

such areas occurs as well as current density thus increasing the deposition in the micro recesses. The rapid consumption and occlusion of the additives is known to account for the diffusion theory. It was further suggested by Winand (1992) that organic additives are either chemically or physically adsorbed on the electrode surface and they tend to cover the electrode active sites rather than covering the entire cathode surface.

According to Habashi (1998) the additives also inhibit the cathodic reaction by being adsorbed on the cathode substrate thus resulting in increased cathodic reaction overpotential. Habashi (1998) noted that a high cathodic overpotential eased the nucleation process and inhibited the formation of large crystallites.

Hasegawa (2007) also reported that the adsorption additives lead to the formation of an adsorption layer, which then alters the deposition overpotential. The researcher also reported the formation of complexes between the additives and metal ions which alter the reaction overpotential.

Varvara et al. (2000) reported the probable action mechanisms for some individual additives (thiourea, gelatine and polyacrylamides). Gelatine and polyacrylamides were reported to influence mass transport as they are thought to form a thick layer in the vicinity of the electrode. Thiourea is understood to act upon charge transfer in two different ways, either through $S^{2-}$ generation and subsequent formation of a sparingly soluble CuS precipitate or through the formation of adsorbed $[Cu\ (tu)_n]^+$ complexes which participate in blocking of the electrode active sites. It was also suggested that in the presence of thiourea the formation of new nuclei is highly favoured as opposed to promoting the growth of already existing copper crystals, this phenomenon results in fine grained deposits. Quinet et al. (2009) also reported the formation of strong bonds between the sulphur atom in thiourea and copper ions.

Yu et al. (2007) reported that thiourea is capable of forming two different compounds with copper ions. The researchers suggested that thiourea forms $Cu_2S$ and a complex $[Cu\ (N_2H_4CS_2)_4]_2SO_4$ in the vicinity of the cathode or indeed

on the cathode surface itself. The formation of the compound $Cu_2S$ was reported to result into an increased number of active sites.

The organic additives are also known to inhibit cation movement in the electric double layer. Vereecken and Winand (1976) suggested that additives interact with water molecules in the electric double layer leading to the formation of a layer with a high viscosity near the cathode substrate. Stankovic and Vukovic (1996) reported that thiourea molecules displace the water molecules thereby altering the composition of the electric double layer where electron transfer is known to occur, as discussed in Section 2.2.1. According to Stankovic and Vukovic (1996), once additives such as thiourea are adsorbed, it becomes increasingly difficult for the hydrated metal ion to reach the double layer where charge transfer occurs and subsequent incorporation of the ion into the metal lattice. The metal ions have to force their passage through the layer of adsorbed molecules for them to reach the surface of the electrode.

Farndon et al. (1995) proposed two mechanisms through which thiourea acts on the cathodic processes during metal deposition. They reported that in the first mechanism thiourea either under goes hydrolysis or is reduced according to Equation 2.54 and Equation 2.55 respectively.

$$H_2NCSNH_2 + H_2O \rightarrow H_2NCONH_2 + H_2S \qquad 2.54$$

$$H_2NCSNH_2 + 2H^+ + 2e^- \rightarrow NH_4CN + H_2S \qquad 2.55$$

According to the researchers, the $H_2S$ which is formed as shown in Equation 2.54 and Equation 2.55 reacts with copper ions to produce CuS. The CuS formed has a low solubility product ($8 \times 10^{-37}$) thus it precipitates out of solution and covers some active sites on the electrode surface leading to inhibition of cathodic processes. In the second mechanism it was suggested that thiourea forms complexes with cupric ions as follows:

In solution:

$$2Cu^{2+} + 2H_2NCSNH_2 \rightarrow 2Cu^{+} + [-SC(=NH)NH_2]_2 + 2H^{+} \quad 2.56$$

On the cathode:

$$2Cu^{2+} + nH_2NCSSNH_2 \rightarrow Cu^{+}(H_2NCSNH_2)_n \quad 2.57$$

$$Cu^{+}(H_2NCSNH_2)_n + e^{-} \rightarrow Cu + nH_2NCSNH_2 \quad 2.58$$

The researchers proposed that at low concentrations thiourea is adsorbed as $CuSCNH_2$ (=NH) and at higher concentrations it is adsorbed as $Cu^{+}(H_2NCSNH_2)_n$.

Fischer (1954) suggested that inhibition occurs as a result of the presence of substances other than the metal ion, $Mn^{+}$, on the surface of the electrode, in the electric double layer or indeed in the diffusion layer. The researcher further suggested four possible outcomes of inhibition on the cathodic reaction as follows;

- A simultaneous reduction of the inhibitor causing a drop in the cathodic current required for the reduction of metal ions and hence a drop in the current efficiency. Reduction of the inhibitor may also result in the contamination of the deposit as a result of the decomposition of the residues of the inhibitor molecule.
- A negative catalytic effect of a pre or post reaction, resulting into an induced reaction overvoltage.
- Changes in the crystallographic orientation and metallographic properties of the deposits.
- Shift in the values of the various overvoltages.

### 2.4.4.3. Adsorption of additives during deposition

In order that the behaviour of the surface active additives is fully understood, an understanding of the adsorption mechanism at the electrode-electrolyte interface

is required. As has been discussed in Section 2.4.4.2, adsorption is one of the mechanisms through which additives influence cathodic reactions. However accurate quantitative determination of the adsorption of organic additives has proved to be challenging as highly sensitive electro-analytical techniques are needed to be able to detect the low concentrations of these additives in the electrolyte (Gale, 1972).Some techniques may be sensitive enough to be able to detect relatively small quantities of adsorbed additives but these often rely on the electrolytic reduction of the additive. It follows therefore that in an electrolyte containing metal ions; it becomes increasingly difficult to distinguish between faradaic metal ion reduction and additive reduction.

Organic additives may be physically or chemically adsorbed on the electrode. Täubert (2006) suggested that the energy of the adsorbate (additive) and that of the surface has an influence on whether chemisorption (chemical adsorption) or physisorption (physical adsorption) occurs. When chemisorption occurs, a chemical bond is formed between the adsorbate and the surface. The bonds formed are usually covalent bonds. Van der Waals forces and electrostatic forces are responsible for physisorption. Loutfy (1971) proposed that surface active additives are adsorbed at an interface as a result of a decrease in their free energy due to either an increase in the bonding energy at the interface or because the free energy at the interface is lower than in the bulk electrolyte. The adsorbability of an additive is highly dependent on its solubility. It is generally accepted that adsorbability increases with decreasing additive solubility (Loutfy, 1971).

Bockris et al. (1998) stated that when organic additives are physically adsorbed on the electrode, their chemical structure remains unchanged. They reported that the bond existing between molecules of the organic compound and the electrode are relatively weak and the adsorbed molecules engage in an exchange with similar molecules in solution as shown by Equation 2.59.This form of organic molecule adsorption is said to be reversible.

$$[\text{Organic}]_{\text{solution}} \leftrightarrow [\text{Organic}]_{\text{adsorbed}} \qquad 2.59$$

The researchers stated that when additives are physically adsorbed, there is no charge transfer between the additive molecules and the substrate. This renders adsorption process as an almost zero current process as depicted in Figure 2.8.

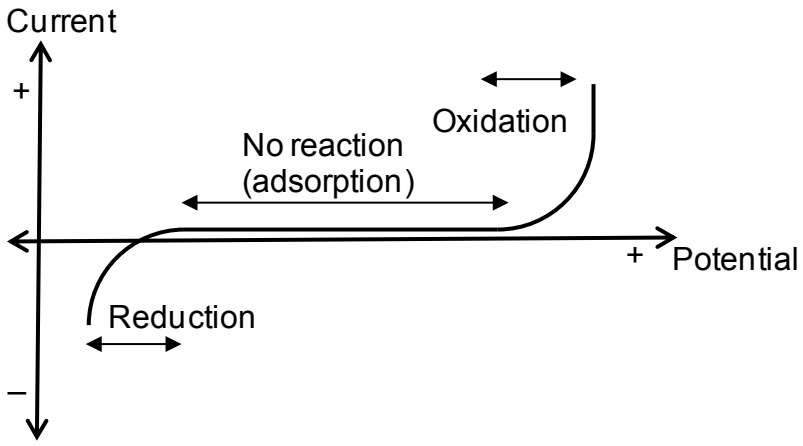


*Figure 2.8.A current-potential profile for additive adsorption on the electrode (after Bockris et al., 1998)*

In chemisorption a charge transfer reaction involving the organic molecule and the electrode surface may occur forming new species which might then be adsorbed on the electrode. A chemisorption reaction maybe written as shown by Equation 2.60, such reactions are not reversible (Bockris et al., 1998).

$$[\text{Organic A}]_{\text{solution}} \xrightarrow{\text{charge transfer}} [\text{Organic B}]_{\text{adsorbed}} \qquad 2.60$$

The amount of molecule adsorbed on the electrode is given in terms of coverage $\Theta$. Coverage defines the fraction of the electrode covered by the additive molecules. The coverage, $\Theta$, is related to the concentration of the additive $c^b$ in the bulk solution. The relationship between $\Theta$ and $c^b$ is described by adsorption isotherms like the Langmuir adsorption isotherm model. This model assumes that N sites exist on the adsorbent of which $N_0$ are unoccupied and $N_1$ are occupied by the additive. It follows therefore that the surface coverage is defined as shown in Equation 2.61

$$\theta = \frac{N_1}{N} \qquad 2.61$$

The Langmuir adsorption isotherm model is defined as shown by Equation 2.62

$$\theta = \frac{Kc^b}{(1 + Kc^b)} \qquad 2.62$$

In applying the Langmuir isotherm it is assumed that at all the available active sites the adsorption energy is not affected by adsorption taking place at nearby sites (Täubert, 2006).

If adsorption takes place by additive molecule dissociation, the Langmuir isotherm takes a new from as according to Equation 2.63.

$$\theta = \frac{K\left(c^b\right)^{\frac{1}{n}}}{1 + K(c^b)^{\frac{1}{n}}} \qquad 2.63$$

Where n is the number of fragments into which the additive molecule has dissociated.

If adsorption takes place on a number of m sites without dissociation, the Langmuir isotherm becomes

$$\frac{\theta}{(1-\theta)^m} = Kc^b \qquad 2.64$$

#### 2.4.4.4. Effect of organic additives on the cathode overpotential

As stated in Section 2.1.3 the degree of deviation away from the equilibrium electrode potential is known as overpotential. The addition of organic additives to the electrolyte results in an increase in the overpotential. It is generally accepted that the overpotential increases as a result of the adsorption of the additive on the electrode surface.

According to Loutfy (1971) the overpotential increases due to the partial blocking of the electrode causing an increase in the current density on the area of the electrode left uncovered. The researcher suggested that if a fraction $\Theta$ of the electrode is covered by the adsorbed additive, the true current density acting on the uncovered surface of the electrode increases from *i* to *i*/(1-$\Theta$).

The true current density in the presence of additives (*i*') is then related to the true current density in the absence additives (*i*) as given in Equation 2.65

$$i' = \frac{i}{(1-\theta)} \qquad 2.65$$

The relationship between the overpotential, η', in the presence of additives and the true current density, i', is shown by Equation 2.66 and is valid only when the reaction rate is charge transfer controlled.

$$\eta' = a + b\ln\frac{i}{(1-\theta)} \qquad 2.66$$

The overpotential in the absence of additives is define by Equation 2.67.

$$\eta = a + b\ln i \qquad 2.67$$

It follows therefore that the increment in the overpotential caused by the coverage of a fraction, $\Theta$, of the electrode is obtained by subtracting Equation 2.66 and Equation 2.67 to give Equation 2.68

$$\Delta\eta = b\ln\frac{1}{(1-\theta)} \qquad 2.68$$

Equation 2.68 remains valid only when the adsorption of additives occurs randomly and their role is largely to act as an inert layer on the electrode.

#### 2.4.4.5. Key findings from previous investigations on the effects of thiourea on copper deposition

Copper cathodes produced in the presence of organic additives are generally of superior quality. They tend to have smooth surfaces, are void free, non-porous and their morphology is usually layered rather than columnar with small crystals thus resulting in reduced dendritic growth.

Guar gum the industry standard organic additive has been used in copper electrowinning as a brightener for many years and is generally dosed within ranges of 0.25 – 5 mg/ℓ.

Vereecken and Winand (1976) investigated the influence of anionic and ionic polyacrylamides (PAM) on cathode quality in comparison with the already known guar gum. The experimental work was carried out using an industrial copper sulphate solution ($Cu^{2+}$ 50 g/ℓ, $Mn^{2+}$ 10 g/ℓ, $Mg^{+}$ 4 g/ℓ, $Co^{2+}$ 1.5 g/ℓ and $H_2SO_4$ 50 g/ℓ).

It was established from that work that both anionic and ionic polyacrylamides gave smooth copper cathodes, with the cationic PAM being superior to the anionic PAM. The polyacrylamides were found to have no influence on the current efficiency and texture orientation of the cathodes. The researchers further noted that the additives were not incorporated in the deposit as the carbon levels in the deposits remained relatively low (< 0.05 mg/ℓ). However, in comparison to guar, PAM was found to be inferior. The actual dosages for both guar and PAM that were used in this test work were not given.

The need for further improvement of the quality of copper, especially for use in the electronic industry has resulted into continued research in the use of additives to produce high quality copper cathodes.

The use of thiourea as an additive in copper electrodeposition has been explored by various researchers because of its capability to act as a brightening as well as a levelling agent. The stable complexes that thiourea is known to form with copper ions inhibit the surface diffusion of adsorbed ions (adions) by blocking the

active sites on the electrode (Quinet et al., 2009). As a result of electrode active site coverage, growth at the active site is inhibited and becomes more pronounced in the recessed areas effecting levelling.

Kang et al. (2007) investigated the effects of thiourea on the deposition of copper from an electrolyte containing 0.5 M copper sulphate, 1 M sulphuric acid, deionised water and thiourea. It was established that smooth and bright deposits were obtainable even at low levels of thiourea. Atomic force microscopy images were used in these studies to determine the grain densities of the deposits produced with 0.083 g/ℓ thiourea and those produced in the absence of thiourea. It was found that deposits formed in a thiourea containing solution (0.083 g/ℓ) gave a grain density of 310 /μm$^2$ while for the thiourea free deposit a grain density of 44 /μm$^2$ was obtained. The formation of deposits with high grain densities in the presence of thiourea was also observed by (Quinet et al., 2009) in their studies. The high grain density obtained in the presence of thiourea was attributed to the inhibition of lateral grain growth and development of large grains. This inhibition action of thiourea was also reported by Krzewska et al. (1984).Formation of smooth deposits in the presence of thiourea is as a result of the inhibition of large grain formation and promotion of the formation of finer grained deposits. It has been suggested in some sections of literature that thiourea slows down crystal growth as a result of its adsorption which blocks the active sites on the cathode.

Kao et al. (2004) also reported the formation of fine grained deposits in the presence of thiourea. They observed that the grain size reduces as thiourea concentration increases as shown in Figure 2.9.

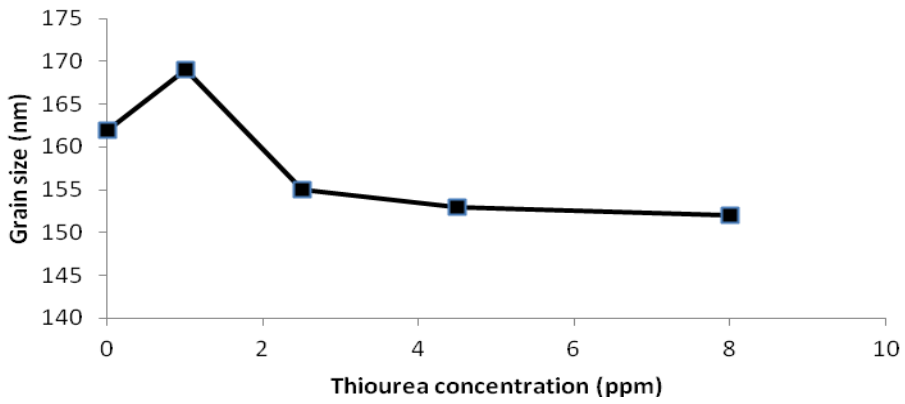


*Figure 2.9. Grain size variation as a function thiourea concentration (after Kao et al., 2004)*

Kang et al. (2007) analysed deposits obtained in the presence of thiourea (using X-ray photoelectron spectroscopy (XPS) and Auger electron spectroscopy) and found that only sulphur was incorporated in the deposit while nitrogen and carbon were only found in trace amounts. According to the researchers, the identification of sulphur in the deposit signified that the adsorbed compound was CuS and not thiourea itself. The researchers further suggested that the inhibition of the surface diffusion of copper adions leading to formation of smooth copper deposits was as a result of the formation of copper sulphide species.

The presence of sulphur, nitrogen and carbon in electrodeposits was also reported by Quinet et al. (2009). The researchers reported that XSP analysis of the deposits obtained in their study showed that sulphur, nitrogen and carbon were present in the deposit. They ascribed the presence of these three elements to the formation of Cu-S-C bonds between thiourea and copper ions. Kao et al. (2004) also reported the presence of sulphur in deposits produced in the presence of thiourea. They reported that a number of spherical particles were observed in the deposits and an energy dispersive x-ray spectroscopy spot analysis of such particles revealed that the particles were mostly composed of copper and sulphur. The researchers further reported that the size of particles increased proportionally with increase in thiourea concentration.

Fabricius et al. (1994) noted that a relatively high number of nuclear densities for smooth deposit formation were obtainable at thiourea concentrations of 10 ppm. At high thiourea concentrations the researchers suggested that the nucleation process was disturbed by the relatively high thiourea-copper complexes adsorbed on the cathode substrate. The researchers further observed that a second anodic peak was encountered during cyclic voltammetry tests. This second anodic peak was ascribed to the dissolution of copper-thiourea complexes. The thiourea concentrations investigated in this work were 0,1,10,100 and 1000 mg/ℓ.

The effects of plating mode employed and the presence of additives in the electrolyte were investigated by Tantavichet and Pritzker (2004). The two modes of plating investigated were the pulse current (PC) and the tradition direct current (DC) method. The use of PC is known to improve copper morphology as compared to DC use even in the absence of additives. PC improves the cation mass transfer, electrode reaction kinetics and the nucleation process thus resulting into production of compact deposits. The two additives that were used in the study were thiourea and chloride ions. The tests were conducted using an acidic sulphate solution, 0.1 M $Cu_2SO_4$ and 1 M $H_2SO_4$, a rotating disk electrode (with 500 rpm speed of rotation), current density of 4 $Adm^{-2}$ for 12 minutes.

The deposits obtained using DC with no additives were observed to be dull with a 38 % reflectance (measure of smoothness). In the presence of 10 mg/ℓ HCl, an even poorer deposit was obtained with only 2 % reflectance. The addition of 20 µM thiourea resulted in improved deposit quality with an 83 % reflectance. This was as expected as thiourea is known to improve deposit morphology as it inhibits large grain formation in preference to the generation of fine grains which is responsible for deposit surface smoothness and brightness. Despite the relatively improved smoothness and brightness, the deposit was observed to exhibit a relatively high micro roughness (>2283 Å). This was attributed to the formation of nodules despite the presence of thiourea, the formation of nodules was also reported in later works by Tantavichet et al. (2009).

According to Alodan and Smyrl (1998) thiourea does not take part in the electrochemical reactions occurring at the electrode, thus the researchers concluded that thiourea has no effect on the current efficiency. This is based on the studies they carried out using a rotating disk electrode (RDE) and thiourea concentrations of 0.5,1,3 and 6 mM in a 0.5 M copper sulphate and 1 M sulphuric acid solution. The researchers also found that thiourea was not incorporated in the deposit. This conclusion is however inconsistent with conclusions made by Tadesse et al. (2013). Tadesse et al. (2013) detected the presence of sulphur and nitrogen in the copper deposits formed in the presence of thiourea. The researchers reported that the sulphur could be as a result of the formation of CuS at the surface of the deposit. The presence of nitrogen was ascribed to possible nitrogen-copper (N-Cu) interactions. The researchers stated that such observations could be as a result of the formation of strong chemical bonds between thiourea and copper or possible incorporation of thiourea in the metal lattice.

Tantavichet et al. (2009) reported that the electrodeposition of copper from a solution containing thiourea required increased polarisation compared to an additive free solution. The researchers ascribed this to the generation of complexes between thiourea, cupric and cuprous ions. A further observation of a decrease in current density was made; current was thought to decrease because of the blocking of the nucleation areas by thiourea. Ntengwe et al. (2010) reported that high thiourea concentrations impede smooth current flow resulting in low current densities. A similar conclusion was made by Tantavichet et al. (2009). According to Goffman and Jordan (1985) addition of excess amounts of thiourea to electrorefining electrolytes results in the formation of cathode deposits with parallel grooves or bands on the surface and may result in the entrapment of sulphur.

Manu and Jayakrishnan (2009) reported in their studies using poly-ethylene glycol (PEG) and chloride ions that organic additives polarised the electrode surface, it was observed in their work that the voltage in the electrolyte

containing PEG increased in the initial stages of deposition as compared to an additive free electrolyte. The researchers attributed this to the adsorption of the organic additive on the electrode surface.

Muresan et al. (2000) investigated the effects of different additives on the morphology and cathodic reduction of copper. The additives investigated included thiourea, horse-chestnut extract (HCE) and IT-85 (ethoxyacetic alcohol and triethyl-benzyl ammonium chloride mixture). The researchers' performed cyclic voltammetry tests as well as electrowinning tests using a copper rotating disc electrode as the working electrode. The voltammograms obtained in these studies showed that the cathodic peak was shifted to more negative values with a corresponding reduction in its area. The researchers reported that the greatest inhibition of the cathodic reaction was observed in the presence of thiourea followed by IT-85. The morphology of the deposits obtained in these studies revealed that fine grained deposits were obtained in the presence of thiourea. It was concluded that the action of thiourea was that of inhibition of the electro crystallisation process as a result of the retardation of the crystal growth process.

### 2.4.5. Effects of selenium and other dissolved impurities on electrowinning

Copper in its pure form finds wide application in sectors such as electrification, electronics and telecommunications. The need to use copper of certain purity comes about because of the desire to take advantage of some inherent properties that copper has in its pure form; as an example, in electrical applications the high conductivity of copper and its ability to be drawn into wires are important properties that cannot be done away with. The presence of impurities such as selenium and tellurium affects the conductivity and annealability of copper. These and other impurities pass into solution during the actual leaching of copper from its ores. The recycling of the cell house spent electrolyte to either the solvent extraction plant or the head of the circuit results in a build up of these impurities in the electrolyte especially for plants which do not have a clearly defined electrolyte bleed system.

Impurities in electrowinning electrolytes include iron, lead, sulphur, manganese, cobalt, zinc, selenium and tellurium. These impurities can affect copper electrowinning in different ways such as altering the physicochemical properties of the electrolyte, taking part in side reactions thus consuming part of the electrowinning current, occlusion or even co-deposition into the copper cathode. The dissolved impurities also have an impact on the electrode kinetics and processes.

Subbaiah and Das (1994) investigated the effects of some impurity metal cations ($Fe^{2+}$,$Fe^{3+}$,$Ni^{2+}$,$Co^{2+}$ and $Mn^{2+}$) on copper electrodeposition and mass transfer coefficient. It was established that the physicochemical properties of the electrolyte were affected in a similar manner, in the presence of ferrous and ferric ions. The electrolyte viscosity and density were observed to increase while the conductivity dropped. Similar observations were also made in the presence of manganese, nickel and cobalt. The changes in the physicochemical properties (viscosity and density) resulted in a drop in the limiting current density and mass transfer coefficient. This in turn resulted in increased power consumption.

Iron is known to adversely affect cathode current through its ionic species ferrous and ferric ions. Ferric ions when present at high concentrations in the electrolyte lower the current efficiency through Equation 2.69.

$$Fe^{3+} + e^{-} \rightarrow Fe^{2+} \qquad E^{0} = +0.77V \qquad 2.69$$

The generated ferrous ion ($Fe^{2+}$) will then get reoxidised to ferric ion by dissolved oxygen generated from the anodic reaction. The generation of ferrous ions and regeneration of ferric ions then becomes recurring, and as such results in a reduced cathode current efficiency. This is so because the reduction of ferric ion according to Equation 2.69 above consumes part of the cathode current. The ferric ions are also known to attack cathode loops according to Equation 2.70.

$$2Fe^{3+} + Cu^{0} \rightarrow 2Fe^{2+} + Cu^{2+} \qquad E^{0} = +0.33V \qquad 2.70$$

This reaction occurs at the solution line and results in cathode drops once the loops are corroded (Biswas and Davenport, 1976). To avoid cathode drops most electrowinning tank houses using the conventional copper starter sheet technology have to harvest their cathodes at relatively low weights (40- 70 kg) compared to electrorefining (100-150 kg) (Biswas and Davenport, 1976). Ferric iron is also known to have detrimental effects on the deposit morphology as a result of its etching effect on the deposit (Arman et al., 2012).

The use of lead alloys as material of construction for anodes is widely practised in most copper electrowinning plants as lead is known be inert and does not easily corrode in sulphuric acid environments. However the ''inert'' lead anodes are found to degrade with time by the oxidation of the surface to lead sulphate and lead oxide. The lead oxide forms a thin film on the lead surface which flakes off resulting in electrolyte and cathode copper contamination. The lead particles get occluded in the cathode product which may affect its annealing properties. The particles are also known to cause short circuits by acting as sites for initiation of dendritic growth. A loss in current efficiency is experienced as a result of these short circuits.

The protective layer formed on the lead is also attacked by dissolved impurities such as manganese. Manganese is entrained in the organic phase as $Mn^{2+}$ during pregnant liquor purification by solvent extraction. It finds its way to the stripping side through entrainment and eventually into the electrowinning tankhouse. $Mn^{2+}$ is a very stable manganese species in sulphuric acid solutions (Cheng et al., 2000). It is oxidised to higher oxidation states at the anode ($Mn^{3+}$ and $MnO_4^-$). The permanganate ion $MnO_4^-$ is a very strong oxidant which attacks the thin protective oxide film on the lead anode surface, this leads to increased anode corrosion rates and results high lead concentration in the electrolyte and subsequent deposit contamination (Cheng et al., 2000). The detrimental effects of manganese were also confirmed by Prengaman et al. (2010). The researchers suggested that manganese attacks the anode as shown by Equation 2.71.

$$Mn^{2+} + PbO_2 + H_2SO_4 \rightarrow MnO_2 + PbSO_4 + 2H^+ \quad 2.71$$

The $PbSO_4$ formed by according to Equation 2.71 converts back to $PbO_2$; this process of reconversion affects the structural stability of the film oxide on the anode surface by making it soft, less adherent and prone to shedding off. Contrasting findings were however earlier reported by Jeffers and Groves (1985). In their investigations the researchers looked at how cathode copper contamination by lead could be mitigated. The following metal ions were used as impurities, magnesium 4.5 g/ℓ, manganese 1.4 g/ℓ, iron 2.8 g/ℓ, aluminium 1.9 g/ℓ and chloride 0.05 g/ℓ in an electrolyte containing 30 g/ℓ copper, 150 g/ℓ sulphuric acid and 100 mg/ℓ cobalt. The results obtained revealed that manganese had no effect on electrowinning; furthermore the lead anode used remained unaffected in the presence of manganese. Only chloride ions were found to accelerate the anode corrosion rate and subsequent contamination of the cathode.

Other impurities such as arsenic and bismuth affect copper deposit properties even when present in minor amounts, a 0.1 % presence of arsenic in the deposit effects its conductivity while bismuth of as low as 0.001 % will result in the deposit being brittle. (Lynch et al., 1991)

Selenium dissolves in leach solution as tetravalent and hexavalent ions and enters the electrowinning tank house if not removed from the electrolyte. Selenium is known to be deleterious in the copper wire cold drawing process (Moskalyk et al., 1998).

Baral et al. (2014) conducted a study on the effects of selenium on the electrodeposition of copper from a sulphate aqueous electrolyte solution. Selenium (as $Na_2SeO_3$) was used as an impurity in the electrolyte and the concentrations studied ranged from 0 to 1000 g/dm$^3$. It was reported from these studies that selenium at concentrations higher than 50 g/dm$^3$ had a notable negative effect on the current efficiency, energy efficiency and quality of deposits obtained. At even higher concentrations of selenium (~1000 g/dm$^3$) co-reduction was observed. The researchers also noted a reduction in the cathodic and

anodic currents at selenium concentration of 100mg/dm$^3$ indicating cathode polarisation. The drop in the current efficiency was attributed to the following possible cathodic reactions as suggested by (Bard et al., 1985):

$$H_2SeO_3 + 4H^+ + 4e^- \leftrightarrow Se + 3H_2O \qquad E^0 = +0.74V \qquad 2.72$$

$$Cu^{2+} + H_2SeO_3 + 4H^+ + 6e^- \leftrightarrow CuSe + 3H_2O \quad E^0 = +0.67V \qquad 2.73$$

$$Cu^{2+} + CuSe + 2e^- \leftrightarrow Cu_2Se \qquad E^0 = +0.5V \qquad 2.74$$

This was further affirmed by analysing the blackish powdery deposits which were formed at the cathode. The deposits were found to contain both copper and selenium thus confirming the formation of CuSe and $Cu_2Se$ by Equation 2.73 and Equation 2.74.

Selenium was also found to affect the quality of deposits, in its absence, bright and smooth deposits were formed. However, by increasing the selenium concentration to 50 g/dm$^3$ smooth but dull bright deposits were obtainable. The deposits obtained at 100 g/dm$^3$ selenium concentration resulted in loose deposits, this was ascribed to internal stresses generated by the selenium in the deposit. Further concentration increases to 500 and 1000 g/dm$^3$ did not allow the copper to deposit, at 1000 g/dm$^3$ a blackish mass covered the cathode, this black deposit was attributed to the formation of CuSe/$Cu_2Se$ at the cathode. X-ray diffraction studies showed that in a pure copper sulphate solution the deposits obtained maintained a (111)> (200)> (220) crystallographic orientation and this same pattern was observed at concentrations of 250 and 500 g/dm$^3$ selenium. At high selenium concentration (1000 g/dm$^3$) foreign peaks attributed to selenium were observed.

Safizadeh et al. (2011) studied the effects of selenium in an electrolyte containing organic additives. Two organic additives (thiourea and gelatine) were used in this study. The researchers used a synthetic solution with a composition of 42 g/ℓ copper sulphate; 18 g/ℓ nickel sulphate, 40 mg/ℓ hydrochloric acid ($Cl^-$) and 160 g/ℓ of sulphuric acid. Thiourea and gelatine were dosed at 4 and 2 mg/ℓ

respectively. The two additives were introduced in the electrolyte simultaneously with thiourea acting as a grain refiner and gelatine acting as a leveller. Selenous acid ($H_2SeO_3$) was used to introduce the impurity selenium in to the electrolyte. It was reported that the presence of selenium in the electrolyte with or without the two additives resulted in reduced cathodic polarisation, black loose particles were also observed on the cathode deposit surface. These black particles were attributed to the formation of copper-selenium compounds. A similar conclusion was made by Baral el at. (2014) in their research as discussed above.

The researchers suggested that the reduction in the cathodic polarisation and formation of black powdery deposits showed that selenium inhibited the preferred effects of the additives. However the researchers did not state how the dosages for the additives were arrived at and what the outcome would have been at slightly higher doses.

An analysis of the deposits using X-ray diffraction (XRD) did not reveal the presence of any compound of copper and selenium. This was attributed to the formation of amorphous composite not detectable by XRD. However energy dispersive spectroscopy revealed the presence of substantial amounts of selenium at certain sites in the deposit. The detrimental effects of selenium on deposit quality have also been reported by Andersen et al. (1983); the researchers reported that copper deposition from selenium containing solution leads to formation of nodular deposits.

## 2.5. Summary

The initial stages in the metal electrodeposition process involve the formation of new nuclei driven by the presence of an electric field. The process is reported to follow three surface steps i.e. charge transfer, surface diffusion and movement of the adsorbed atom after electron transfer into a preferred nucleation site. After initial nuclear formation the deposit then grows by incorporation of other diffusing atoms into the metal lattice. The types of electrodeposits formed depend on a number of factors with the two prominent ones being the operating current density and the level of cathodic process inhibition. The inhibition of the cathodic processes may be achieved through the use of organic additives. Depending on the current density and the level of inhibition, deposits with different characteristics may be produced, ranging from smooth and compact deposits to rough, nodular and even powdery deposits.

The use of organic additives in the copper electrowinning influences the electrodeposition process resulting in the production of high quality deposits. It has been reported that organic additives promote progressive nucleation rather than instantaneous nucleation. Formation of complexes with copper cations is one of the mechanisms through which organic additives act, these complexes are adsorbed on the cathode substrate and subsequently affecting the delivery of copper on the nucleation sites. Thiourea in particular is reported to act upon the charge transfer step by forming complexes with copper. At high concentrations the additives are reported to negatively affect the limiting current density.

Dissolved impurities on the other hand negatively affect the electrowinning process by lowering the current efficiency, occlusion in the cathode deposit and even co-deposition. Impurities such as iron are reported to lower the cathodic current efficiency by undergoing reduction from ferric to ferrous iron. Selenium at high concentrations is reported to undergo co-reduction with copper and gets incorporated in the deposit. The occlusion and co-deposition of dissolved impurities affects the physical and mechanical properties of copper deposits.

# 3. Experimental

The experimental work in this study was divided into two categories: electrochemical and electrowinning tests. Electrochemical tests were carried out in order to get preliminary information on the effects of selenium and thiourea on the reduction of copper ions during cathodic electrodeposition, while electrowinning tests were carried out to gain an understanding of the aforementioned factors on electrowinning efficiency and cathode quality.

## 3.1. Electrochemical tests

### 3.1.1. Materials

All the electrochemical tests were performed using synthetic solutions prepared from reagent grade chemicals and deionised water. The synthetic solution contained 0.01 M $Cu^{2+}$ as copper sulphate, and 1 M sulphuric acid. The chemicals used in synthetic solution preparation are listed in Table 3.1. The synthetic solution preparation procedure is outlined in APPENDIX A. Selenium and thiourea was varied as shown in Table 3.2.

*Table 3.1. List of chemicals used in the electrochemical experiments.*

| Reagent name | Source | Grade | Molecular weight (g/mol) |
|---|---|---|---|
| Copper(II) sulphate ($CuSO_4.5H_2O$) | Merck | AR | 249.68 |
| Concentrated sulphuric acid($H_2SO_4$) | KIMIX | AR | 98.08 |
| Selenious acid ($H_2SeO_3$ ) | Sigma Aldrich | AR | 128.97 |
| Thiourea ($CH_4N_2S$) | KIMIX | CP | 76.12 |

### 3.1.2. Methodology

A number of electrochemical techniques are available for investigating electrode reactions; however cyclic voltammetry is most often the first choice technique for obtaining preliminary information about electrode reactions. In this study cyclic voltammetry was employed to investigate the effects of varying concentrations of

selenium and thiourea on the cathodic reduction of cupric ions. Some basic principles of cyclic voltammetry are discussed in Section 2.3.1.

#### 3.1.2.1. Experimental design

The electrochemical tests were out carried out using a one factor at a time (OFAT) approach. Selenium and thiourea were initially investigated separately at 3 different levels. The OFAT approach was used so as to fully understand the effects of selenium and thiourea. It was also desired to investigate any possible interactions between selenium and thiourea hence a combination of the two was also investigated. As discussed in Section 2.4.3.3, improved PGM recovery as well as selenium and tellurium precipitation were observed at thiourea concentrations of 200 % and 320 % excess, therefore these two levels of thiourea concentration were considered in this study. It was also desired to observe the effects of thiourea at a lower concentration and 100 % excess thiourea was chosen as a low value. Selenium was investigated at values of 20, 57 and 150 mg/ℓ with 57 mg/ℓ being the concentration of selenium in the electrolyte before the selenium and tellurium removal stage. A low and high value of 20 and 150 mg/ℓ respectively were investigated to determine the effects of variations in selenium concentration. The cyclic voltammetry tests were performed at a scan rate of 10 mV/s and sweep range of -0.5 V to +0.5 V for copper and copper-selenium solutions as well as copper-thiourea solutions. The sweep range was chosen so as to encompass the standard copper reduction potential (0.34 V). For selenium alone the sweep range considered was between 2 V and 0.25 V. For thiourea the potential was swept between -0.25 V and 1.3 V. The specific sweep ranges for selenium and thiourea were selected based on literature findings.Table 3.2 shows a summary of the variable factors considered in the electrochemical studies while the fixed factors are shown in Table 3.3.

*Table 3.2. Summary of variable factors and factor values used in the electrochemical tests*

| Thiourea (%excess) | Selenium (mg/ℓ) | Thiourea-selenium interaction | |
|---|---|---|---|
| | | Thiourea | Selenium |
| 100 | 20 | 5 mg/ℓ | 10 mg/ℓ |
| 200 | 57 | 10 mg/ℓ | 57 mg/ℓ |
| 320 | 150 | 200 % excess | 150 mg/ℓ |

*Table 3.3. Summary of fixed factors and factor values used in the electrochemical tests*

| Factor | Factor Value |
|---|---|
| Temperature (˚C) | 25 |
| Working electrode Rotational speed (rpm) | 1000 |
| Copper ($Cu^{2+}$) concentration (M) | 0.01 |
| $H_2SO_4$ concentration (M) | 1 |
| Sweep rate (mV/s) | 10 |

### 3.1.2.2. Experimental setup

A 3 electrode system as shown in Figure 3.1 was used in this study. The set up consisted of a 175 ml jacketed multi-port electrolytic cell, a 5 mm diameter rotating disk platinum electrode as the working electrode, a saturated calomel reference electrode and graphite counter electrode. The system was equipped with a Gamry RDE710 control unit for regulating the rotational speed of the working electrode and an Interface 1000 Potentiostat (Model 04085) for maintaining the potential of the working electrode at a desired value with reference to the reference electrode. The running and real time monitoring of the experiments as well as data collection and analysis was achieved by use of the

Gamry PHE200$^{TM}$ physical electrochemistry software installed on an external computer which was connected to the system through a USB cable.

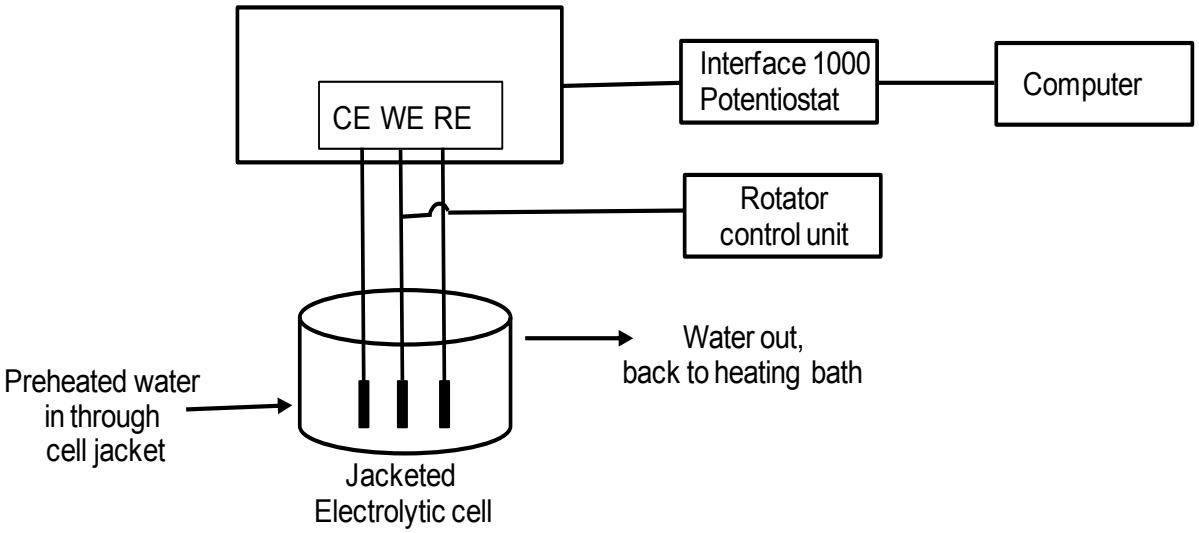


*Figure 3.1. Schematic diagram of the experimental setup*

To avoid electrolyte contamination with the reference electrode filling solution, a bridge tube fitted with a vycor frit at the bottom to allow movement of ions was used to hold the reference electrode and establish contact between the electrolyte and the reference electrode. The tube cavity was filled with the same electrolyte as that in the cell. The temperature of the electrolyte was controlled using a HAAKE D1 heating bath, with water as a heating medium circulated through the jacket of the electrolytic cell.

### 3.1.2.3. Electrode cleaning

To ensure that accurate and reproducible voltammetry results are obtained, the working electrode was cleaned and polished to a mirror finish after each experimental run. A Buehler micro cloth and a Buehler 0.05 µm alumina suspension were used in cleaning and polishing of the electrode.

The micro-cloth was attached onto a glass plate by means of its adhesive back. A few drops of the alumina suspension solution were then applied to the cloth.

The electrode was first rinsed using a squeeze bottle with de-ionised water as cleaning medium to remove any encrusted material. With its face down, the electrode was then placed onto the glass plate onto which a micro-cloth has been attached. The electrode was then polished using a smooth figure-eight motion while ensuring that even pressure is applied. The polishing process was carried out for about 5-10 minutes after which the electrode was thoroughly rinsed using de-ionised water and dried before being mounted on to the rotator shaft in readiness for the next experimental run.

#### 3.1.2.4. Experimental procedure

About 125 ml of the synthetic electrolyte solution was introduced into the 175 ml electrolytic cell. The circulation of preheated water through the cell jacket was then started. The water was circulated throughout the experiment duration so as to maintain the electrolyte temperature at a desired value. The temperature of both the water and the electrolyte was verified using mercury in glass thermometer. The three electrodes were then securely placed into the electrolytic cell through the provided ports on the cell cover, ensuring that the electrodes are correctly immersed in the electrolyte. The counter electrode was placed as close as possible to the working electrode (distance of <1 cm) so as to minimise ohmic drop through the electrolyte as resistance through the electrolyte was not compensated for. The rotation speed of the working electrode was then gradually increased from its rest state (0 rpm) to a final working speed of 1000 rpm. It has been reported in literature that with a rotating electrode the accuracy of the electrochemical test results is enhanced compared to solid electrodes. As stated in Section 3.1.2.2 , the physical electrochemistry software was used in this study. The cyclic voltammetry function within the physical electrochemistry function was chosen and settings for the desired sweep potentials and sweep rate (10 mV/s) were entered. The system was then run to generate potential versus current graphs (voltammograms).

## 3.2. Electrowinning tests

### 3.2.1. Materials

The electrowinning tests were conducted using a synthetic copper sulphate solution. The solution contained about 63 g/ℓ $Cu^{2+}$, 33 g/ℓ $Ni^{2+}$, 1.2 g/ℓ $Fe^{3+}$ and 35 g/ℓ $H_2SO_4$ simulating industry standard electrolyte. The chemicals used are listed in Table 3.4.

*Table 3.4. List of chemicals used in the electrowinning tests.*

| Reagent name | Source | Grade | Molecular weight (g/mol) |
|---|---|---|---|
| Copper(II) sulphate ($CuSO_4.5H_2O$) | Merck | AR | 249.68 |
| Concentrated sulphuric acid ($H_2SO_4$) | KIMIX | AR | 98.08 |
| Selenious acid ($H_2SeO_3$) | Sigma Aldrich | AR | 128.97 |
| Thiourea ($CH_4N_2S$) | KIMIX | CP | 76.12 |
| Ferric sulphate ($Fe_2(SO_4)_3$) | KIMIX | AR | 399.88 |
| Nickel sulphate ($NiSO_4.6H_2O$) | KIMIX | AR | 262.85 |

### 3.2.2. Methodology

The electrowinning tests were performed in order to effectively investigate the effects of varying concentrations of thiourea and selenium on the morphology of copper electrodeposits, the electrowinning current efficiency as well as any possible chemical contamination. The copper deposits produced in the electrowinning tests were subjected to microscopic examination to study their morphology and chemical composition in the presence and absence of thiourea and selenium.

It was also desired to investigate how the electrowinning efficiency would be affected by the presence of thiourea and selenium in the electrolyte. The actual weight of deposit produced was compared with the theoretical weight of deposit expected taking into account the electrode current and electrowinning time.

#### 3.2.2.1. Experimental design

The electrowinning experiments were conducted in a similar manner as the electrochemical tests following a one factor at a time (OFAT) approach. This was in order to fully elucidate the effects that each factor will have on the morphology of the electrodeposits as well as on the electrowinning current efficiency. The levels at which the factors were investigated are identical to the ones used in the electrochemical tests although one extra level of 10 mg/ℓ thiourea was also investigated. The 10 mg/ℓ level was added so as to simulate industrial practice where additives are added in the ranges of 5 mg/ℓ to 20 mg/ℓ. Some electrodeposits were also produced in the absence of both thiourea and selenium. The tests were carried out at a fixed potential (400 mV vs. SHE) for duration of 3 hours. The deposition potential was chosen based on the cyclic voltammetry results. In the cyclic voltammetry tests copper reduction was observed to occur at 200 mV vs. SCE or 441 mV vs. SHE. A potential of 600 mV vs. SHE was also considered to ascertain the effect of higher potential during electrowinning in the presence of excess thiourea.

#### 3.2.2.2. Experimental setup

The experimental setup used for electrowinning experiments was the same as that described in Section 3.1.2.2 and used for the electrochemical tests. The electrowinning tests were run at a constant potential while monitoring the current at the working electrode. In order to achieve this, the controlled potential coulometry function was selected from the Gamry PHE200$^{TM}$ physical electrochemistry software. A controlled potential coulometry experiment is a long term electrolysis experiment in which the potential is held at a set value allowing the electrochemical species to be reduced or oxidised while the current is monitored.

#### 3.2.2.3. Experimental procedure

The electrowinning tests were conducted in a 175 ml jacketed electrolytic cell into which a predetermined volume (150 ml) of synthetic solution was introduced.

With the three electrodes securely in place, the circulation of preheated water through the cell jacket was started in order to maintain the electrolyte temperature at a desired value of 25°C. The rotation speed of the working electrode was then gradually increased form its rest position to a final working speed of 500 rpm. The controlled potential coulometry function was then selected from the Gamry PHE200™ physical electrochemistry software and values for the potential, electrowinning time and working electrode rotational speed entered before running the system for the selected duration of the experiment (3 hours). At the end of the experiment, the deposit obtained was washed insitu using copious amounts of deionised water. The sample was then harvested from the electrode and washed further using deionised water before being air dried and stored away in a sample container for analysis.

### 3.2.2.4. Analytical methods

The concentrations of the different elements in the solution samples were analysed using inductively coupled plasma optical emission spectrometry (ICP-OES). The elements analysed using this technique were copper, iron, nickel and selenium.

The morphology of the electrodeposits was analysed by scanning electron microscope (SEM). Back scattered images of the electrodeposit samples were obtained using a Merlin Zeiss brand SEM instrument. X-ray maps were also obtained to detect specific sites and overall distribution of the elements present on the deposits. The Merlin Zeiss brand SEM instrument was equipped with a Gemini II column for enhanced high resolution imaging utilising advanced detection modes. For chemical composition analysis the instrument uses an Oxford X-mass 20 $mm^2$ detector utilising energy dispersive x-ray spectroscopy (EDX). The quantification of the elements detected was done using Aztec 3.0 SP1 software.

# 4. Results and discussion

## 4.1. Electrochemical tests

As discussed in Section 3.2.1 cyclic voltammetry was used to characterise the effects of selenium and thiourea on the cathodic reduction of cupric ions ($Cu^{2+}$). To come up with a base case for both selenium and thiourea, cyclic voltammetry tests were conducted in acidified base synthetic solutions containing cupric ions or selenium or thiourea alone. The results obtained are discussed in the following sections. The repeatability of the cyclic voltammograms is also shown in APPENDIX B.

### 4.1.1. Cyclic voltammogram for copper

Figure 4.1 shows the voltammogram obtained from a solution containing only cupric ions with sulphuric acid as a background electrolyte (standard electrolyte). During the cathodic sweep a peak C1 is observed at about -0.2 V vs. SCE corresponding to the copper reduction reaction as shown by Equation 2.22 . In the anodic direction a sharp peak A1 is observed at 0.35 V vs. SCE corresponding to the copper dissolution reaction. After the anodic peak A1, the current decays to zero an indication that the $Cu^0$ sites formed on the electrode surface during the cathodic sweep have been fully oxidised. This observation is in agreement with similar observations made by Grujicic and Pesic (2002) and Baral et al. (2014).

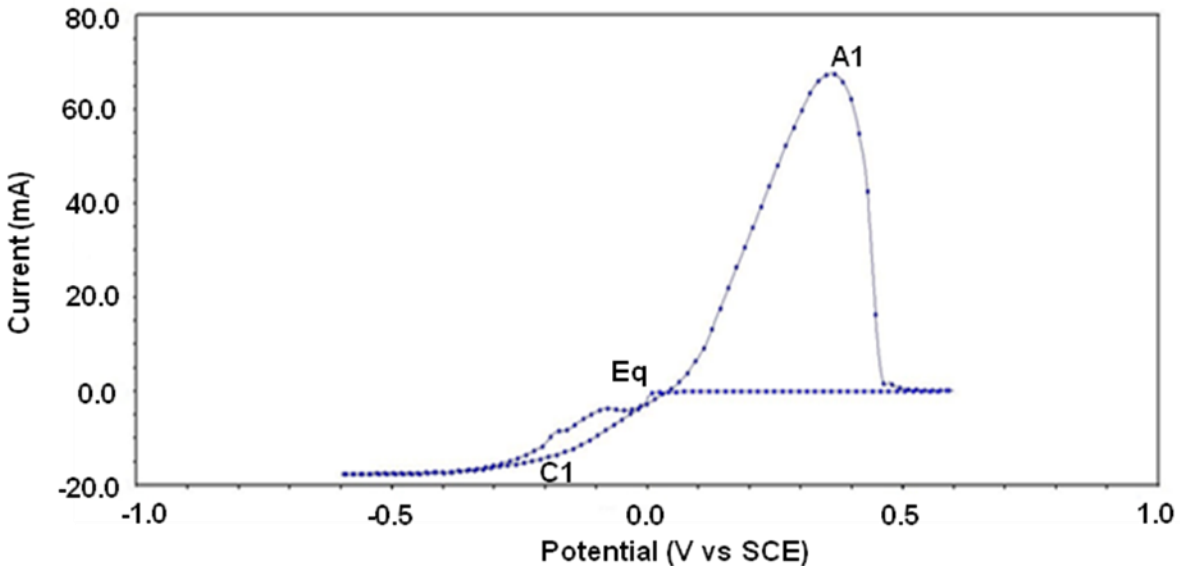


*Figure 4.1.Cyclic voltammogram for copper in 0.01 M $Cu^{2+}$ ions and 1 M sulphuric acid at 25˚C*

A cross over between the anodic and cathodic current lines was observed at the point denoted Eq on Figure 4.1. This cross over potential has also been observed elsewhere (Grujicic and Pesic, 2002; Barin et al., 2000; Safizadeh et al., 2012).The cross over potential was as a result of the difference in the copper cathodic (deposition) and anodic (dissolution) potentials (Grujicic and Pesic, 2002).

### 4.1.2. Cyclic voltammogram for selenium

In this study cyclic voltammetry tests done using solutions with selenium concentrations of between 20 and 250 mg/ℓ showed no noticeable peaks in both the anodic and cathodic directions, it was therefore not possible to characterise the response of selenium at such concentrations. Baral et al. (2014) and Safizadeh et al. (2012) conducted cyclic voltammetry tests on selenium using solutions containing 1000 mg/ℓ and 600 mg/ℓ selenium respectively. Safizadeh et al. (2012) reported that at lower concentrations of 60 mg/ℓ selenium, the voltammograms obtained were not reproducible. It is not well understood at this point why redox reactions involving selenium were not observed at such concentrations (20 and 250 mg/ℓ). At 600 mg/ℓ selenium and 1 M sulphuric acid,

two cathodic peaks (C1 and C2) and three anodic peaks (A1, A2 and A3) were observed as shown in Figure 4.2. Similar voltammograms were also observed by Santos and Machado (2004) in perchloric acid, Carbonnelle and Lamberts (1992) in sulphuric acid and Kowalik (2014).

The first cathodic peak C1 at about 0.28 V vs. SCE (or 0.521 V vs. SHE) with its corresponding anodic peak A1 may be associated to the four electron reduction of selenium according to Equation 2.27 while peaks C2 and A2 are associated with the reduction and dissolution of selenium respectively as shown by Equation 2.29. The third anodic peak A3 (0.69 V vs. SCE) may be ascribed to the dissolution of a platinum-selenium compound formed according to Equation 4.1. A similar peak was reported at 0.72 V vs. SCE by Carbonnelle and Lamberts (1992). The formation PtSe was also reported by Santos and Machado (2004). Carbonnelle and Lamberts (1992) stated that the formation of the platinum-selenium compound was as a result of the presence of platinum oxide on the electrode surface. Selenium is reported to interact with solid metal electrodes as shown by Equation 2.38. Kowalik (2014) also reported strong interactions between selenium and the noble gold electrode.

$$H_2Se + PtO \rightarrow PtSe + H_2O \qquad 4.1$$

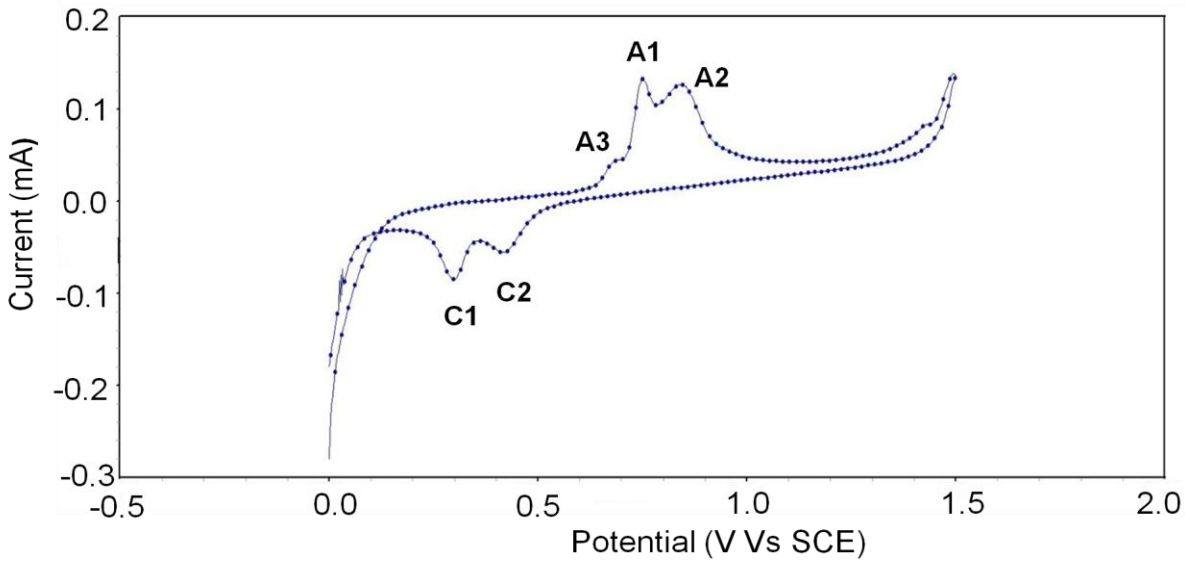


*Figure 4.2. Cyclic voltammogram for 600 mg/ℓ selenium and 1 M sulphuric acid at 25˚C*

### 4.1.3. Cyclic voltammogram for thiourea

Figure 4.3 shows the voltammogram obtained from tests done in a 0.05 mM thiourea and 1 M sulphuric acid solution. The voltammogram obtained in this study is comparable to those obtained by Bolzan et al. (1999) and Shevtsova et al. (2005).

As can be seen from Figure 4.3, a small reduction current is observed between -0.25 V and 0.3 V, between 0.3 V and 0.65 V current increases leading to the formation of an anodic wave. From 0.7 V the current increases gradually culminating into an anodic peak at about 1.1 V. Bolzan et al. (1999) reported that the oxidation of thiourea occurs in two stages. The initial oxidation stage was reported to occur between 0.4 V and 0.7 V (vs. SCE) while the second oxidation stage occurred at potentials above 0.7 V. The anodic wave between 0.3 V and 0.65 V observed in this study corresponds to the initial oxidation of thiourea while the observed increase in current at potentials more positive to 0.7 V corresponds to the second stage of thiourea oxidation. In the first oxidation stage soluble formamidine disulphide is formed while in the second stage thiourea and other adsorbed residues are oxidised (Bolzan et al., 1999). The two stage electro oxidation of thiourea was also reported by Cofre and Bustos (1993). Bolzan et al. (1999) proposed some reaction paths for the first and second oxidation stages of thiourea. In the first stage the researchers proposed that thiourea oxidation occurred as shown by Equation 4.2 to Equation 4.4.

$$[\mathrm{Pt}] + (\mathrm{H_2N})_2\mathrm{CS} \leftrightarrow [\mathrm{Pt}]((\mathrm{H_2N})_2\mathrm{CS})_{\mathrm{ads}} \quad 4.2$$

$$[\mathrm{Pt}]((\mathrm{H_2N})_2\mathrm{CS})_{\mathrm{ads}} \rightarrow [\mathrm{Pt}] + [(\mathrm{H_2N})_2\mathrm{CS}^{\bullet}]^{+} + \mathrm{e}^{-} \quad 4.3$$

$$2[(\mathrm{H_2N})_2\mathrm{CS}^{\bullet}]^{+} \rightarrow (\mathrm{H_2N})_2(\mathrm{HN})_2\mathrm{C_2S_2} + 2\mathrm{H}^{+} \quad 4.4$$

Pt in this case refers to the platinum electrode surface. Equation 4.2 represents the adsorption of thiourea on to the electrode, the adsorbed thiourea is then oxidised according to Equation 4.3 producing a soluble radical which dimerises to produce formamidine disulphide as shown by Equation 4.4.

According to the researchers, the second thiourea oxidation stage proceeds as shown by Equation 4.5 to Equation 4.8. Adsorbed thiourea is oxidised according to Equation 4.5 producing sulphenic acid.

$$[\mathrm{Pt}]((\mathrm{H_2N})_2\mathrm{CS})_{\mathrm{ads}} + \mathrm{H_2O} \rightarrow [\mathrm{Pt}] + [(\mathrm{H_2N})_2\mathrm{CSOH_2}]^{2+} + 2\mathrm{e}^- \quad 4.5$$

The sulphenic acid was reported to undergo decomposition according to Equation 4.6 producing urea, adsorbed sulphur and some protons.

$$[(\mathrm{H_2N})_2\mathrm{CSOH_2}]^{2+} \rightarrow [\mathrm{Pt}](\mathrm{S})_{\mathrm{ads}} + (\mathrm{H_2N})_2\mathrm{CO} + 2\mathrm{H}^+ \quad 4.6$$

Urea is further oxidised to produce nitrogen, carbon dioxide and hydrogen ions according to Equation 4.7, while the adsorbed sulphur is also oxidised forming sulphate ions according to Equation 4.8.

$$((\mathrm{H_2N})_2\mathrm{CO})_{\mathrm{ads}} + \mathrm{H_2O} \rightarrow \mathrm{N_2} + \mathrm{CO_2} + 6\mathrm{H}^+ + 6\mathrm{e}^- \quad 4.7$$

$$[\mathrm{Pt}](\mathrm{S})_{\mathrm{ads}} + 4\mathrm{H_2O} \rightarrow [\mathrm{Pt}] + \mathrm{SO_4^{2-}} + 8\mathrm{H}^+ + 6\mathrm{e}^- \quad 4.8$$

The reaction path proposed by Bolzan et al. (1999) is consistent with findings reported by Shevtsova et al. (2005). Shevtsova et al. (2005) reported that at more positive potentials both thiourea and formamidine disulphide undergo complete oxidation to produce carbon dioxide, cyanide and sulphide ions. The absence of a reduction peak during the cathodic scan indicates that thiourea does not undergo reduction at the potentials studied (-0.25 V to 1.3 V). Thiourea reduction has been reported to occur at more negative potential values of around -1.6 V vs. SCE (Mouanga and Bercot, 2011).

Figure 4.4 shows the voltammogram obtained from the tests done in a potential range restricted to the copper reduction and oxidation process (-0.5 V to 0.5 V). As can be seen from the voltammogram, no peaks were observed in both the cathodic and anodic directions. This could imply that thiourea is not electrochemically active at such potentials. However thiourea maybe oxidised by cupric ions as stated in Section 2.4.2.2 with the cupric ions acting as oxidising

agents within that potential range leading to the formation copper-thiourea complexes.

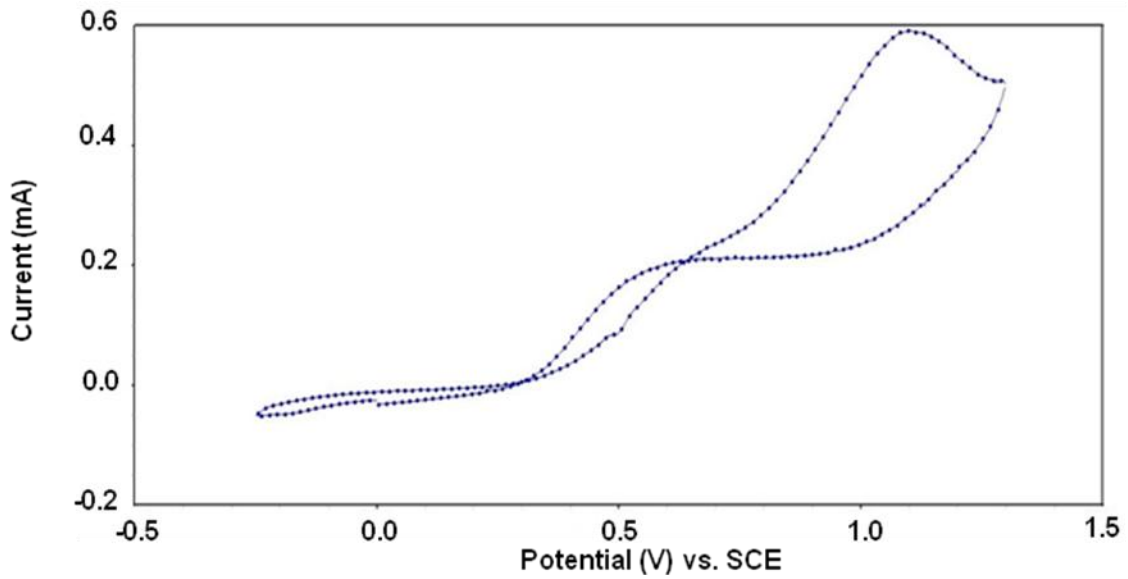


*Figure 4.3. Cyclic voltammogram for thiourea in 0.05 mM thiourea and 1 M sulphuric acid at 25°C with potential scan range of -0.25 V to 1.3 V*

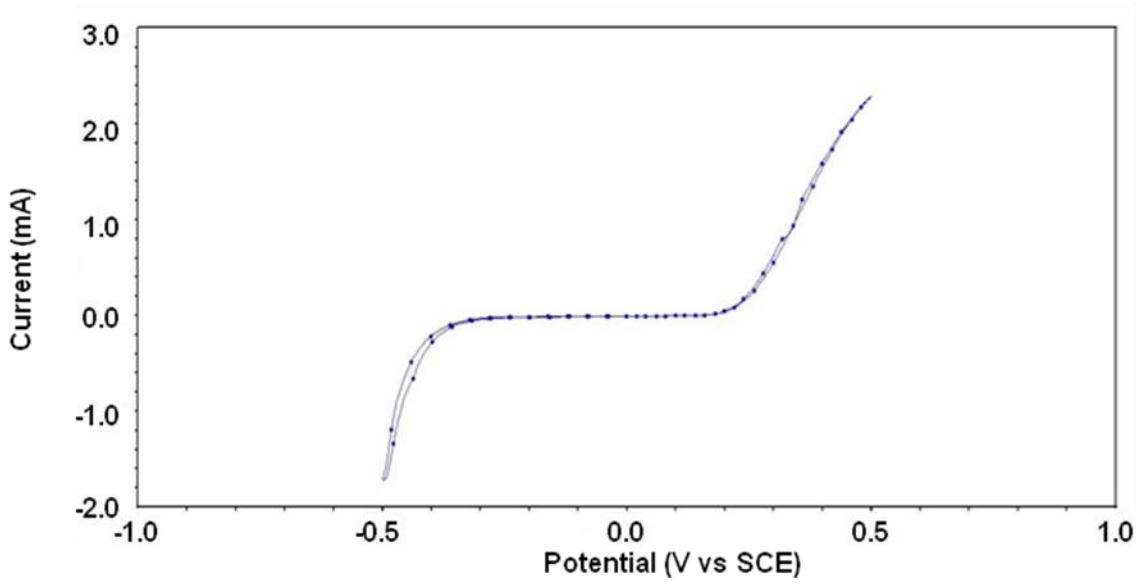


*Figure 4.4. Cyclic voltammogram for thiourea in 0.05 mM thiourea and 1 M sulphuric acid at 25°C with potential scan range of -0.5 V to 0.5 V*

### 4.1.4. Effects of thiourea

The effect of excess thiourea on the cathodic reduction of cupric ions was investigated at 3 different levels as stated in Section 3.1.2.1. The presence of thiourea in the electrolyte at the three levels investigated resulted in a shift in the cathodic peak to more negative values as shown in Figure 4.5. A corresponding reduction in the size of the anodic peak (reduction in anodic current) was also observed as the concentration of thiourea increased; this was an indication that excess thiourea polarised the working electrode resulting in a reduction in the electrode reaction efficiency. The shift in the cathodic overpotential in the presence of thiourea has been reported by several researchers (Gomez et al., 2009; Muresan et al., 2000; Varvara et al., 2001; Alodan and Smyrl, 1998; Tadesse et al., 2013). As has been discussed in Section 2.4.4.2 and Section 2.4.4.4, additives act by partially blocking the electrode surface thus increasing the current density on the uncovered areas of the electrode, this in turn results in an increase in the reaction overpotential (Habashi, 1998; Loutfy, 1971). The shift in the reduction potential that was observed in this study may thus be ascribed to an increase in the reaction overpotential as a result of electrode active site coverage by thiourea.

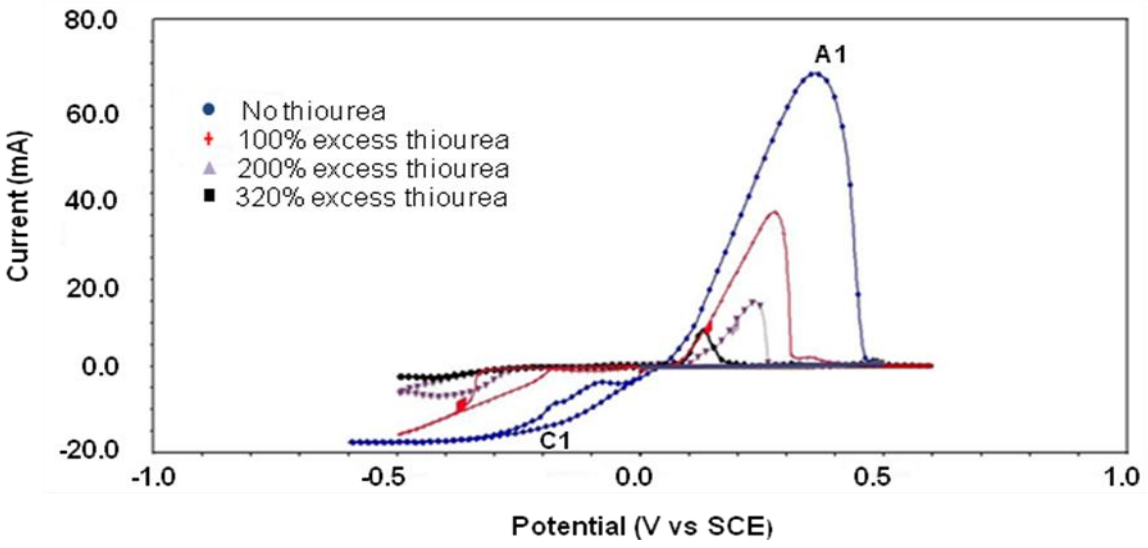


*Figure 4.5.Cyclic voltammogram for copper ($Cu^{2+}$ 0.01 M) with varying concentrations of thiourea, 100 %, 200 % and 320 % excess in 1 M sulphuric acid at 25 C*

As mentioned in Section 2.4.4.3, coverage of the electrode active sites may occur through the physical adsorption of thiourea on the electrode surface or through the formation of Cu-Tu complexes. Thiourea is known to form complexes with copper ions as discussed in Section 2.4.2.1and Section 2.4.2.2. The ability of the thiourea molecule to donate an electron allows it to form complexes with metals such as copper and nickel (Jin et al., 2002). Hibbert (1993) suggested that the formation of complexes between metal ions and ligands may result in a shift in the reduction potential by as much as 1 volt in either direction as shown by Equation 2.16. However, neither cathodic peaks nor anodic peaks were observed relating to the formation and oxidation of complexes at 100 % and 200 % excess thiourea. It is therefore suggested that the dominant mode of inhibition observed at these conditions was that of physical adsorption of thiourea. The adsorption of additives is considered as an almost zero current process as discussed in Section 2.4.4.3 and therefore difficult to detect in a voltammetry test.

At 320 % excess thiourea, however, a second more positive anodic peak A2 as shown in Figure 4.6 was observed which was absent in voltammograms obtained with solutions containing only copper (II) sulphate, Figure 4.1 and that containing only thiourea, Figure 4.3 and Figure 4.4. The peak A2 can therefore be attributed to the oxidation of complexes formed between copper and thiourea adsorbed on the electrode surface at high thiourea concentrations. The observation made in this study is consistent with findings made by Fabricius et al. (1994). The researchers further suggested that at concentrations high enough to result in the appearance of peak A2, formation of smooth and homogeneous deposits was not possible. At lower concentrations of 100 % and 200 % excess thiourea, Figure 4.7 and Figure 4.8 respectively, peak A2 was absent. The appearance of peak A2 at 320 % excess thiourea could therefore be used as diagnostic criteria for solutions containing high concentrations of thiourea to produce compact and homogenous deposits as suggested by Fabricius et al. (1994).

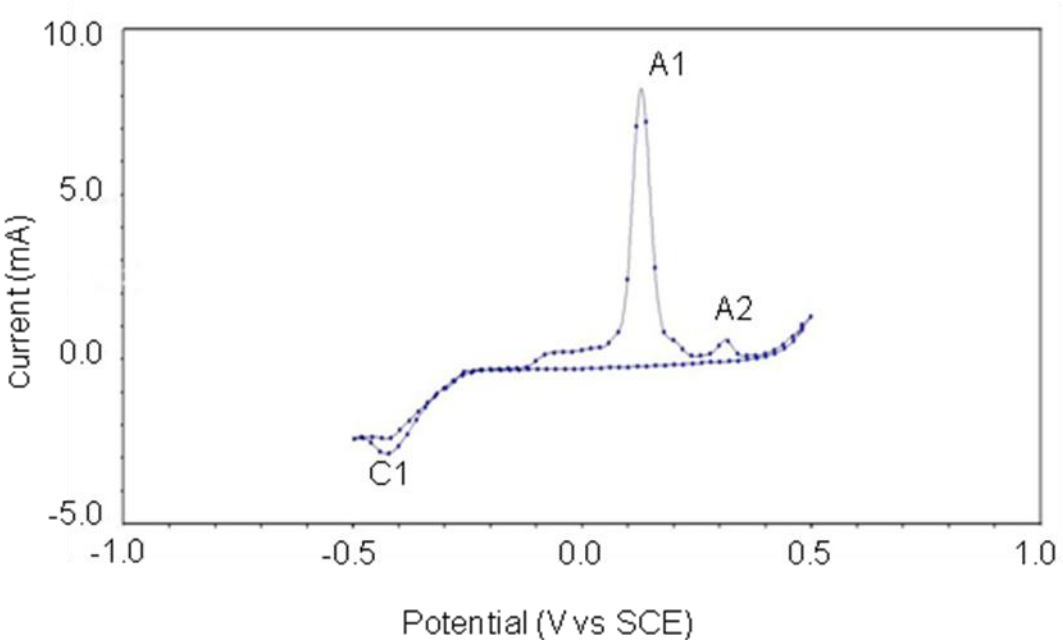


*Figure 4.6.Cyclic voltammogram for copper in 0.01 M $Cu^{2+}$ and 1 M sulphuric acid in the presence of 320 % excess thiourea at 25˚C*

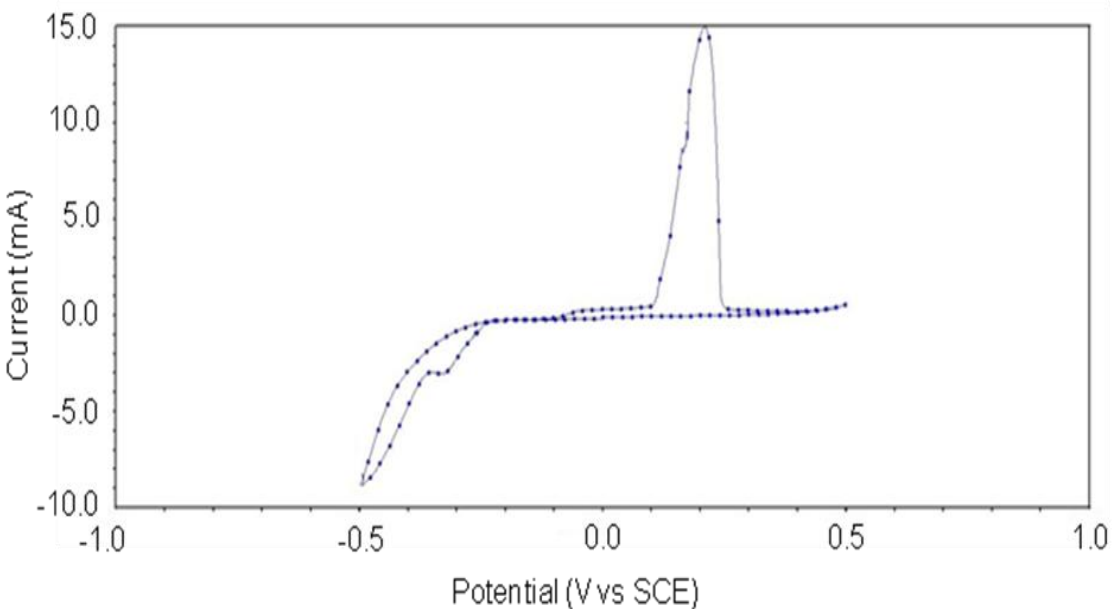


*Figure 4.7.Cyclic voltammogram for copper in 0.01 M $Cu^{2+}$ and 1M sulphuric acid in the presence of 200 % excess thiourea at 25˚C*

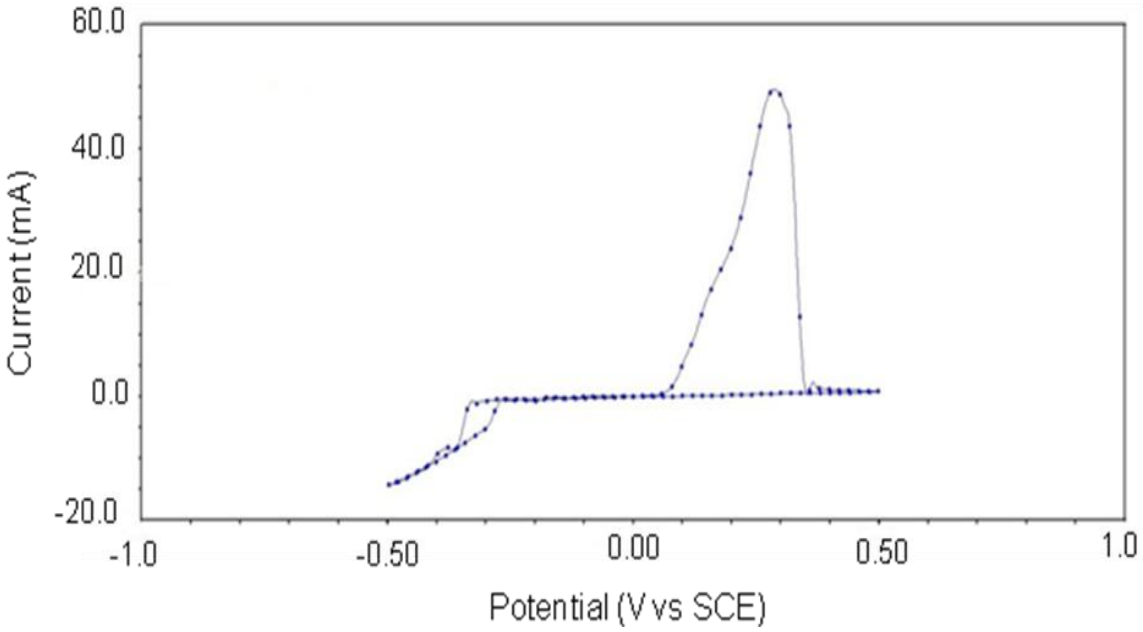


*Figure 4.8. Cyclic voltammogram for copper in 0.01 M $Cu^{2+}$ and 1 M sulphuric acid in the presence of 100 % excess thiourea at 25˚C*

### 4.1.5. Effects of selenium

Figure 4.9 to Figure 4.11 show the voltammograms obtained in the electrochemical investigation of the effects of selenium on the reduction of cupric ions at varying concentrations of 20 mg/ℓ, 57 mg/ℓ and 150 mg/ℓ respectively. The general form of the voltammograms is similar to that obtained in an acidified copper sulphate solution with no addition of impurity (Figure 4.1). This is an indication that the primary reaction taking place is the reduction of cupric ions as was the case in an impurity and additive free electrolyte. However in the presence of different concentrations of selenium, a second cathodic peak is observed at about 0.11 V vs. SCE as can be seen from the voltammograms. The size of this peak increases as the concentration of selenium increases. The appearance of this second cathodic peak may be ascribed to the simultaneous reduction of cupric ions and selenium according to Equation 4.9 as suggested by Carbonnelle and Lamberts (1992).

$$2Cu^{2+} + H_2SeO_3 + 4H^+ + 8e^- \leftrightarrow Cu_2Se + 3H_2O \qquad 4.9$$

Carbonnelle and Lamberts (1992) observed a similar peak at about 0.16 V vs. SCE in their study of copper-selenium solution (0.001 M $Cu^{2+}$ and 0.00024 M $Se^{4+}$) in 0.1 M sulphuric acid. The increase in the size of the peak with increase in selenium concentration could imply that Equation 4.9 is dependent on the concentration of selenium in the electrolyte.

The principle difference in the current work and the work done by Carbonnelle and Lamberts (1992), is that in the current work the sweep range was restricted to the region where cupric ion reduction and oxidation is expected to occur (-0.5 V to 0.5 V), while Carbonnelle and Lamberts (1992) had an extended sweep range of between -0.5 V and 1.5 V. It was therefore possible for Carbonnelle and Lamberts (1992) to observe the oxidation of the copper selenide compound formed as shown by Equation 4.9. In the current study, a black insoluble mass was instead found at the electrode surface, Figure 4.12, this could be attributed to the fact that a shorter sweep range was considered and the oxidation of such a compound could not be observed. Other researchers have reported the presence of a black mass at the cathode surface which they attributed to the formation of a copper selenide compound (Baral et al., 2014; Safizadeh et al., 2012). It is therefore suggested that the black mass at the electrode as shown by Figure 4.12 could be a copper selenide compound.

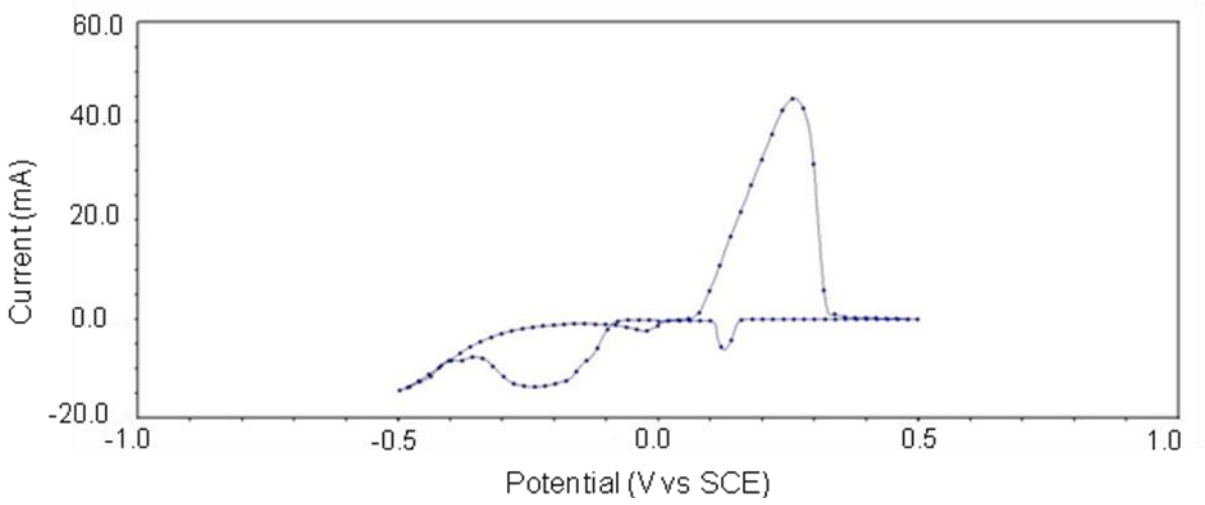


*Figure 4.9. Cyclic voltammogram for copper in 0.01 M $Cu^{2+}$ and 1 M sulphuric acid in the presence of 20 mg/ℓ selenium at 25˚C*

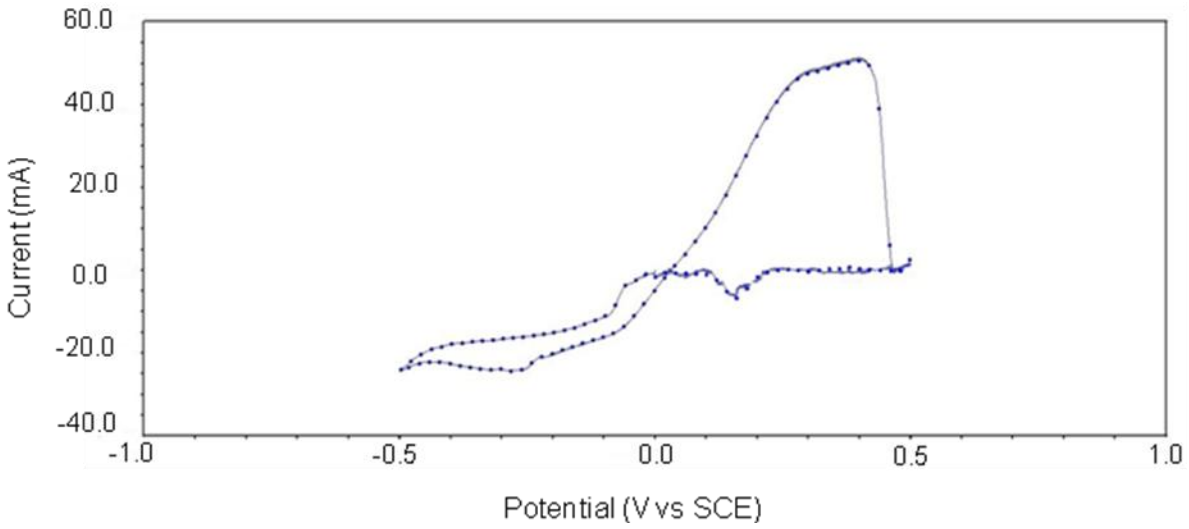


*Figure 4.10. Cyclic voltammogram for copper in 0.01 M $Cu^{2+}$ and 1 M sulphuric acid in the presence of 57 mg/ℓ selenium at 25˚C*

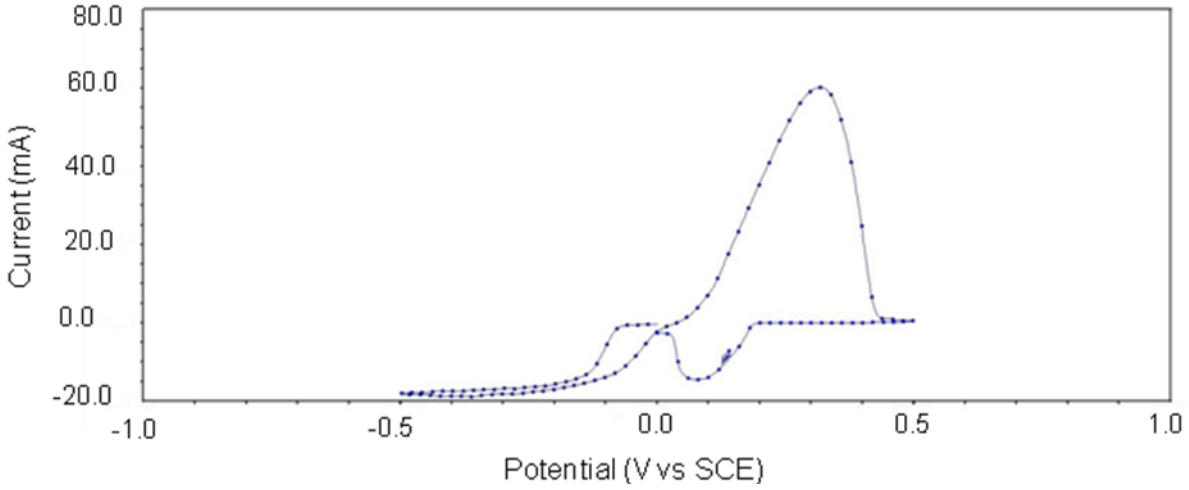


*Figure 4.11. Cyclic voltammogram for copper in 0.01 M $Cu^{2+}$ and 1 M sulphuric acid in the presence of 150 mg/ℓ selenium at 25˚C*

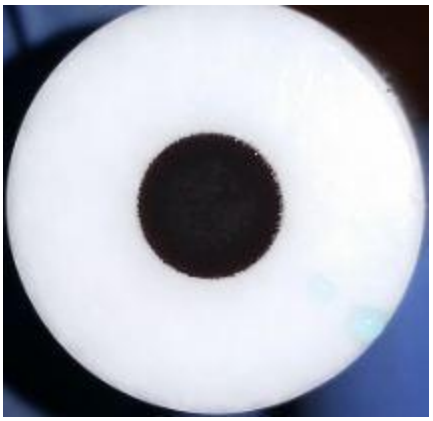

*Figure 4.12. Image showing the appearance of the working electrode after a cyclic voltammetry test in 0.01 M $Cu^{2+}$ and 1 M sulphuric acid in the presence of 150 mg/ℓ selenium*

### 4.1.6. Combined effect of thiourea and selenium

Figure 4.13 shows the voltammogram obtained in the presence of both selenium and thiourea at different concentrations. Thiourea was added at concentrations of 10 mg/ℓ and 200 % excess while selenium was added at 5 mg/ℓ, 57 mg/ℓ and 150 mg/ℓ. It can be seen from the figure that in all the three cases investigated, a shift in the cathodic potential to more negative values is observed in comparison to the voltammogram obtained in a standard electrolyte, Figure 4.1, an indication of cathode polarisation. As expected, the highest polarisation was observed from the electrolyte containing 200 % excess thiourea and 150 mg/ℓ selenium, followed by 10 mg/ℓ thiourea and 57 mg/ℓ selenium. A second anodic peak C2 similar to that observed in the copper-selenium solutions as discussed in Section 4.1.5 was also observed in solution containing 10 mg/ℓ thiourea and 57 mg/ℓ selenium. It is interesting to note that with 200 % excess thiourea and 150 mg/ℓ selenium the peak was not present. This could possibly mean that the high concentration of thiourea inhibited the formation of the copper selenide compound suggested in Section 4.1.5 through Equation 4.9. The mechanism through which such an inhibition would occur is however not clear at this stage. One possibility could be that the thiourea inhibited the smooth flow of both selenium and copper ions to the electrode surface thus no copper-selenium compound could be formed. At 10 mg/ℓ thiourea and 5 mg/ℓ selenium peak C2

was also not observed, this could be attributed to the low concentration of selenium added. As seen in Section 4.1.5 , peak C2 increased with increase in selenium concentration an indication that the formation of the copper selenide compound was dependent on the concentration of selenium.

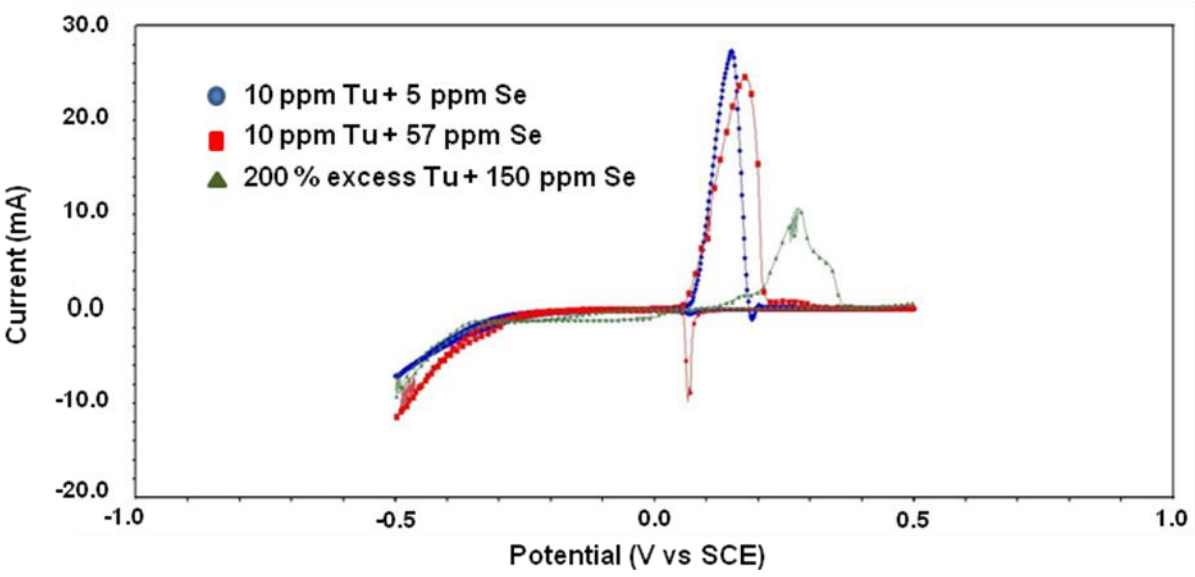


*Figure 4.13. Cyclic voltammogram for the combined effect of thiourea and selenium in 0.01 M $Cu^{2+}$ and 1 M sulphuric acid at 25˚C*

## 4.2. Electrowinning tests

As stated in Section 3.2.2 copper electrodeposits were experimentally produced in the absence and presence of thiourea and selenium. The electrodeposits produced were then analysed using scanning electron microscopy (SEM) to study the surface morphology while the chemical composition was studied by energy dispersive x-ray spectroscopy (EDX). The results obtained are presented and discussed in the following sections.

### 4.2.1. Electrowinning in the absence of thiourea

The deposition of copper from acidic copper sulphate solutions has been studied and reported by several researchers. It has been reported that the nucleation process during deposition in the absence of any additives is often controlled by the prevailing local conditions at the growth site (Pablo et al., 2002). It has been reported that when deposition takes place in the absence of an additive, the quality of the deposit produced depends solely on the kinetics of the cupric ion reduction reaction, Equation 2.22.

Figure 4.14 shows an SEM image of a copper electrodeposit that was obtained from a solution containing about 63 g/ℓ $Cu^{2+}$, 33 g/ℓ $Ni^{2+}$, 1.2 g/ℓ $Fe^{3+}$ and 35 g/ℓ $H_2SO_4$. The deposit was produced at a constant potential for duration of 3 hours. It can be seen from Figure 4.14 that the deposit obtained was characterised by a relatively rough and dull surface. This was as expected, as electrodeposits produced in the absence of any additives are said to be granular and rough (Fabricius et al., 1994). This is so because the deposition process follows the instantaneous deposition mechanism taking place on a small nuclear number density. As has been discussed in Section 2.1.1, instantaneous nucleation occurs when all the available nucleation sites on the electrode surface are instantaneously converted into nuclei. The instantaneous nucleation mechanism perpetuates grain growth leading to the formation of coarse grained and rough deposits.

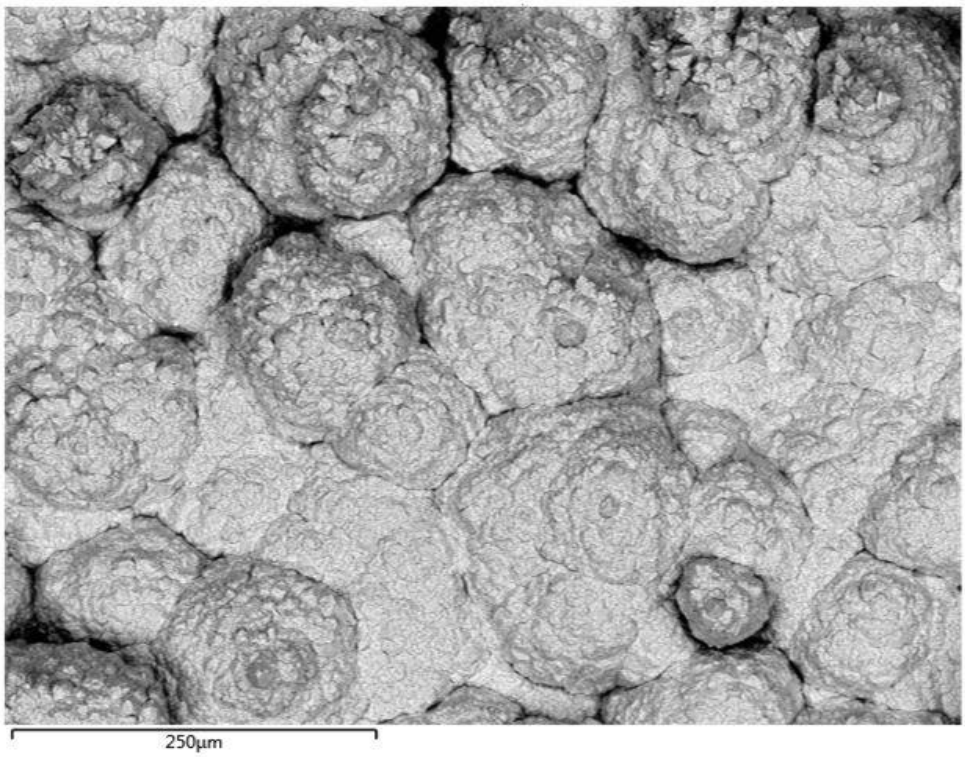


*Figure 4.14. Scanning electron microscopy (SEM) image of a copper electrodeposit obtained in a standard electrolyte solution at constant potential.*

Fabricius et al. (1994) suggested that during instantaneous nucleation, the electrocrystallisation process is often fast, taking place on a relatively few number of nucleation sites which are formed instantaneously on the electrode surface. It has also been reported that during instantaneous nucleation the formation of new nuclei is terminated very early on in the initial stages of electrocrystallisation resulting in the formation of coarse grained deposits as grain growth is favoured over the formation of new nuclei. Figure 4.15 shows an SEM image of the grain structure for the electrodeposit shown in Figure 4.14. It can be seen that the deposit consisted of well-developed grains growing independently of each other. This affirms the fact that grain growth was favoured over the formation of new nuclei as is the case during instantaneous nucleation occurring in the absence of additives.

The rough surface observed may also be attributed to a lack of leveling, as deposition was done in the absence of an additive or leveling agent. As

mentioned in Section 2.1, electrode surfaces contain some surface imperfections or defects which act as nucleation sites. These defects may vary in size and texture resulting in the presence of micropeaks and microrecesses on the electrode surface. The micropeaks usually have a higher current density and are closer to the diffusion layer. Schilardi et al. (1998) reported that a high number of depositing cupric ions are captured at the micropeaks while a relatively small number reports to the recessed areas. Therefore, in the absence of a leveling agent (additive) growth is more pronounced on the micropeaks than in the microrecesses. This often results in uneven and rough deposits as has been observed in this study.

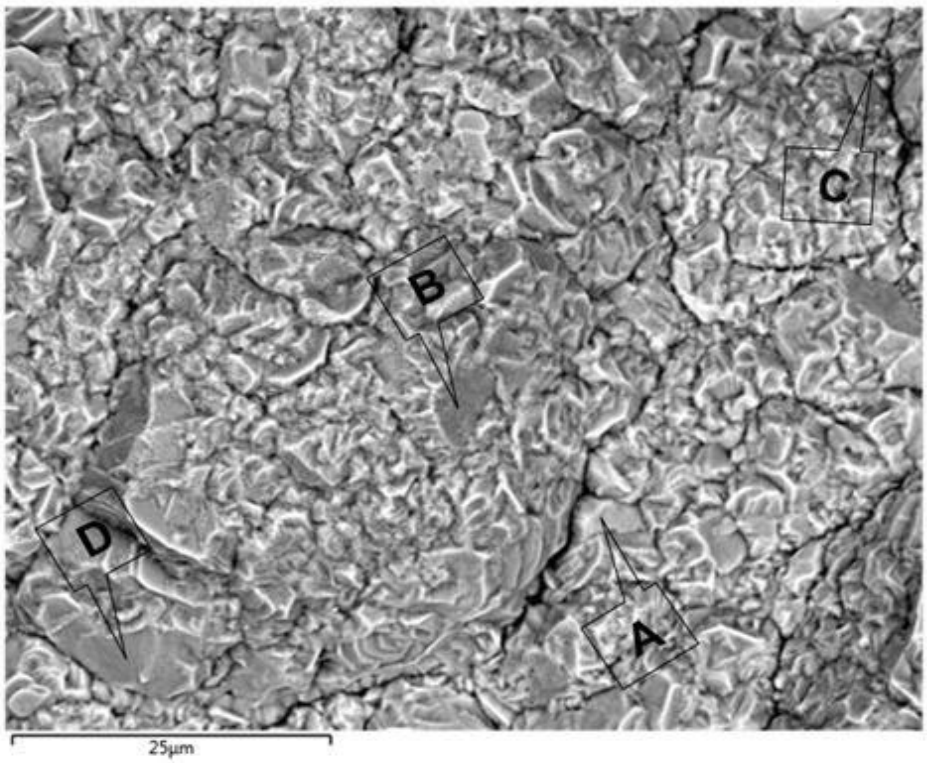


*Figure 4.15. Scanning electron microscopy (SEM) image showing the grain structure of a copper electrodeposit obtained from a standard electrolyte*

Table 4.1 shows a summary of the elemental composition of the electrodeposit shown by Figure 4.15. The electrodeposit was relatively pure with trace amounts

of impurities picked nickel, sulphur and iron. The oxygen detected may have resulted from the oxidation of the deposit. The carbon observed could have resulted from the graphite counter electrode.

*Table 4.1. Spot elemental composition of certain sites from the deposit obtained in a standard electrolyte*

| Site | Elemental composition (Wt%) | | | | | | |
|---|---|---|---|---|---|---|---|
| | Cu | S | O | N | Ni | Fe | C |
| A | 97.23 | 0.02 | 0.18 | - | - | - | 2.55 |
| B | 96.43 | 0.07 | 0.73 | - | 0.04 | 0.07 | 2.71 |
| C | 97.46 | - | 0.49 | - | 0.03 | - | 2.01 |
| D | 95.52 | - | 0.44 | - | - | - | 4.04 |

### 4.2.2. Electrowinning in the presence of thiourea

The electrowinning and electrorefining of copper in the presence of thiourea has been investigated extensively and various findings reported by a number of researchers (Muresan et al., 2000; Mirkova et al., 1994; Tadesse et al., 2013). It is, however, worth mentioning that most of the work reported has focused on the effects of thiourea at relatively low concentrations (10-50 mg/ℓ), only a limited number of researchers have reported on the effects of thiourea at relatively high concentrations. In this study the effects of thiourea have been investigated at concentrations much higher than those reported and applied in industrial electrowinning operations as well as lower concentrations applicable to industrial practice. The results obtained are presented and discussed in the following sections.

#### 4.2.2.1. Effects of low thiourea concentrations on cathode morphology

Figure 4.16 shows the SEM image of an electrodeposit obtained in the presence of 10 mg/ℓ thiourea. As can be seen the electrodeposit obtained was smooth and planar in comparison to that obtained in the absence of thiourea (see Figure 4.14). This was as expected and in good agreement with published literature where the presence of controlled amounts of thiourea has been reported to result into smooth electrodeposits (Quinet et al., 2009; Tadesse et al., 2013; Fabricius et al., 1994). Thiourea inhibits the cathodic copper reduction process resulting

into a progressive nucleation mechanism. This action leads to the formation of fine grained and smooth electrodeposits. Habashi (1998) reported that additives inhibit the cathodic reaction resulting in an increase in the cathodic reaction overpotential. According to Habashi (1998) the increase in the cathodic reaction overpotential eases the nucleation process and inhibits the formation of large grains and promotes the formation of fine grains that are responsible for the formation of smooth electrodeposits. The inhibiting effect of thiourea and increase in the cathodic overpotential as reported by other researchers has also been observed in this study through cyclic voltammetry (refer to Section 4.1.4). It can therefore be assumed that the smooth deposit obtained in this study as seen in Figure 4.16 was as a result of thiourea influencing the electrocrystallisation process through inhibition of the cathodic reaction thus promoting the progressive nucleation mechanism to predominate leading to the continuous formation of new nuclei and increasing the nuclear number density. The continuous formation of new nuclei can be affirmed by referring to Figure 4.17. It can be inferred from Figure 4.17 that the continuous formation of new nuclei was favored over crystal growth; this is evidenced by the relatively high number of fine grains observed in the deposit as opposed to large grains. The presence of fine grains in electrodeposits (as seen in Figure 4.17) has been reported by several researchers to be responsible for the formation of smooth deposit surfaces (Varvara et al., 2001; Muresan et al., 2002; Fabricius et al 1994; Bonou et al., 2002; Kumar et al., 2011). The observation made by the aforementioned researchers agrees well with findings made in this study where a fine grained structure and smooth electrodeposit surface have been observed.

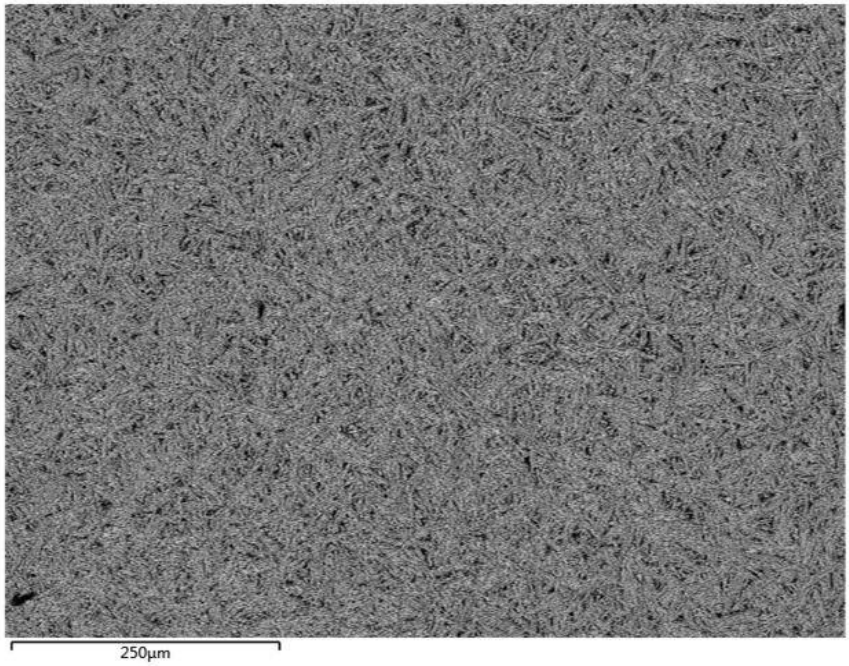


*Figure 4.16. Scanning electron microscopy (SEM) image of a copper electrodeposit obtained from a standard electrolyte containing 10 mg/ℓ thiourea at a constant potential of 400 mV.*

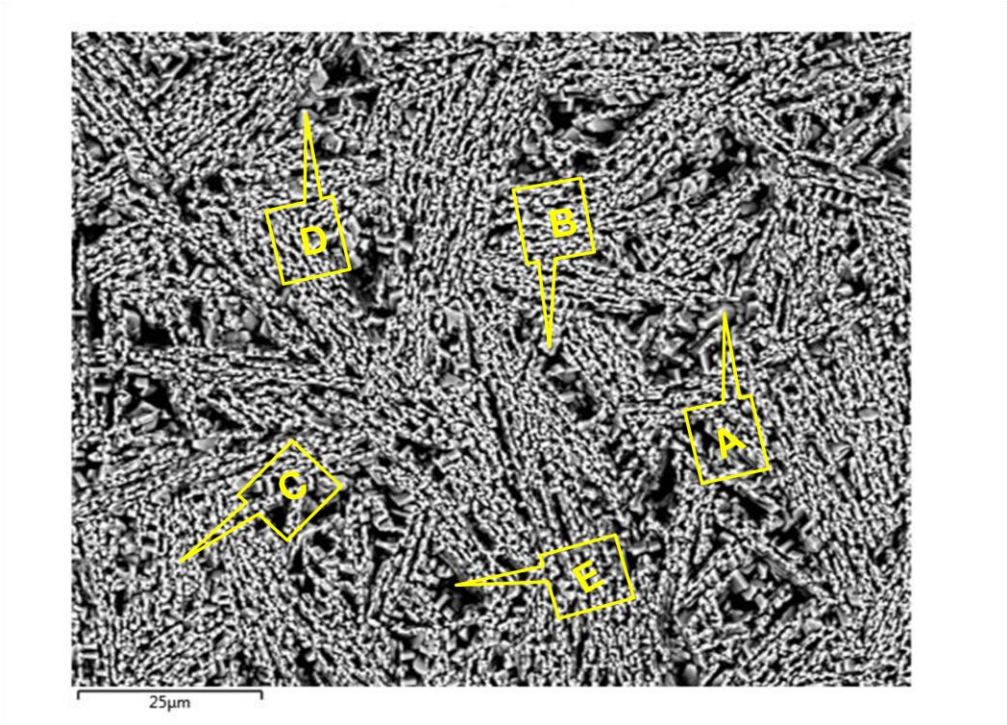


*Figure 4.17. Scanning electron microscopy (SEM) image showing the grain structure of a copper electrodeposit obtained from standard electrolyte containing 10 mg/ℓ thiourea at a constant potential of 400 mV.*

The smooth and planar deposit obtained in this study may also be attributed to the leveling action of thiourea. The leveling action occurs through the preferential or selective adsorption of thiourea or thiourea-copper complexes onto the electrode active sites. This results into a non uniform distribution of current on the electrode such that the ratio of the current in the recessed areas to that on the micropeaks (electrode active sites) is greater than unity. This retards growth at the micropeaks and allows growth to occur in the recessed areas thus effecting leveling. Oniciu and Muresan (1991) also reported that as a result of the blocking of the active sites, metal atoms are displaced towards the microrecesses thus increasing the growth rate in the recessed areas resulting into a planar deposit surface. The evidence of thiourea adsorption on the active sites in this study may be taken as the presence of void like spaces as can be seen on Figure 4.17 as was also suggested by Tadesse et al., 2013. The two processes leading to the formation of smooth deposits as discussed (continued nucleation and blocking of active sites) occur simultaneously.

Table 4.2 shows some EDX results taken at random spots as shown in Figure 4.17. It can be seen from the results that the deposit was relatively pure with minimal evidence of contamination from thiourea or any of the other chemicals in the electrolyte. It would have been expected that with the proposed adsorption of thiourea on the active sites, as discussed above, impurities drawn from thiourea would have been detected in the electrodeposit but this was not the case. This could be ascribed to the possible desorption of the additive. According to Schilardi et al. (1998), desorption occurs due to a reduction in the radius of curvature at the surface protrusions following lateral growth as deposition proceeds. The desorption of thiourea during deposition has also been reported by Pablo et al. (2002).

*Table 4.2. Spot elemental composition of specific sites from an electrodeposit obtained from an electrolyte containing 10 mg/ℓ thiourea*

| Site | Elemental composition (Wt%) | | | | | | |
|---|---|---|---|---|---|---|---|
| | Cu | S | N | O | Ni | Fe | C |
| A | 99.19 | - | - | 0.37 | - | - | 0.56 |
| B | 96.86 | - | - | 0.40 | - | - | 2.74 |
| C | 96.53 | 0.03 | - | 0.54 | - | - | 2.90 |
| D | 98.28 | 0.05 | - | 0.38 | - | - | 1.30 |
| E | 97.75 | - | - | 0.33 | - | - | 1.92 |

#### 4.2.2.2. Effects of excess thiourea amounts on cathode quality

Figure 4.18 [A] to [C] show digital images of the electrodeposits that were obtained in the presence of varying concentrations of thiourea. At 100 % excess thiourea, a coherent and homogeneous electrodeposit was obtained as can be seen from Figure 4.18 [A]. However at higher concentrations of 200 % and 320 % excess thiourea the quality of the deposits obtained deteriorated. The deposits became brittle and could only be harvested in the form of flakes as in the case of 320 % excess thiourea concentration (Figure 4.18 [C]). The formation of brittle deposits in the presence of high concentrations of thiourea was also reported by Andersen et al. (1983). It should, however, be mentioned that the actual thiourea concentration referred to as high by Andersen et al. (1983) was not specified. The weight of the deposits obtained was also observed to decrease with increasing thiourea concentration.

The poor deposition characteristics observed in the presence of high thiourea concentrations agrees well with observations made in the cyclic voltammetry tests (refer to Section 4.1.4). Thiourea was observed to inhibit the cathodic reduction of cupric ions. An increase in the reduction overpotential in the presence of thiourea was observed thus confirming its inhibiting effect on the cathodic reduction reaction. This increase in the overpotential implies that an overpotential higher than the standard copper deposition overpotential was required in order to deposit enough metal. This could be the reason as to why low weight deposits were observed with increased excess thiourea concentration considering that the electrowinning tests were done at a constant potential. In the

cyclic voltammetry tests done at 320 % excess thiourea a second oxidation peak ascribed to the re-oxidation of copper-thiourea complexes was observed (see Figure 4.6). Indeed as suggested by Fabricius et al. (1994) and as has been observed in this study, the appearance of the second anodic peak signifies a thiourea concentration too high for the formation of a coherent and homogenous deposit. This is affirmed by the quality of deposit obtained at 320 % excess thiourea concentration as can been seen from Figure 4.18 [C].

A reasonable explanation of the poor deposition characteristics observed in the presence of high thiourea concentrations could also be drawn from processes taking place in the electric double layer and the diffusion layer during deposition. As discussed in Section 2.4.4.2 one of the probable mechanisms through which thiourea acts is by its adsorption on the active sites during copper discharge. In the process of covering the active sites, thiourea displaces water molecules from the electric double layer and as such altering the composition and the properties of the double layer through which electron discharge occurs (Stankovic and Vukovic, 1996).

The thiourea also forms a layer of adsorbed molecules within the double layer through which hydrated copper ions must penetrate to approach the electrode surface where charge transfer occurs and subsequent incorporation into the metal lattice occurs (Stankovic and Vukovic, 1996). It can therefore be suggested that as the concentration of thiourea increases, the metal ions find it increasingly difficult to penetrate through this layer of adsorbed thiourea molecules. This action results in an increase in the charge transfer overpotential and as such inhibits metal deposition.

[A] [B] [C]

*Figure 4.18. Digital images of electrodeposits obtained in the presence of varying concentrations of thiourea [A] 100 %, [B] 200 % and [C] 320 % excess thiourea*

Figure 4.19 shows the SEM image of the deposit obtained in the presence of 100 % excess thiourea. Although a relatively coherent and homogeneous electrodeposit was obtained, the surface quality of this deposit was observed to be poor. This can be inferred from both the digital and SEM images, Figure 4.18 [A] and Figure 4.19 respectively. The deposit surface was uneven exhibiting a degree of roughness. It would have been expected that in the presence of thiourea a known leveling agent a smooth deposit would be obtained. However, that was not the case, as evidenced by the quality of the deposit obtained as shown by Figure 4.19. This may be ascribed to an imbalance in the concentration of thiourea as suggested by Nuňez (2005). Nuňez (2005) suggested that a high thiourea concentration results in a sudden increase in the local overpotential at some sites, thus resulting in a breakdown of such passivated surfaces and hence perpetuating growth at such sites resulting in an uneven electrodeposit. Stankovic and Vukovic (1996) also suggested that thiourea exhibits a limit on the inhibition-concentration relationship beyond which its preferred effects may not observed.

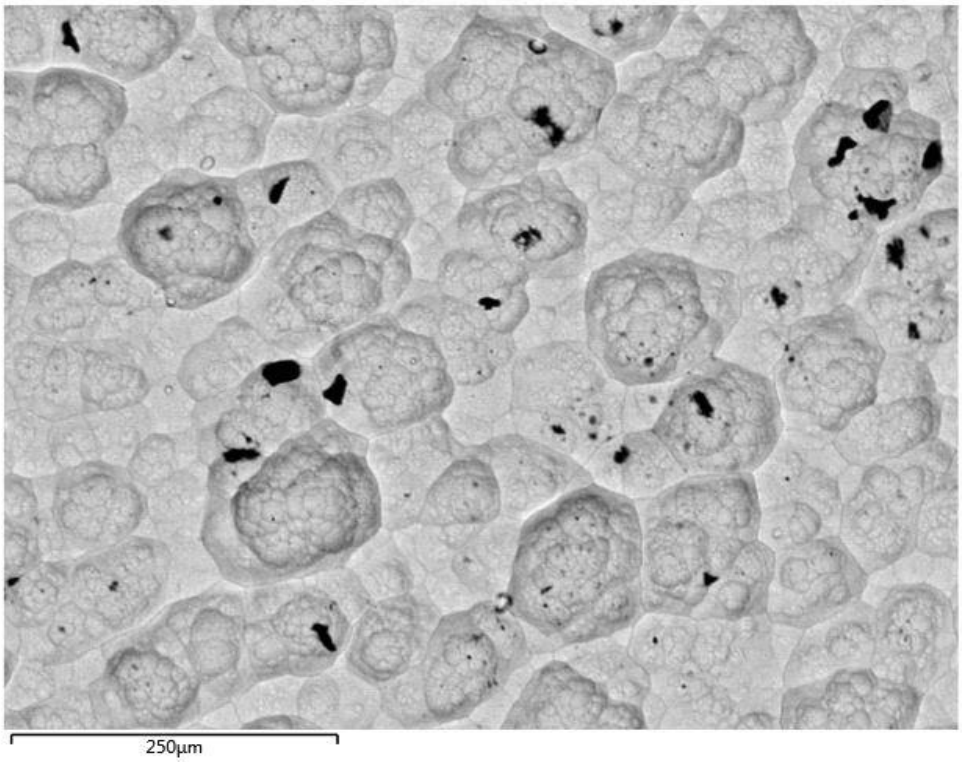


*Figure 4.19. Scanning electron microscopy (SEM) image of an electrodeposit obtained from a solution containing 100 % excess thiourea at constant potential and 25˚C.*

The impurity levels in the electrodeposits obtained in the absence and presence of thiourea is shown by Figure 4.20. It is evident from Figure 4.20 that in the presence of thiourea a substantial amount of impurities carbon, sulphur and nitrogen were detected. Figure 4.21 shows an SEM image of impurities carbon and sulphur incorporated into an electrodeposit produced at 200 % excess thiourea. The distribution of the two impurities is as shown by Figure 4.22 [B] and [D]. It can be inferred from Figure 4.21 that the impurities were directly embedded in the metal matrix.

As has been discussed in Section 2.4.2 carbon, sulphur and nitrogen are constituent elements of the thiourea molecule whose chemical formula is given as $CH_4N_2S$. The presence of carbon, nitrogen and sulphur in electrodeposits produced from thiourea containing electrolytes has also been reported elsewhere (Tadesse et al., 2013; Kang et al., 2008; Alodan and Smyrl, 1998). However Kang et al. (2008) argued that the levels of nitrogen and carbon detected in their

deposits were low and therefore concluded that thiourea was not incorporated in the deposit but rather CuS was responsible for the blocking of the electrode active sites. In contrast Tadesse et al. (2013) concluded that the presence of nitrogen and sulphur in the deposits could be as a result of direct incorporation of thiourea in the metal lattice. In this study it was observed that the levels of nitrogen, sulphur and carbon had a high dependency on the concentration of thiourea in the electrolyte. The impurities were observed to increase with increasing thiourea concentration. It is therefore suggested that the impurities may have originated from thiourea itself.

The probable mechanisms through which carbon, sulphur and nitrogen maybe incorporated in the electrodeposits include direct incorporation of thiourea reagent molecules as suggested by Nuňez (2005) or through the formation on copper-thiourea complexes. Thiourea may also be incorporated in the electrodeposit through the formation of strong chemical bonds with copper species. Rodriguez et al. (1991) reported that the nitrogen atom in nitrogen containing additives such as thiourea forms strong and stable adsorbates through chemisorption onto copper surfaces. This action coupled with the high concentration of thiourea considered in this study may have resulted into the incorporation of substantial amounts of the three impurities in the electrodeposits. Thiourea is also reported to form strong chemical bonds with cupric ions through its sulphur atom. Some specific spots analysed by EDX and the corresponding elemental compositions are shown in Figure 4.23 and Table 4.3 respectively. It must be mentioned that the spot analysis elemental composition did not however show any direct relationship with thiourea stoichiometric composition.

As discussed in Section 2.4.4.2 thiourea may be hydrolysed or indeed reduced according to Equation 2.54 and Equation 2.55 respectively producing $H_2S$. The $H_2S$ then reacts with copper ions forming a sparingly soluble CuS. The CuS participates in blocking the electrode active sites and may thus be incorporated in the deposit as deposition proceeds leading to deposit contamination with sulphur.

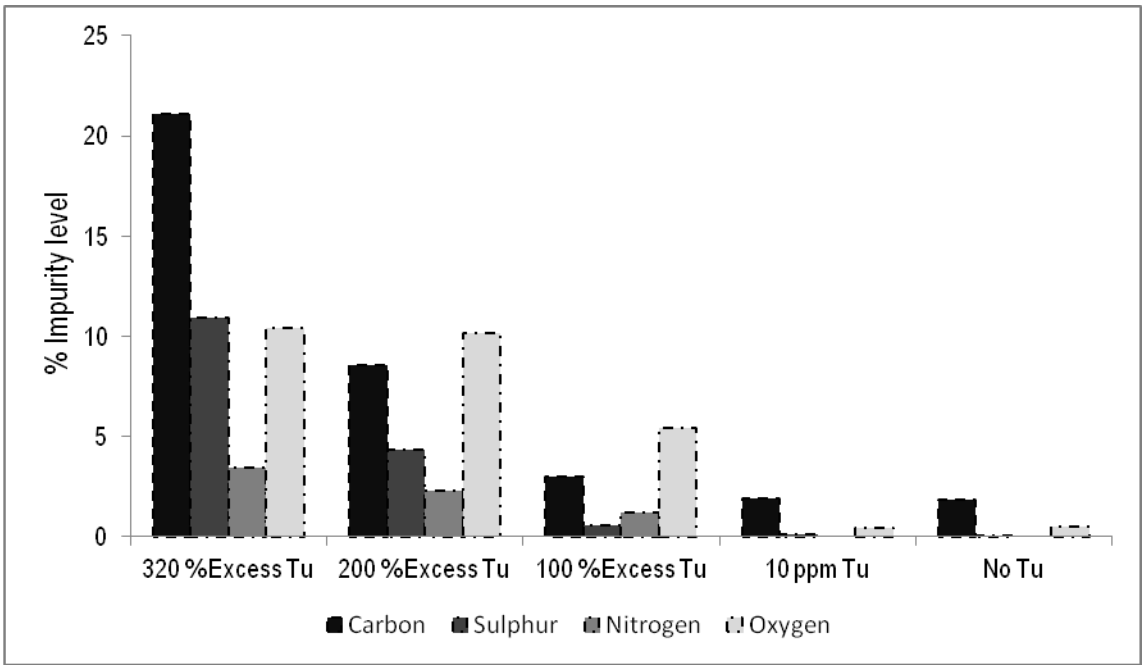


*Figure 4.20. Impurity levels detected from electrodeposits obtained the presence of varying concentrations of thiourea.*

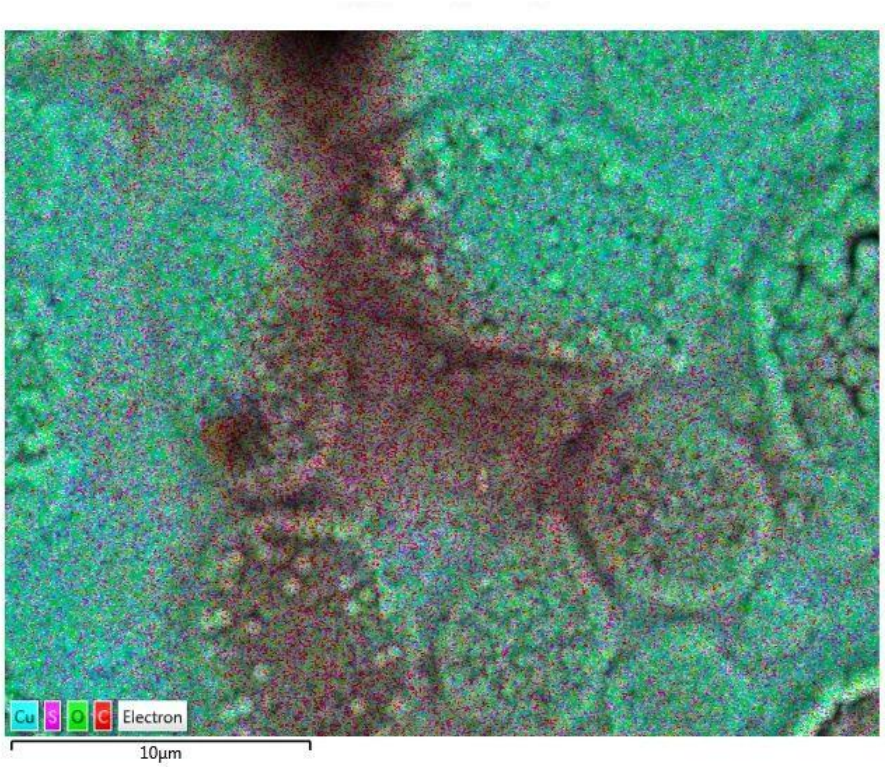


*Figure 4.21. Scanning electron image of an electrodeposit obtained from an electrolyte containing 200 % excess thiourea showing incorporated impurities carbon and sulphur*

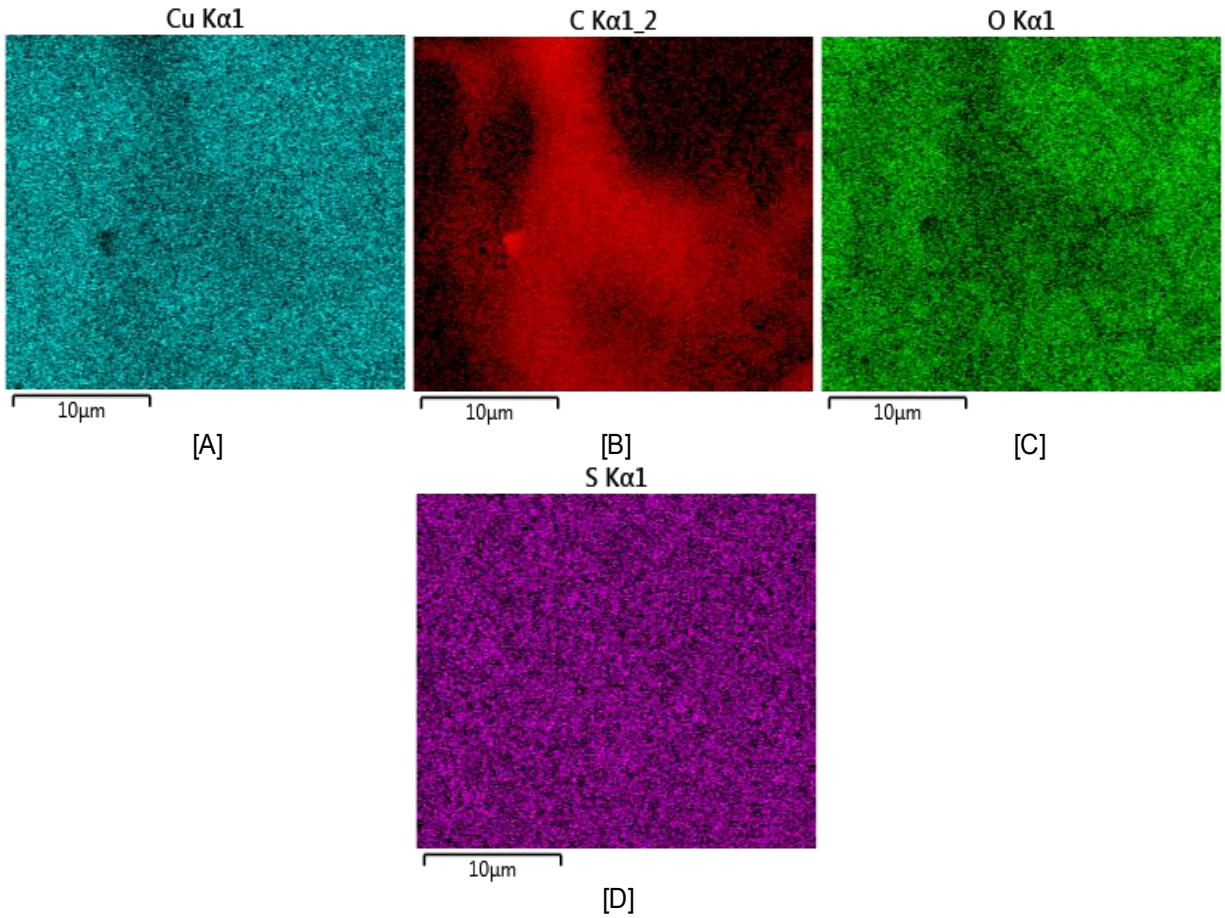


*Figure 4.22. Elemental maps showing the distribution of elements in an electrodeposit obtained from an electrolyte containing 200 % excess thiourea, [A]-copper, [B]-carbon, [C]-oxygen and [D]-sulphur*

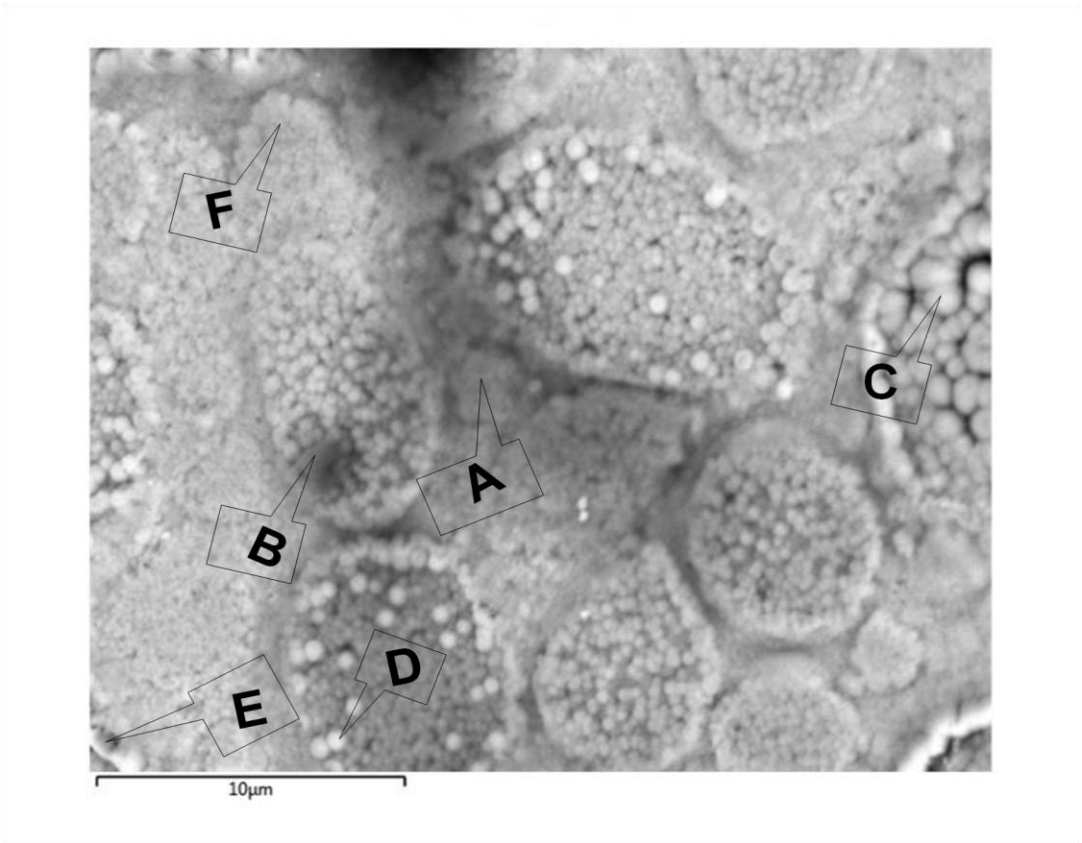


*Figure 4.23. Scanning electron image of an electrodeposit obtained from an electrolyte containing 200 % excess thiourea showing some specific sites sampled.*

*Table 4.3. Spot elemental composition of specific sites from an electrodeposit obtained from an electrolyte containing 200 % excess thiourea.*

| Site | Elemental composition (Wt %) | | | | | | |
|---|---|---|---|---|---|---|---|
| | Cu | S | O | N | C | Ni | Fe |
| A | 42.99 | 8.01 | 4.81 | - | 44.20 | - | - |
| B | 37.56 | 8.56 | 5.82 | - | 48.06 | - | - |
| C | 77.45 | 3.17 | 10.76 | 0.81 | 7.81 | - | - |
| D | 89.94 | 1.34 | 7.32 | - | 1.40 | - | - |
| E | 84.48 | 1.16 | 9.19 | 0.77 | 4.40 | - | - |
| F | 70.64 | 0.97 | 7.95 | 1.07 | 19.38 | - | - |

#### 4.2.2.3. Effects of excess thiourea on electrowinning efficiency

Figure 4.24 shows the current-time graphs obtained in the presence of varying concentrations of thiourea. The current obtained was seen to decrease with increasing thiourea concentration. The average cathodic current observed in the absence of thiourea was 56.55 mA. The introduction of 10 mg/ℓ thiourea resulted into a drop in the average current to about 49.43 mA. In the presence of excess thiourea the current dropped to 38.54, 37.80 and 23.40 mA for 100, 200 and 320 % excess respectively.

Oniciu and Muresan (1991) reported that most organic additives employed in metal deposition increase the cathode polarisation thus resulting into a reduced current density at a constant potential. Bockris and Razumney (1967) also reported that adsorbed additives or inhibitors reduce the cathodic current during constant potential metal deposition due to their negative catalytic activity on the deposit electrocrystallisation process. The reduction in the current observed in this study may therefore be ascribed to the polarisation of the platinum working electrode by adsorbed thiourea. The polarising effect (reduction in current) of thiourea observed in the electrowinning tests is consistent with observations made in the cyclic voltammetry tests (refer to Section 4.1.4). The presence of thiourea in the electrolyte during cyclic voltammetry resulted into a shift (or an increase) in the cathodic overpotential to more negative values. This is an indication of electrode polarisation through electrode active site coverage by thiourea. Bockris and Razumney (1967) further reported that due to an increase in the concentration of an additive (and thus a subsequent increase in coverage) the overpotential increases such that the relationship $\frac{d|\eta|}{d\theta}$ increases and becomes more positive. As a consequence the cathode current decreases and a subsequent reduction in the current density will be observed.

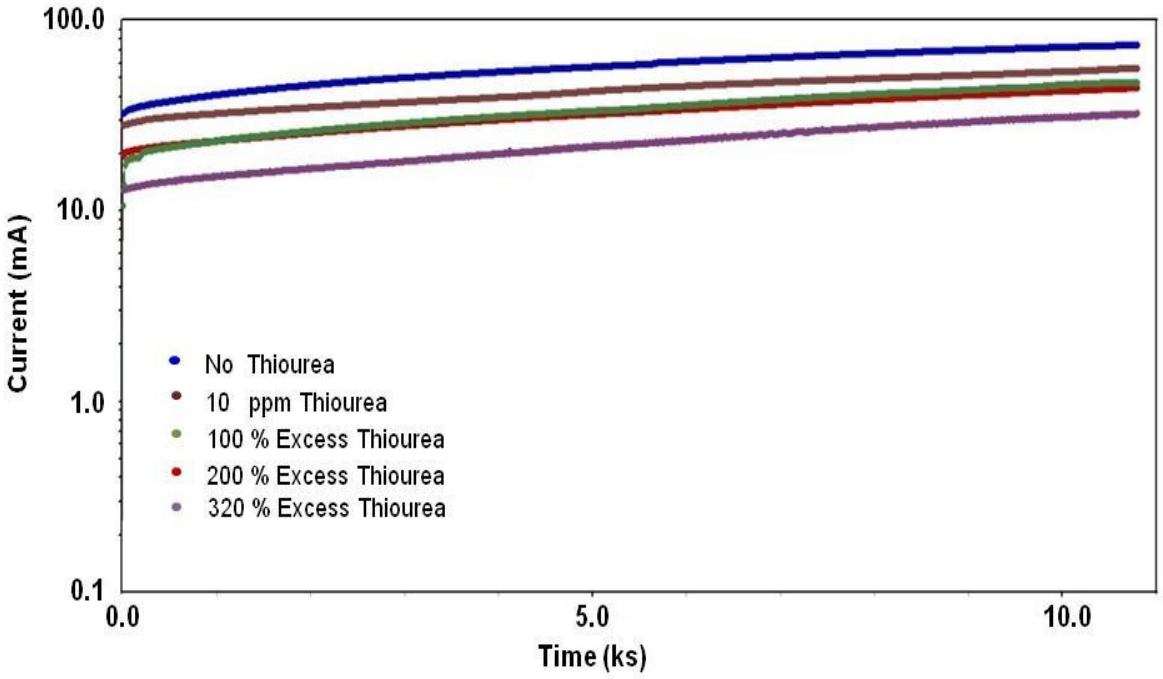


*Figure 4.24. Current transients showing the effect of varying thiourea concentration on the cathodic current during cupric ion reduction*

Figure 4.25 summarises the current efficiencies obtained in the presence of varying thiourea concentrations. The current efficiencies obtained had a strong dependency on the concentration of thiourea in the electrolyte. It was observed that the current efficiencies dropped with increasing thiourea concentration. The highest drop in the current efficiency was observed at a maximum thiourea concentration of 320 % excess. The drop in the current efficiency could be ascribed to the polarising effect of thiourea on the electrode. In this study, the polarising effect of thiourea has been confirmed in both the cyclic voltammetry and electrowinning tests. As mentioned in Section 2.1.3 electrode polarisation results in a drop in the efficiency of the electrochemical processes taking place at the electrode. Winand (1992) also proposed that a drop in the current efficiency during deposition in the presence of an additive could be as a result of simultaneous reduction of the additive. This then results in a drop in the partial current density required for the reduction of metal ions and subsequently of the current efficiency. As discussed in Section 2.4.4.2 thiourea may be reduced according to Equation 2.54 and Equation 2.55. The decrease in the current

efficiency observed could therefore be attributed possible simultaneous thiourea reduction.

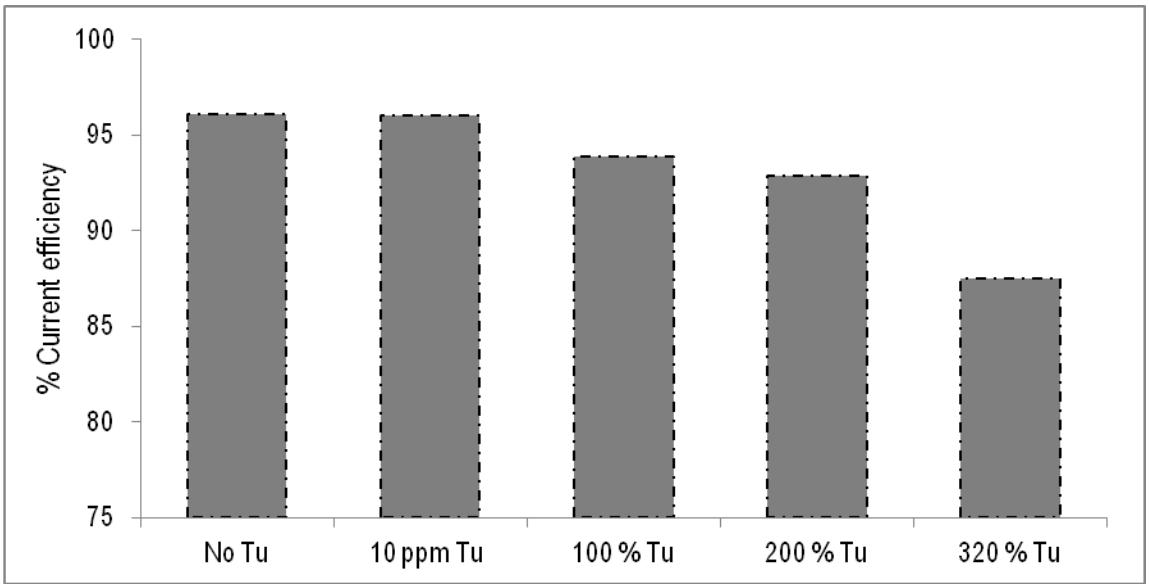


*Figure 4.25. Current efficiencies obtained from electrowinning tests done in the presence of varying thiourea concentrations.*

### 4.2.2.4. Electrowinning at higher potential

It was desired to observe if a higher deposition potential would mitigate the adverse effects of excess thiourea on electrowinning efficiency and deposit quality. Therefore an electrowinning test was conducted at a potential of 600 mV. The concentration of thiourea considered in this test was 320 % excess. Figure 4.26 shows the digital image of the electrodeposit obtained at 600 mV. As can be seen a flaky and brittle deposit similar to that obtained at 400 mV and 320 % excess thiourea was obtained. However the weight of the deposit obtained at 600 mV was higher than that obtained at 400 mV. This is consistent with the higher cathodic current observed at 600 mV in comparison to that observed at 400 mV as can be seen from Figure 4.27. The current efficiency was also higher at 600 mV, namely 90.47 % compared to 87.46 % obtained at 400 mV. Figure 4.28 shows a comparison of the levels of carbon, sulphur and nitrogen detected in both deposits produced at 400 and 600 mV. It can be seen from Figure 4.28 that the deposition potential could not help in mitigating the adverse effects of excess

thiourea on deposit chemical quality. The levels of nickel and iron detected in this deposit were relatively low at 1.95 % and 0.23 % respectively.

*Figure 4.26. Digital image of electrodeposit produced at 600 mV in the presence of 320 % excess thiourea.*

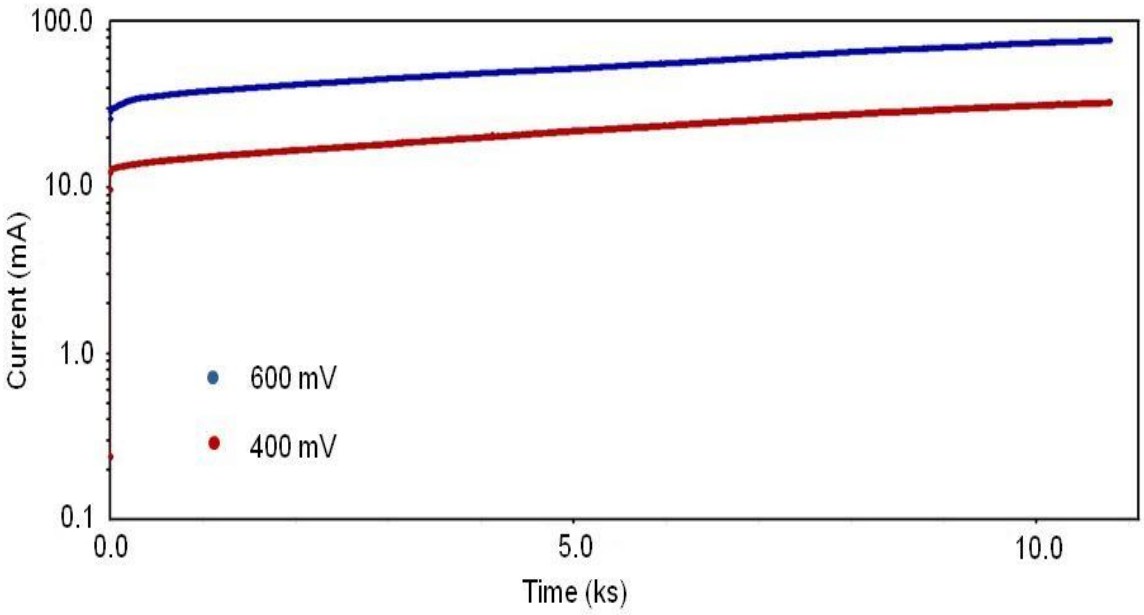


*Figure 4.27. Current transients showing cathodic current at two different potentials in the presence of 320 % excess thiourea.*

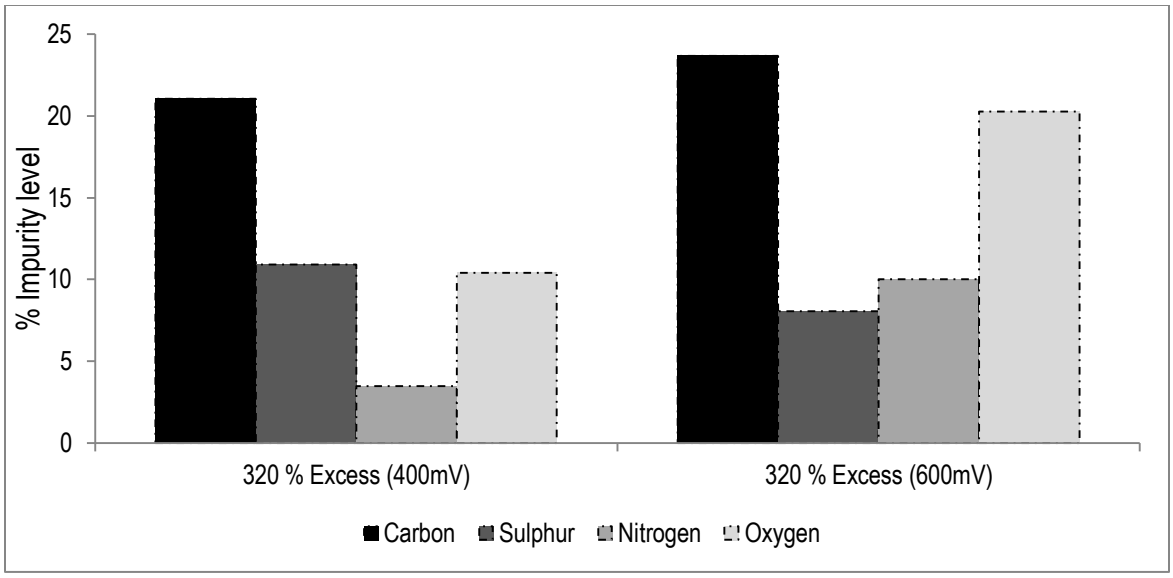


*Figure 4.28. Comparison of impurity levels, carbon, sulphur and nitrogen in electrodeposits produced at different potentials in the presence of 320 % excess thiourea.*

## 4.2.3. Electrowinning in the presence of selenium

### 4.2.3.1. Effects of selenium on cathode morphology

Figure 4.29 [A] to [C] show digital images of the electrodeposits that were obtained in the presence of varying concentrations of selenium. As can be seen the electrodeposits appeared dark in colour with the intensity of the darkness increasing with increased selenium concentration. The dark appearance of the electrodeposits is consistent with the observation made in the cyclic voltammetry tests. A dark coating on the electrode surface was also observed in the cyclic voltammetry tests done in an electrolyte containing 0.1 M copper and 150 mg/ℓ selenium (see Figure 4.12). The appearance of this dark coating on the electrodeposits could be attributed to the formation of a copper-selenide compound as discussed in Section 4.1.5. However it is noteworthy that the formation of the black mass as suggested in Section 4.1.5 according to Equation 4.9 occurred at about 0.11 V vs. SCE. It is therefore imperative to state that the formation of blackened electrodeposits during the electrowinning tests may have occurred through a different reaction pathway considering that the electrowinning tests were done at a constant potential of 0.4 V vs. SCE. It is

therefore suggested that the formation of the copper selenium compound during the electrowinning tests may have occurred through Equation 2.73 whose standard electrode potential is 0.67 V vs. SHE or 0.426 V vs. SCE.

The electrodeposits obtained in the presence of selenium were also observed to exhibit very poor edge quality. Such growth was not observed from the test done in the absence of selenium. The edge quality was observed to deteriorate with increased selenium concentration. It is however not known at this stage why the presence of selenium in the electrolyte resulted into poor electrodeposit edge quality.

*Figure 4.29. Digital images of electrodeposits obtained in the presence of varying concentrations of selenium [A] 20 mg/ℓ, [B] 50 mg/ℓ and [C] 150 mg/ℓ*

Figure 4.30 to Figure 4.32 show the SEM images of the electrodeposits obtained from solutions containing selenium at different concentrations. It can be seen from the images that the presence of selenium in the electrolyte resulted into the formation of nodules on the electrode surface. The size of the nodules was observed to increase with increasing selenium concentration in the electrolyte. Selenium particulates have been reported to act as seeds for nodule formation. The formation of nodules in the presence of selenium has also been reported by other researchers (Andersen et al., 1983). Andersen et al. (1983) reported that selenium being a good semi–conducting element assumes the prevailing electrode potential once it comes into contact with the cathode substrate. This allows cupric ions to deposit on the selenium particulate surface as well as the

planar electrode surface. The growth of copper from the two fronts (planar electrode and selenium particulate) occurs sufficiently such that the selenium particulate is cemented into the copper deposit matrix.

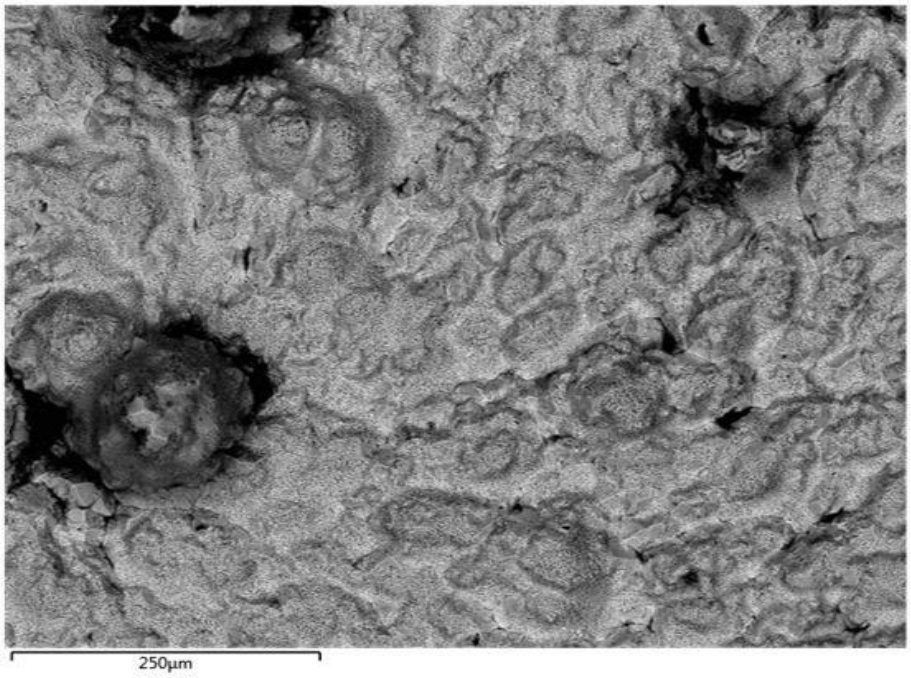


*Figure 4.30 . Scanning electron microscopy (SEM) image of an electrodeposit obtained from an electrolyte containing 20 mg/ℓ Se at constant potential and 25˚C.*

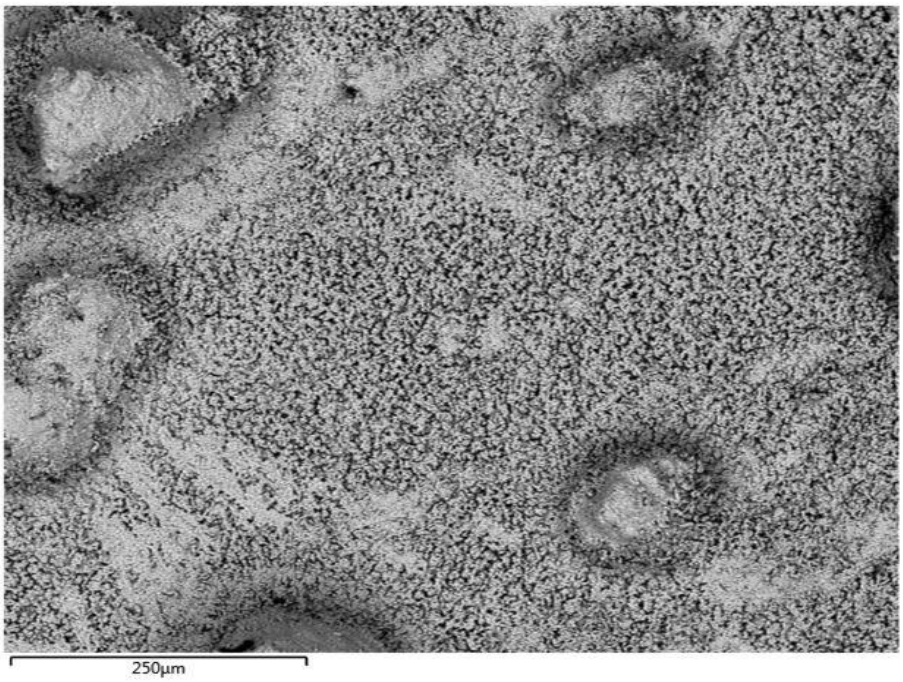


*Figure 4.31. Scanning electron microscopy (SEM) image of an electrodeposit obtained from an electrolyte containing 57 mg/ℓ Se at constant potential and 25˚C*

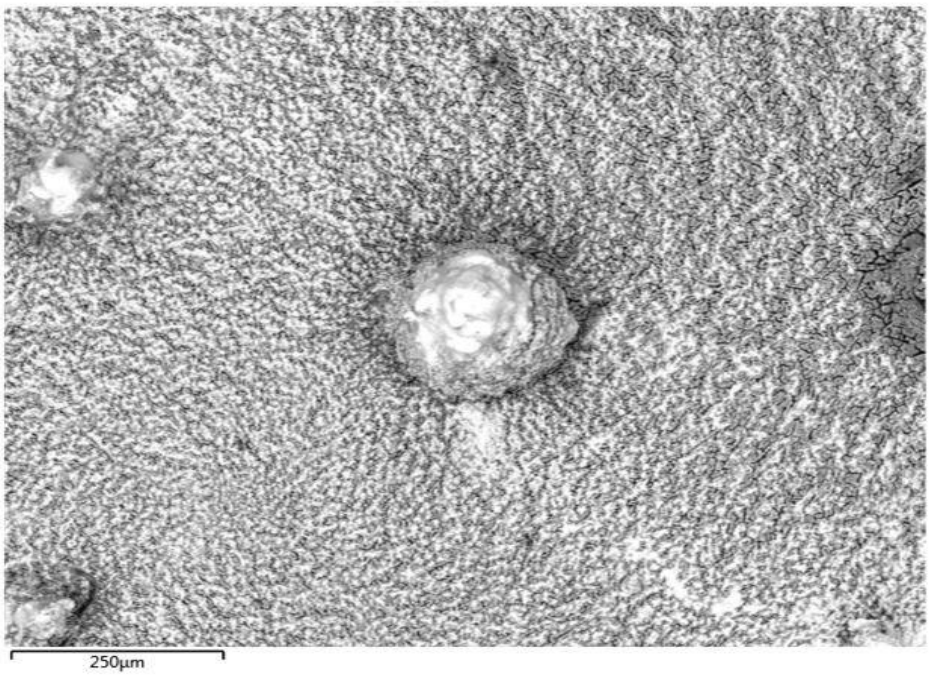


*Figure 4.32. Scanning electron microscopy (SEM) image of an electrodeposit obtained from an electrolyte containing 150 mg/ℓ Se at constant potential and 25˚C*

The mechanism of nodule formation in the presence of selenium as suggested by Andersen et al. (1983) agrees well with observations made in this study. It was observed through energy dispersive spectroscopy that high selenium concentrations were found around the nodules. Figure 4.33 shows an image of an electrodeposit produced in the presence of selenium, the associated elemental maps are shown by Figure 4.34 [A] to [F]. It can be seen from Figure 4.34 [C] that at or around the nodules the concentration of selenium was higher as compared to the planar surface. This was confirmed by doing spot analysis of some random areas on one of the nodules. It was revealed that indeed the concentration of selenium was highest on the nodules as be seen from Figure 4.35 and Table 4.4. The concentration of other elements such as iron, nickel and carbon was low as can be seen from Figure 4.34 [D] to [F].

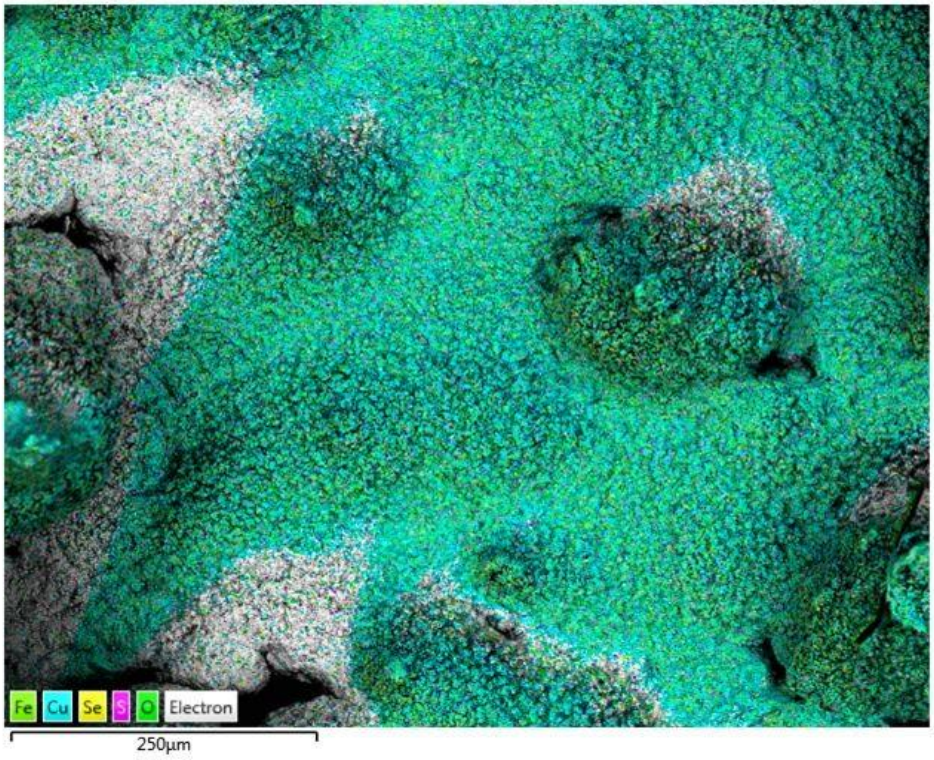


*Figure 4.33. Scanning electron microscopy image of an electrodeposit obtained from an electrolyte containing 150 mg/ℓ Se at constant potential and 25˚C*

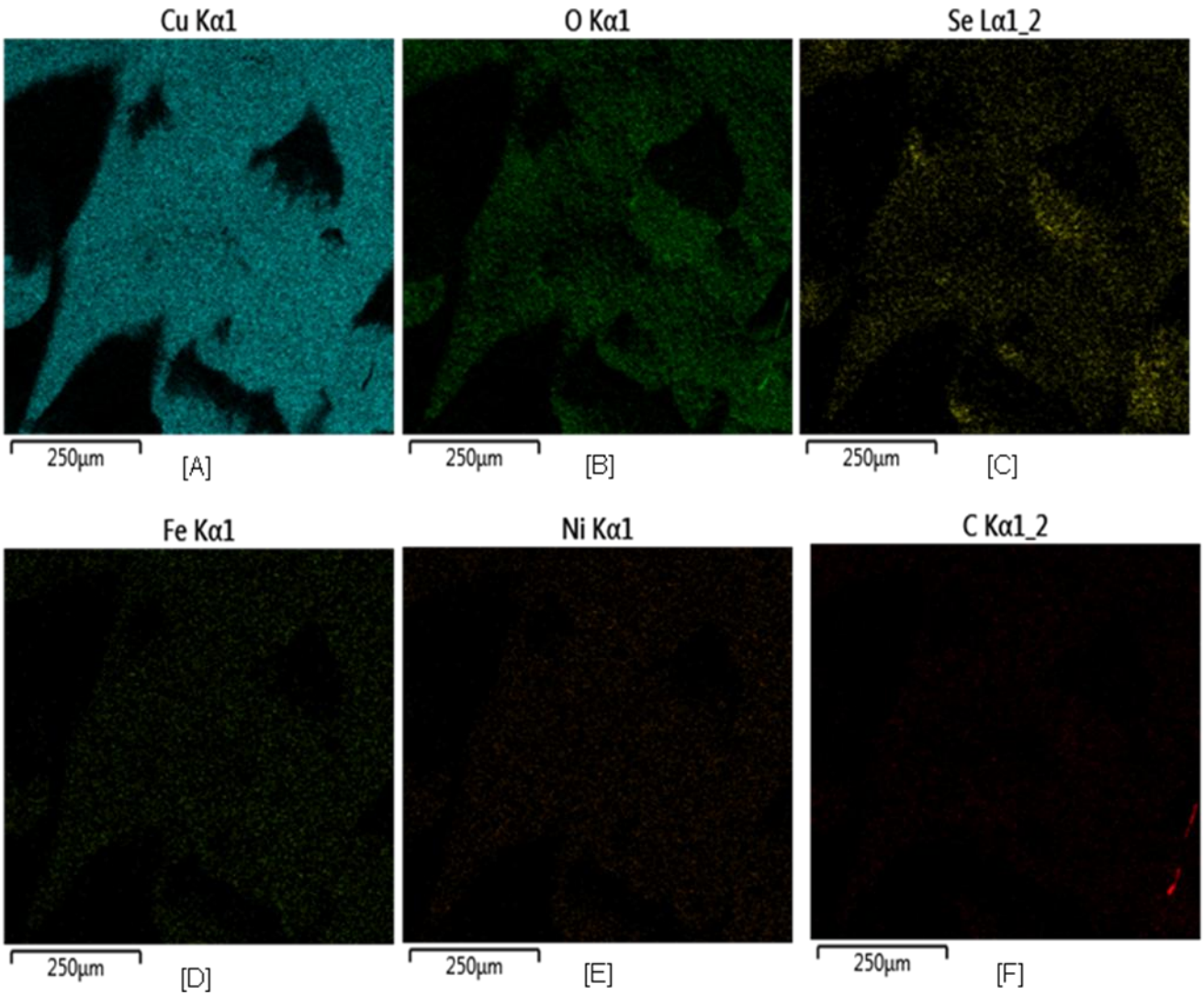


*Figure 4.34. Elemental maps showing the distribution of elements on an electrodeposit obtained from an electrolyte containing 150 mg/ℓ Se, [A]-copper, [B]-oxygen, [C]-selenium, [D]-iron, [E]-nickel and [F]-carbon*

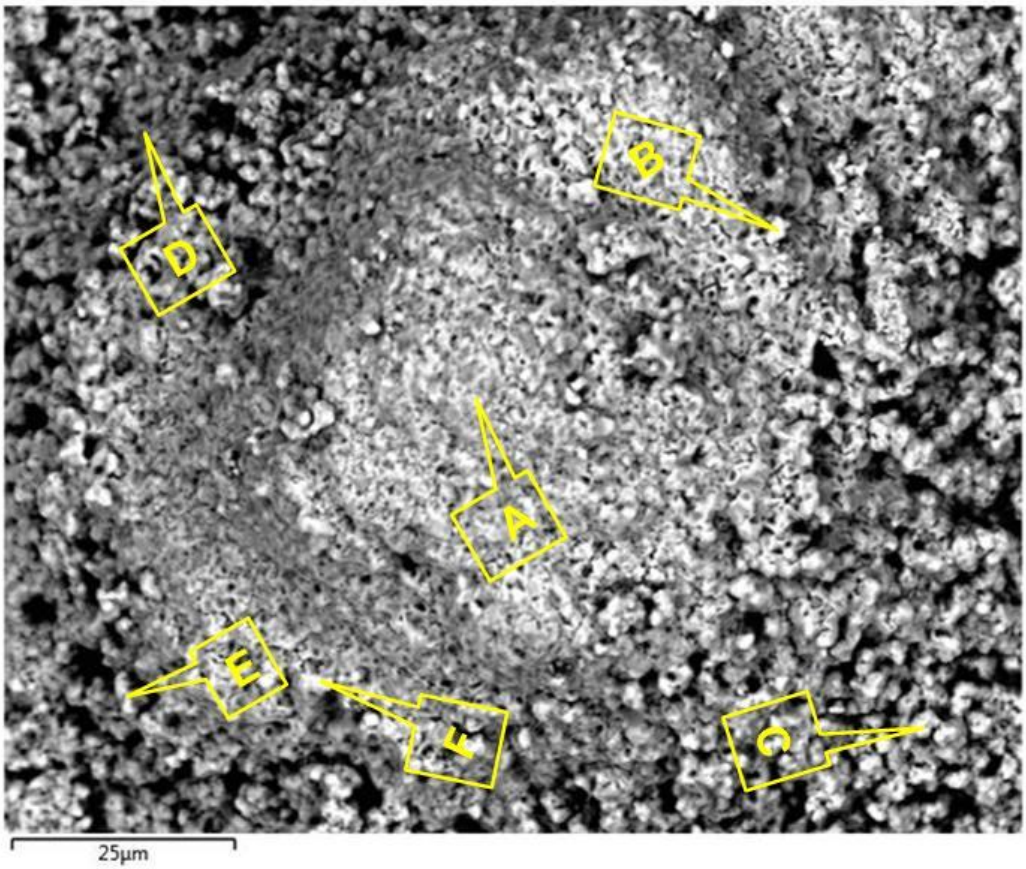


*Figure 4.35. Scanning electron microscopy (SEM) image of a nodule formed on the surface of an electrodeposit obtained from an electrolyte containing 150 mg/ℓ Se*

*Table 4.4. Spot elemental composition of specific sites from a surface nodule observed on an electrodeposit obtained from an electrolyte containing 150 mg/ℓ Se*

| Site | Elemental composition (Wt %) | | | | | | |
|---|---|---|---|---|---|---|---|
| | Cu | S | O | Ni | Fe | C | Se |
| A | 76.29 | 0.13 | 9.12 | - | - | 3.10 | 11.36 |
| B | 77.25 | - | 6.28 | - | - | 3.95 | 12.51 |
| C | 78.08 | 0.14 | 10.29 | 0.21 | - | 4.14 | 7.14 |
| D | 92.90 | - | 4.11 | - | - | 1.96 | 1.03 |
| E | 78.72 | - | 14.68 | - | - | 4.21 | 2.39 |
| F | 75.43 | - | 10.87 | - | - | 4.70 | 9.01 |

#### 4.2.3.2. Effects of selenium on electrowinning efficiency

The effects of selenium on the copper electrowinning efficiency were investigated at three levels as shown in Table 3.2. In the presence of selenium the cathodic current was observed to increase significantly at a concentration of 150 mg/ℓ as shown by Figure 4.36. The increase in the cathodic current was not significant at selenium concentrations of 20 mg/ℓ and 57 mg/ℓ. The increase in the cathodic current in the presence of selenium can be attributed to side reactions taking place other the reduction of copper ions. It was evident in the cyclic voltammetry tests that selenium takes part in chemical reactions with copper ions leading to the formation of copper selenide compounds (refer to Section 4.1.5). The formation of the copper selenide compound was further confirmed in the electrowinning tests as discussed in Section 4.2.3.1. As has been discussed in Section 4.1.5 the formation of the copper selenide compound showed a strong dependency on the concentration of selenium in the electrolyte. In the cyclic voltammetry tests done in the presence of 150 mg/ℓ selenium a black mass covered the electrode surface (see Figure 4.12). This is consistent with findings made in the electrowinning tests were a significant increase in the cathodic current was observed in the presence of 150 mg/ℓ selenium.

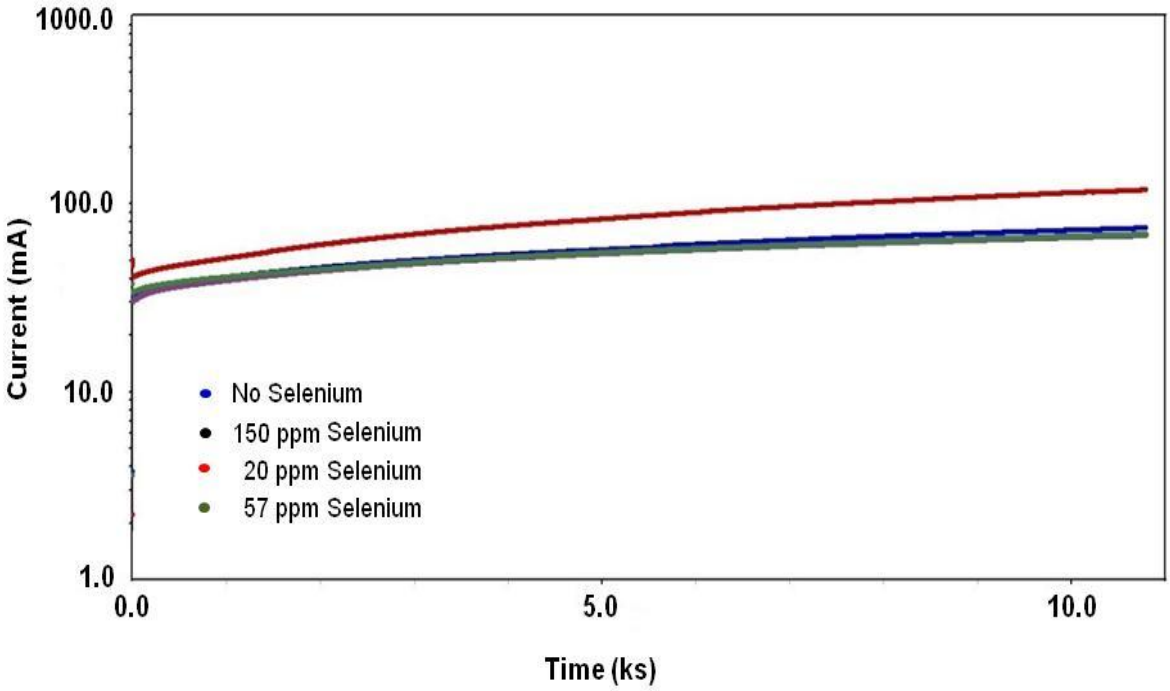


*Figure 4.36. Current transients showing the effects of varying selenium concentration on the cathodic current during cupric ion reduction*

The current efficiencies obtained in the presence of selenium were also negatively affected as shown by Figure 4.37. At 20 mg/ℓ selenium a current efficiency of 95.96 % was obtained. At selenium concentrations of 57 mg/ℓ and 150 mg/ℓ, current efficiencies of 94.78 % and 85.35 % were observed respectively. The drop in the current efficiencies in the presence of selenium may be attributed to current consumption through the simultaneous reduction of selenium according to Equation 2.73 to Equation 2.74 as suggested by Baral et al. (2014) and Bard et al. (1985). The drop in the current efficiency observed in this study is consistent with findings made by Baral et al. (2014)

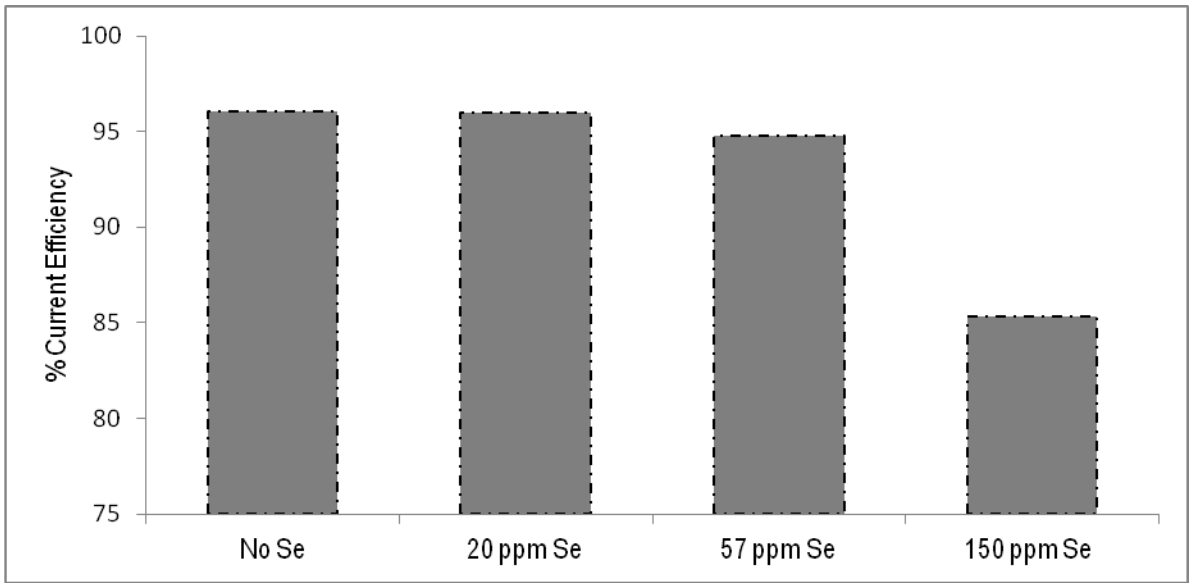


*Figure 4.37. Current efficiencies obtained in the absence and presence of varying selenium concentration*

# 5. Conclusions and Recommendations

The electrochemical behaviour of cupric ions in the presence of varying concentrations of thiourea and selenium has been investigated. It has been observed that both thiourea and selenium interact with the cathodic reduction of cupric ions. The effects of both thiourea and selenium on the morphology and chemical quality of the electrodeposits as well as the electrowinning efficiency were also successfully investigated.

The conclusions drawn from the aforementioned studies are summarised in the following sections:

## 5.1. Effects of excess thiourea on copper electroreduction

The effects of excess thiourea on the electroreduction of copper ions have been investigated using cyclic voltammetry. It has been shown in this study that excess thiourea polarises the electrode resulting into a significant increase in the electrode overpotential. This was evident at all the three levels of excess thiourea investigated (100 %, 200 % and 320 %). The polarising effect observed showed a strong dependency on the concentration of thiourea in the electrolyte. The electrode polarisation increased with increasing thiourea concentration. As a result of the electrode polarisation the efficiency of cupric ion reduction was lowered. The reduction overpotential increased from 200 mV vs. SCE in the absence of thiourea to between 300 mV and 450 mV vs. SCE in the presence of excess thiourea. Further, an observed decrease in the cupric reduction peak as well as the oxidation peak was made. The observation was ascribed to electrode polarisation.

## 5.2. Effects of excess thiourea on cathode quality and electrowinning efficiency

It is clear from the experimental results obtained that excess thiourea negatively affected the morphology and the chemical composition of copper electrodeposits.

Substantial amounts of impurities carbon, sulphur and nitrogen were detected by EDX from the deposits obtained in the presence of thiourea. The impurity levels increased with increasing thiourea concentration. At lower thiourea concentrations only trace amounts of sulphur were detected.

The electrodeposits obtained at concentrations of 200 % and 320 % excess thiourea were brittle and flaky. At 100 % excess thiourea, a coherent deposit was obtained but the deposit surface was rough. The preferred effects of thiourea as a leveling agent through its ability to retard growth at the electrode active sites were not observed at the excess amounts investigated.

The effects of excess thiourea on the electrowinning efficiency were evaluated in terms of the current efficiency and the current density. The current efficiency showed a strong dependency on the thiourea concentration. A decrease in current efficiency was observed with increasing thiourea concentration. A current efficiency of 93.88 % was observed at 100 % excess thiourea while at 200 % and 320 % excess thiourea, current efficiencies of 92.87 % and 87.46 % were obtained, respectively.

## 5.3. Effects of selenium on copper electroreduction

It has been shown through cyclic voltammetry that selenium interacts with cupric ions at the negative electrode during copper electrodeposition. A second cathodic peak was encountered during the electroreduction of cupric ions in the presence of selenium. This second cathodic peak was ascribed to the simultaneous reduction of cupric ions and selenium. This observed interaction between copper and selenium implies that the efficiency of the copper reduction reaction is lowered. Part of the current required for cupric ion reduction is consumed by the selenium ion reduction.

## 5.4. Effects of selenium on cathode quality and electrowinning efficiency

The influence of selenium on the morphology of copper deposits was evaluated using SEM. It was found that selenium led to the formation of nodules on the electrodeposit surface. The formation of nodules in the presence of selenium was attributed to the semiconducting properties of selenium. Selenium assumes the electrode potential once in contact with the electrode surface. As a consequence copper ions deposit onto the selenium particulates leading to the formation of nodules (Andersen et al., 1983). It was also observed that selenium contaminated the electrodeposits. The current efficiency was observed to drop significantly at a selenium concentration of 150 mg/ℓ. A marginal drop in the current efficiency was also observed at concentrations of 57 mg/ℓ and 20 mg/ℓ.

## 5.5. Suitability of thiourea as a Se/Te precipitating agent

The results obtained in this study have indicated that the presence of excess thiourea (as proposed for Se and Te precipitation) is detrimental to copper electrowinning. It has been shown through electrochemical and electrowinning tests that excess thiourea inhibits the cathodic reduction of copper ions and leads to the formation of poor quality cathodes. The cathodes produced in the presence of excess thiourea were highly contaminated with carbon, sulphur and nitrogen which are thiourea constituent elements. The presence of excess thiourea amounts also resulted in a drop in the current efficiencies. The current efficiencies dropped to 93.88 %, 92.87 % and 87.46 % in the presence of 100 %, 200 % and 320 % excess thiourea compared to 96.06 % in the absence of thiourea.

## 5.6. Recommendations

The following are the recommendations to be considered regarding this work:

- Experimental work in which other additives with depolarizing properties are used should be considered to try and counter the polarising effect of excess thiourea observed in this study.
- Electrowinning tests using an electrolyte from which selenium and tellurium have been removed in the manner proposed by the previous work should be considered. This will assist in consolidating the current work and the work which provided impetus to this study.

# 6. References

Alekperov, A., 1974. Electrochemistry of selenium and tellurium. *Russian Chemical Reviews,* 43(1974), pp. 235-247.

Alodan, M. & Smyrl, W., 1998. Effect of thiourea on copper dissolution and deposition. *Electrochimica Acta,* 44(1998), pp. 299-309.

Andersen, T. N., Pitt, C. & Livingston, L., 1983. Nodulation of electrodeposited copper due to suspended Particulate. *Journal of Applied Electrochemistry,* 13(1983), pp. 429-438.

Andersen, T., Wright, C. & Richards, K., 1973. *Important electrochemical aspects of electrowinning copper from acid leach solutions.* Salt Lake City Utah, Paper presented at the International Symposium on Hydrometallurgy.

Arman, E., Yazici, E. Y., Haci, D. & Faith, E., 2012. *The influence of impurity ions on the eletcrowinning of copper from waste PCBs leaching solutions.* Bodrum, Turkey, XIII International Mineral Processing Symposium.

Ayowole, A. S., 2013. *Antimony recovery from complex copper concentrates through hydro and electrometallurgical processes.* PhD thesis,Minerals and metals research laboratory division of sustainable process engineering, Lulea University of Technology.Sweden.

Baral, A., Sarangi, C.K., Tripathy, B.C., Bhattacharya, I.N., Subbaiah. T., 2014. Copper electrodeposition from sulfate solutions—Effects of selenium. *Hydrometallurgy,* 146(2014), pp. 8-14.

Barin, C. S., Correia, A. N. & Machado, S. A., 2000. The effect of concentration on the electrocrystallisation mechanism for copper on platinum ultramicro electrodes. *Journal of the Brazillian Chemical Society,* 11(2), pp. 175-181.

Baub, E. & Schiffner, T., 1971. The inluence of thiourea on the electrolytic deposition of copper in acid copper sulphate electrolytes, Translated paper from:. *Metalloberflache,* 25(4)(1971), pp. 114-117.

Bello, Y., 2014. *Tellurium and Selenium precipitation from copper sulphate solutions: Master of Engineering thesis, Department of process Engineering, Stellenbosch University. South Africa.*

Beukes, N. & Badenhorst, J., 2009. *Copper electrowinning: theoretical and practical design.* Johannesburg, The Southern African Institute of Mining and Metallurgy, Hydrmetallurgy conference 2009.

Bircumshaw, L., 2008. *Base Metal Refinery process overview.* Lonmin Internal Communication, 16 April 2008.

Biswas, A. & Davenport, W., 1976. *Extractive metallurgy of copper.* 1st ed. Quebec: Pergamon Press.

Bockris, J. O., Reddy, A. K. & Gamboa-Aldeco, M., 1998. *Modern elecrochemistry 2A.* 2nd ed. New York: Kluwer Academic/Plenum Publishers.

Bockris, O. J. & Razumney, G., 1967. *Fundamental aspects electrocrystallisation.* New York: Plenum press.

Bolzan, A., Wakenge, I., Salvarezza, R. & Arvia, A., 1999. Electrochemical response of thiourea and formamidine disulphide on polycrystalline platinum in aqueous 0.5 M sulphuric acid. *Electroanalytical Chemistry,* 475(1999), pp. 181-189.

Bonou, L., Eyraud, M., Denoyel, R. & Massiani, Y., 2002. Influence of additives on Cu electrodeposition mechanisms in acid solutions:direct current study supported by non-electrochemical measurements. *Electrochimica Acta,* 47(2002), pp. 4139-4148.

Brookins, D., 2012. *Eh-pH diagrams for geochemistry.* Springer Science and Business Media.

Carbonnelle, P. & Lamberts, L., 1992. A voltammetric study of the electrodeposition of the Cu + Se system. *Electroanalytical chemistry,* 340(1992), pp. 53-71.

Carbonnelle, P. & Lamberts, L., 1992. Electrochemical study of the copper-selenium system using carbon paste electrode. *Electrochimica Acta,* 37(8), pp. 1321-1325.

Charles, P. H. & Hannaert, 1970. *Fluid-bed cementation of selenium contained in a copper electrolyte. Copper Metallurgy Proceedings, AIME.* Denver.

Cheng, C., Hughes, C., Barnard, K. & Larcombe, K., 2000. Manganese in copper solvent extraction and electrowinning. *Hydrometallurgy,* 58(2000), pp. 135-150.

Christian, G. D., Buffle, J. & Haerdi, W., 1979. Study of selenium(IV) at a dropping mecury electrode by cyclic voltammetry with triangle polarisation. *Electroanalytical chemistry,* 109(1980), pp. 187-194.

Cofre, P. & Butos, A., 1994. Voltammetric behaviour of the Cu(II)-thiourea system in sulphuric acid medium at platinum and glassy carbon electrodes. *Journal of Applied Electrochemistry,* 24(1994), pp. 564-568.

Cui, W., 2014. *Effect and interaction of commercial additives and chloride ions in copper electrowinning. Masters dissertation. Missouri University of technology.* Columbia.

Davenport, W., King, M., Schlesinger, M. & Biswas, A., 2002. *Extractive metallurgy of copper.* 4th ed. Pergamon press.

Deni, R. M., 1994. *The effect of addition agents on cathodic overpotential and cathode quality in copper electrorefining. Masters thesis,* Laurentian University: Canada.

Donald.R.Weir, Kerfoot, D & Scheie, H. C., 1982. *Removal of Selenium (IV) and (VI) from acidic copper sulphate solutions.* United States Patent, Patent No. 4330508.

Fabian, C. P., 2005. *Copper electrodeposition in the presence of guar or activated polyacrylamide. PhD thesis, Chemical Engineering Department, James Cook University,* Australia.

Fabricius, G., Kontturi, K. & Sundholm, G., 1994. Influence of thiourea on the nucleation of copper from acid sulphate solutions. *Electrochimica Acta,* 39(1994), pp. 2353-2357.

Farndon, E. E., Walsh.F.C & S.A, C., 1995. Effect of thiourea,Benzotriazole and 4,5-Dithioctane-1,8-Disulphonic acid on the kinetics of copper deposition from dilute acid sulphate solutions. *Journal of Applied Electrochemistry,* 22(1995), pp. 574-583.

Gale, R. J., 1972. *Amino acids as additives in copper electrodeposition. PhD. thesis, Faculty of Graduate studies and Research, McGill University, Montreal,* Canada.

Goffman, M. & Jordan, T., 1985. *Method of thiourea addition to electrolyte solutions useful for copper refining.* Texas, United States of America.

Gomez, H., Lizama, H., Suarez, C. & Valenzuela, A., 2009. Effect of thiourea concentration on the electrochemica behaviour of gold and copper electrodes in the presence and absence of Cu(II) ions. *Chilean Chemical Society,* 54(4), pp. 439-444.

Grujicic, D. & Pesic, B., 2002. Electrodeposition of copper:the nucleation mechanisms. *Electrochimica Acta,* 47(2002), pp. 2901-2912.

Gupta, P. C., 1963. Analytical chemistry of the thiocarbamides.I. Quantitative determination of thiourea. *Zeitschrift Analyticsche Chemie,* 196(1963), pp. 412-429.

Habashi, F., 1998. *Principles of extractive metallurgy volume 4 amalgam and electrometallurgy.* Quebec: Metallurgie Extractive Quebec.

Hasegawa, M., 2007. *Fundamental analysis of electrochemical copper deposition for fabrication of submicrometer interconnects. PhD thesis,* Japan: Department of Applied Cemistry, Waseda University.

Jeffers, T. & Groves, R., 1985. *Minimising lead contamination in copper produced by solvent extraction-electrowinning.*

Jin, S., Ghali, E. & St-Amant, G., 2002. *Effects of formamidine disulphide on the cathode polarisation behaviour of copper cathode in acid sulphate electrolyte at 65oC.* China, Yunan Science Technology Press.

Kang, M. S., Kim, S.-K., Keecho, K. & Jae Jeong, K., 2008. The influence of thiourea on copper electrodeposition: Adsorbate identification and effect on electrochemical nucleation. *ScienceDirect,* 516(2008), pp. 3761-3766.

Kao, Y. L., Tu, G. C., Huang, C. A. & Chang, J. H., 2004. The annealing behaviour of copper deposit electroplated in sulphuric acid bath with varying concentrations of thiourea. *Materials Science and Engineering A,* 382(2004), pp. 104-111.

Kirchnerova, J. & Purdy, W. C., 1981. The mechanism of the electrochemical oxidation of thiourea. *Analytica Chimica Acta,* 123(1981), pp. 83-95.

Kowalik, R., 2014. Microgravimetric studies of selenium electrodeposition onto different substrates. *Archives of Metallurgy and Materials,* 59(3), pp. 871-877.

Krzewska, S., Podsiadly, H. & J, P., 1980. Studies on the reaction of copper(II) with thiourea. *Journal of Inorganic and Nuclear Chemistry,* 42(1980), pp. 89-94.

Kumar, S. K., Biswas, K. & Balasubramanian, R., 2011. Mechanism of film growth of pulsed electrodeposition of nanocrystalline copper in presence of thiourea. *Journal of Nanoparticle Reseach,* 13(2011), pp. 6005-6012.

Kuzeci, E. & Kammel, R., 1989. *Application of voltammetry in hydrometallurgical dissolution and deposition processes.* Process Control and Automation in Hydrometallurgy.

Lai, Y., Lui, F., Li, J., Zhang, Z., Liu, Y., 2009. Nucleation and growth of selenium electrodeposition onto tin oxide electrode. *Electroanalytical Chemistry,* 639(2010), pp. 187-192.

Lottering, C., 2012. *Precipitation of rhodium from a copper sulphate leach solution in the selenium/tellurium removal section of a base metal refinary,* South Africa: Final Year Thesis, Stellenbosch University.

Loufty, R., 1971. *Electrosorption effects of organic additives on the cathodic overpotential of copper electrodeposition. PhD dissertation. University of Western Ontario.* Canada.

Lynch, D. C., Akagi, S. & Davenport, W., 1991. Thermochemical nature of minor elements in copper smelting mattes. *Metallurgical Transactions,* pp. 677-688.

Manu, R. & Jayakrishnan, S., 2009. Influence of additives and the effect of aging in modifying surface topography of electrodeposited copper. *Electrochemical Society,* 156(2009), pp. 215-221.

Martens, D. A., 2003. *Selenium. United States Department of Agriculture,* Arizona.

Mattsson, E. & Bockris, J., 1959. Galvanostatic studies of the kinetics of deposition and dissolution in the copper + copper sulphate system. *Transaction Farady Society,* 55(1959), pp. 1586-1601.

Merchant, H. D., 1995. *Defect structure, Morphology and Properties of Deposits,* Ohio.

Mirkova, L., Petkova, N., Popova, I. & Rashkov, S., 1994. The effect of some surface active additives upon the quality of cathodic copper deposits during the electro-refining process. *Hydrometallurgy,* 36(1994), pp. 201-213.

Moskalyk, R., Alfantazi, A., Tombalakian, A. & Valic, D., 1999. Anode effects in electrowinning. *Minerals Engineering,* 12(1999), pp. 65-73.

Mouanga, M. & Bercot, P., 2011. Electrochemical analysis of thiourea on platinum in non-aqueous electrolyte. *International Journal of Electrochemical Science,* 6(2011), pp. 1007-1013.

Mulwanda, J., 2014. *Recovery of dissolved platinum group metals from a pregnant copper sulphate leach solution by precipitation.* Master of Engineering thesis, Stellenbosch University. South Africa.

Muresan, L., Varvara, S., Maurin, G. & Dorneanu, S., 1999. The effect of some organic additives upon copper electrowinning from sulphate electrolytes. *Hydrometallurgy,* 54(2000), pp. 161-169.

Ntengwe, F. W., Mazana, N. & Samadi, F., 2010. The effect of impurities and other factors on the current density in electro-chemical reactors. *International journal of ChemTech Research,* 2(2010), pp. 1289-1300.

Oniciu, L. & Muresan, L., 1991. Some fundamental aspects of levelling and brightening in metal electrodeposition. *Journal of Applied Electrochemistry,* 21(1991), pp. 565-574.

Pablo, F., Albano, E. V. & Salvarezza, R., 2002. Interface dynamics for copper electrodeposition: The role of organic additives in the growth mode. *Physical Review E,* 042601 66(2002), pp. 1 -4.

Pasa, A. A. & Munford, M. L., 2006. Electrodeposition. *Encyclopedia of Chemical Processing,* 10(2006), pp. 821-832.

Paunovic, M. & Schlesinger, M., 2006. *Fundamentals of electrochemical deposition.* 2nd ed. Hoboken, New Jersey: John Wiley and Sons Inc..

Paunovic, M., Schlesinger, M. & Snyder, D. D., 2010. *Mordern electroplating.* 5th ed. John Wiley & sons, Inc.

Prengaman, D. R., Ellis, T. W. & Mirza, H. A., 2010. *New lead anodes for copper electrowinning.* International Workshop on Process Hydrometallurgy.

Quinet, M., Lellamand, F., Ricq, L., Hihn, J.Y., Arnould, C., Mekhalif, Z., 2009. Influence of organic additives on the initial stages of copper electrodeposition on polycystalline Platinum. *Electrochimica Acta,* 54(2009), pp. 1529-1536.

Ratajczak, H., Pajdowski, L. & Ostern, M., 1975. Polarographic studies on aqueos formamidine disulfide solutions I and II. *Electrochimica Acta,* 20(1975), pp. 427-434.

Safizadeh, F., Lafront, A.-M., Ghali, E. & Houlachi, G., 2011. An investigation of the influence of selenium on copper deposition during electrorefining using electrochemical noise analysis. *Hydrometallurgy,* 111(2012), pp. 29-34.

Saji, V. S. & Lee, C.-W., 2013. Selenium electrochemistry. *RSC Advances,* 3(2013), pp. 10058-10077.

Santos, M. C. & Machado, S. A., 2004. Microgravimetric, rotating ring-disc and voltammetric studies of the underpotential deposition of selenium on polycrystalline platinum electrodes. *Journal of Eletcroanalytical Chemistry,* 567(2004), pp. 203-210.

Schilardi, P., Mendez, S., Salvarezza, R. & Arvia, A., 1998. Evolution of the growth front for copper electrodeposition followed by real time imaging. *Langmuir,* 14(1998), pp. 4308-4314.

Schlesinger, M., King, M., Sole, K. & Davenport, W., 2011. *Extractive metallurgy of copper.* 5th ed. Asterdam: Elsevier.

Shevtsova, O., Bek, Y. R., Zelinskii, A. & Vais, A., 2006. Anodic behaviour of gold in acid thiourea solutions: A voltammetry and quartz microgravimetry study. *Elektrokhimiya,* 42(3), pp. 279-285.

Stankovic, Z. D. & Vukovic, M., 1996. The influence of thiourea on kinetic parameters on the cathodic and anodic reaction at different metals in H2SO4 solution. *Electrochimica Acta,* 41(16), pp. 2529-2535.

Tadesse, B., Horne, M. & Jonas, A.-M., 2013. The effect of thiourea,L(-)ctsteine and glycine additives on the mechanisms and kinetics of copper electrodeposition. *Journal of Applied Electrochemistry,* 43(2013), pp. 1185-1195.

Tantavichet, N. & Pritzker, M. D., 2004. Effect of plating mode, thiourea and chloride on the morphology of copper deposits produced in acidic sulphate solutions. *Electrochimica Acta,* 50(2004), pp. 1849-1861.

Tantavichet, N., Somsak, D. & Orawan, C., 2009. Influence of the interaction between chloride and thiourea on copper electrodeposition. *Electrochimica Acta,* 55(2009), pp. 240-249.

Varvara, S., Muresan, L., Nicoara, A., Maurin, G., Popescu, I.C., 2000. Kinetic and morphological investigation of copper electrodeposition from sulfate electrolytes in the presence of an additive based on ethoxyacetic alcohol and triethyl-benzyl-ammonium chloride. *Materials Chemistry and Physics,* 72(2001), pp. 332-336.

Weir, D. R., Kerfoot, D. & Hofirek, Z., 1982. *Removal of Selenium from acidic Copper/Nickel Solutions, Sherrit Gordon Mines.* United States Patent, Patent No. 4374808.

Winand, R., 1992. Electrocrystallisation-theory and applications. *Hydrometallurgy,* 29(1992), pp. 567-598.

Woollacott, L. & Eric, R. H., 1994. *Mineral and metal extraction:An overview.* Johannesburg, The South African Institute of Mining and Metallurgy.

Yu, Run-lun., Liu, Qing-ming., Qiu, Ghuan-zhou., Fang, Zheng., Yang, Peng., Tan, Jian-Xi., 2008. Inhibition behabiour of some mixed additives upon copper electrowinning. *Trans Nonferrous Met Soc China,* 18(2008), pp. 1280-1284.

Zuman, P. & Somer, G., 1999. Polarographic and voltammetry behaviour of selenious acid and its use in analysis. *Talanta,* 51(2000), pp. 645-665.

# APPENDIX A: SYNTHETIC SOLUTION PREPARATION

The procedure that was followed in the preparation of the synthetic solution was as outlined below:

- 200 ml of deionised water was initially added to a 500 ml beaker.
- A known volume of sulphuric acid was then added. The volume of acid required to achieve a desired molarity was calculated using Equation A-1.
- Calculated amounts of the salts, copper (II) sulphate, nickel sulphate and ferric sulphate were then added into the beaker.
- Required amounts of thiourea or selenium were then added based on the experimental plan.
- Deionised water was then used to make up the solution up to a final volume of 300 ml.
- During preparation, the solution was continuously stirred at 600 rpm using a Dragon Lab magnetic stirrer (model MS-H280-Pro) to ensure complete dissolution of the salts.

$$Vol_{acid} = \frac{M_r M(\%\ acid\ purity) Vol_{final}}{\rho_{acid}} \qquad \text{A-1}$$

# APPENDIX B: CYCLIC VOTAMMETRY REPEATABILITY

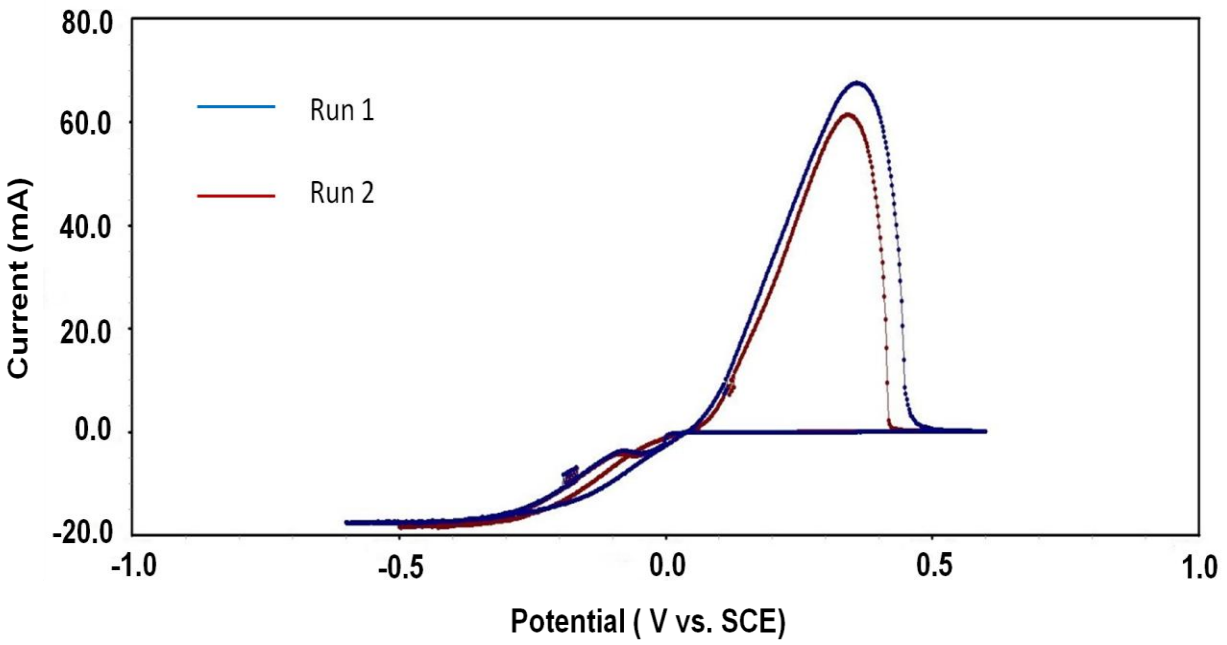


*Figure B.1. Cyclic voltammograms obtained for 0.01 M $Cu^{2+}$ and 1 M sulphuric acid at 25˚C.*

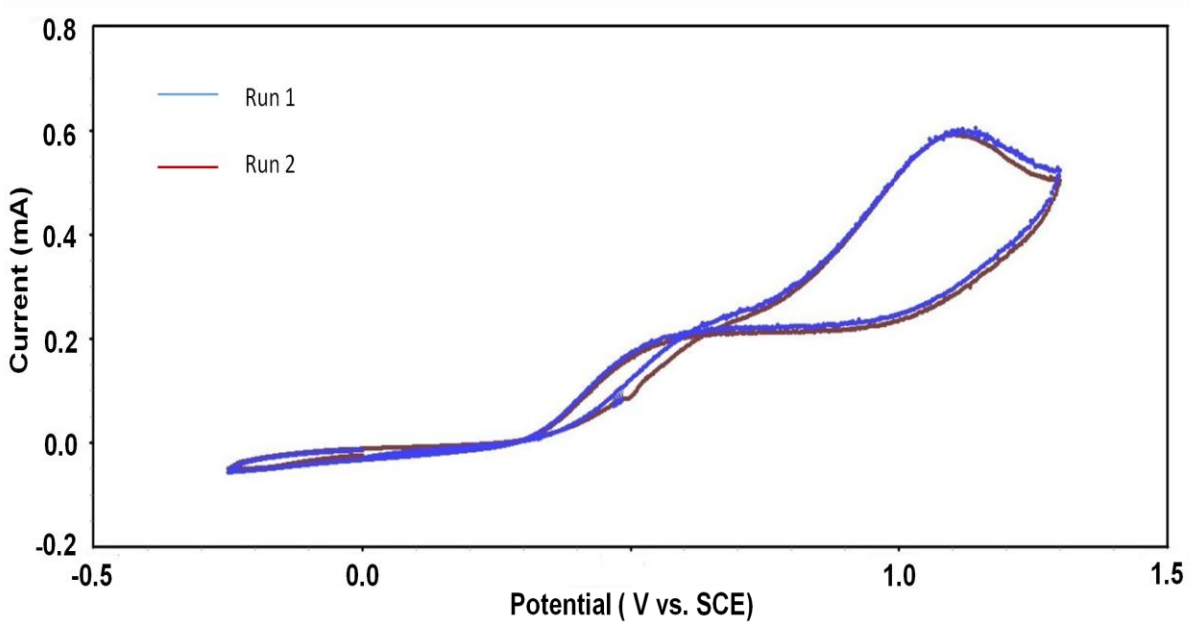


*Figure B.2. Cyclic voltammograms obtained for 0.05 mM and 1 M sulphuric acid at 25˚C.*

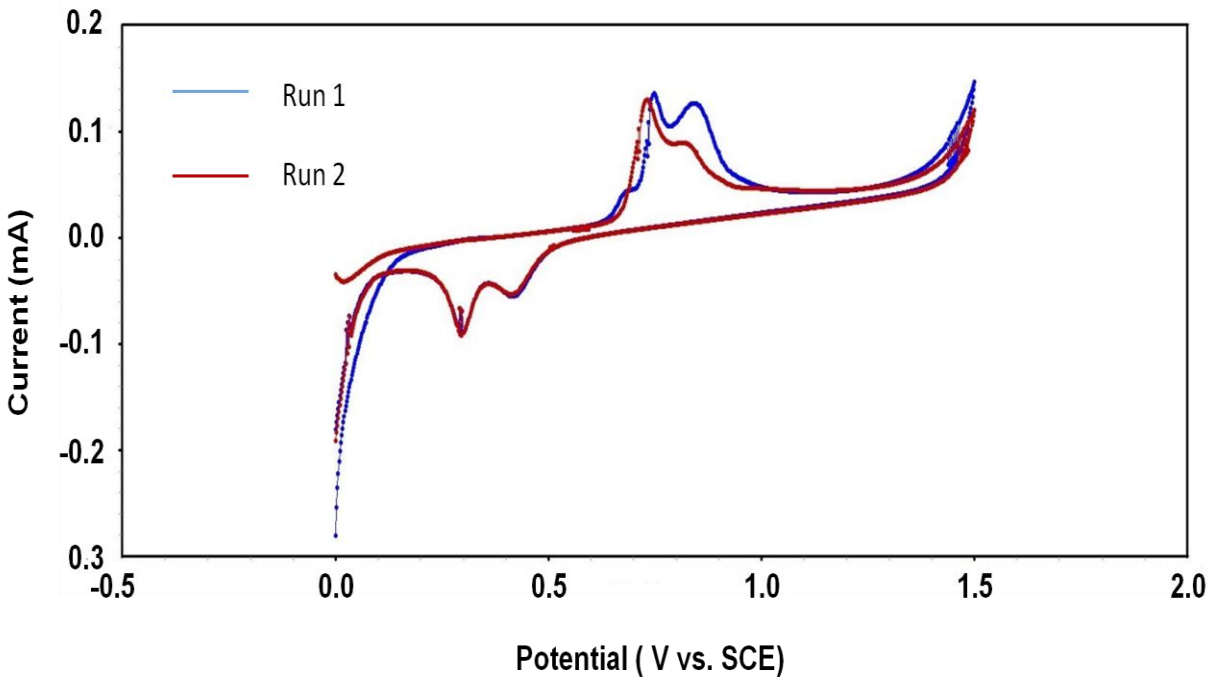


*Figure B.3 Cyclic voltammograms obtained for 600 ppm Se and 1 M sulphuric acid at 25˚C*

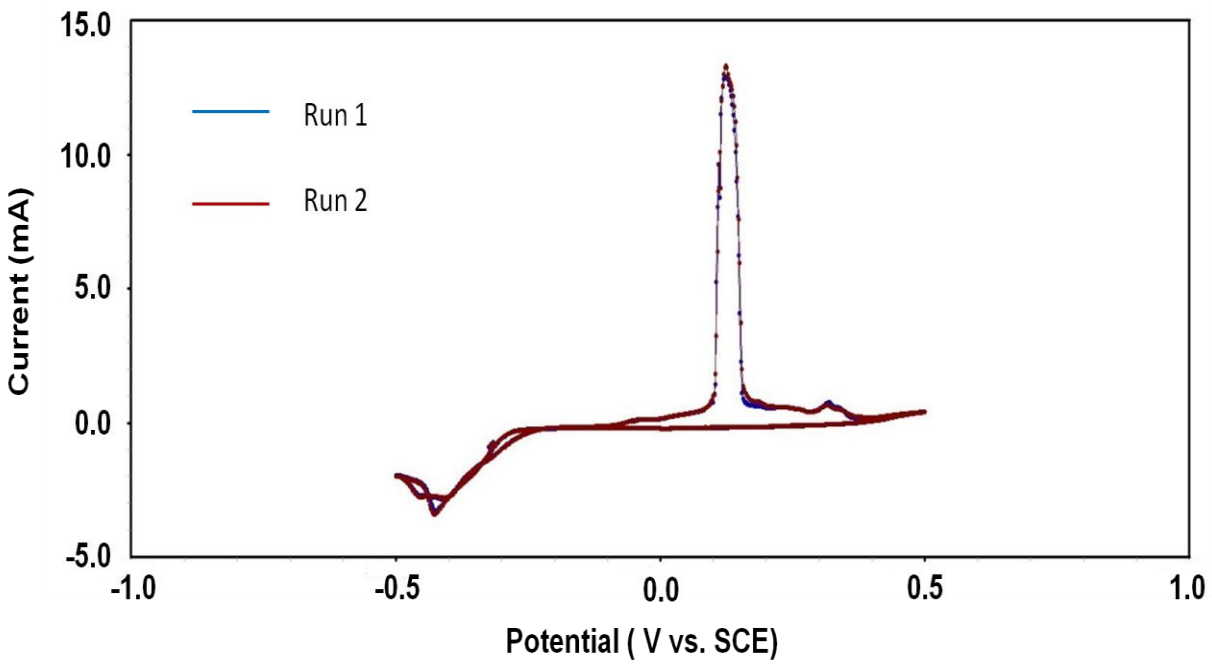


*Figure B.4. Cyclic voltammograms obtained for 0.01 M $Cu^{2+}$, 320 % excess thiourea and 1 M sulphuric acid at 25˚C.*

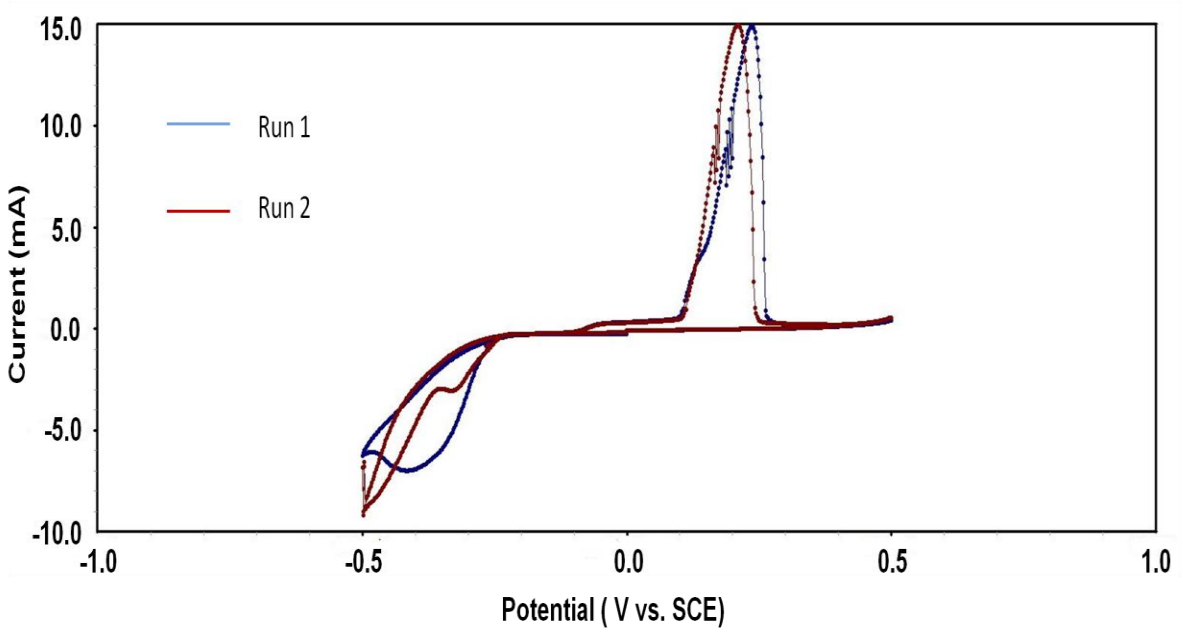


*Figure B.5. Cyclic voltammograms obtained for 0.1 M Cu2+, 200 % excess thiourea and 1 M sulphuric acid at 25˚C.*

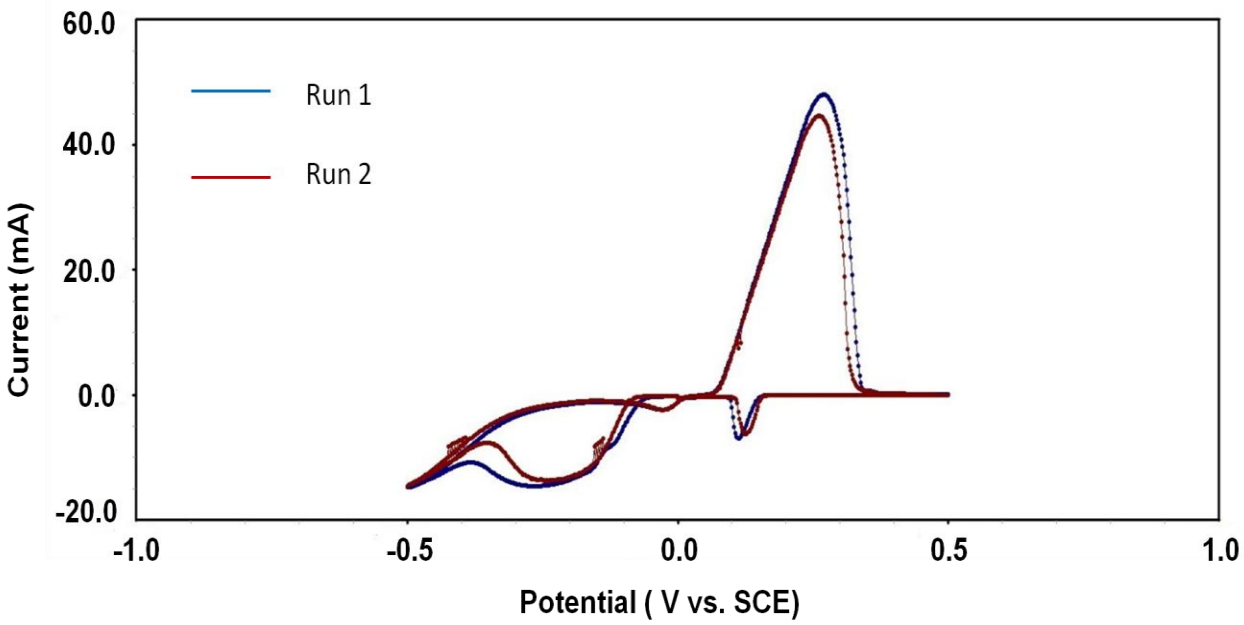


*Figure B.6. Cyclic voltammograms obtained for 0.01 M $Cu^{2+}$ , 20 mg/ℓ selenium and 1M sulphuric acid at 25˚C.*

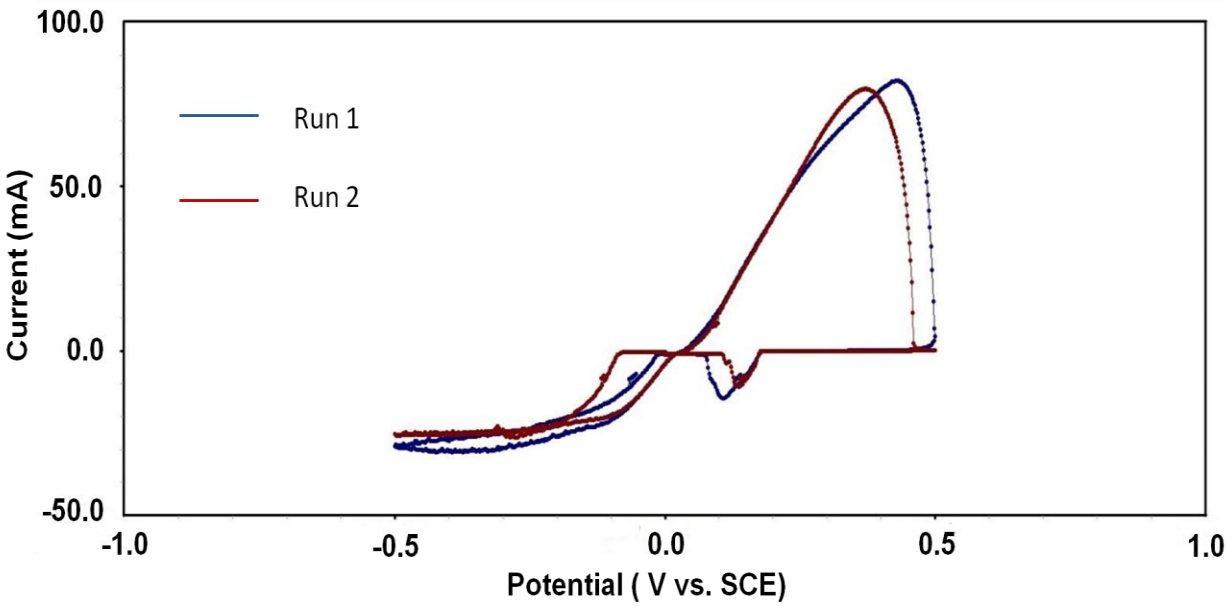


*Figure B.7. Cyclic voltammograms obtained for 0.01 M $Cu^{2+}$, 57 mg/ℓ selenium and 1 M sulphuric acid at 25 ˚C.*

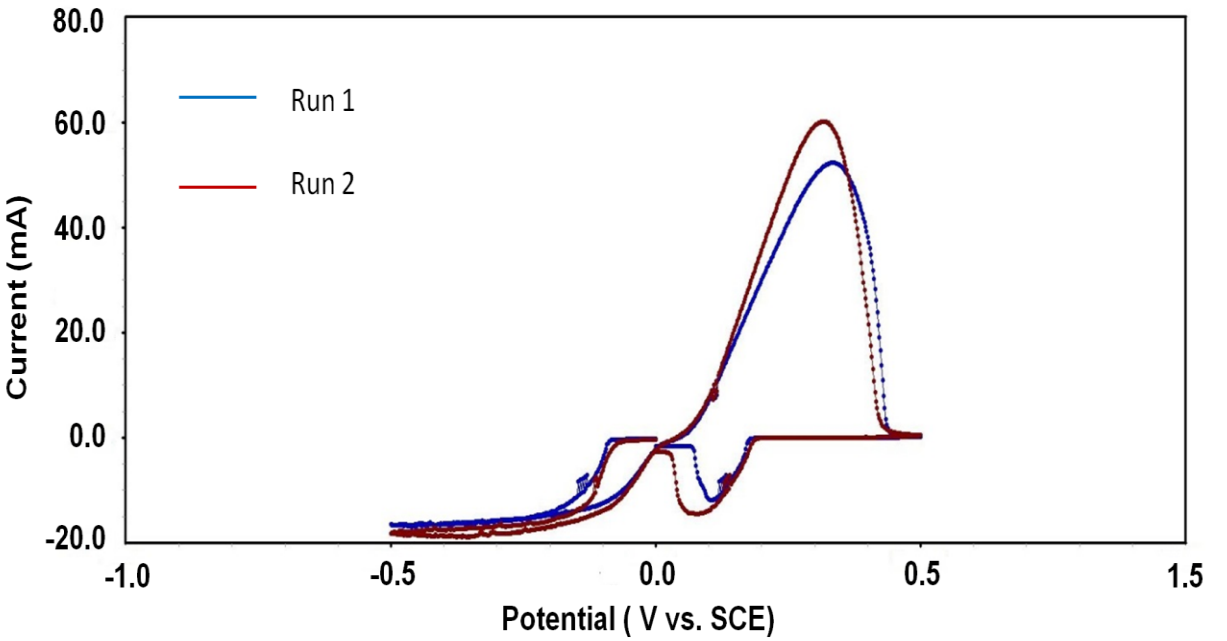


*Figure B.8. Cyclic voltammograms obtained for 0.01 M Cu2+, 150 mg/ℓ selenium and 1 M sulphuric acid at 25˚C.*

# APPENDIX C: EXPERIMENTAL DATA

*Table C.1. ICP results for test performed in the presence of thiourea*

| Test conditions | Sample ID | Cu (g/ℓ) | Fe (g/ℓ) | Ni (g/ℓ) |
|---|---|---|---|---|
| 320 % Excess | Initial | 63.49 | 1.28 | 31.85 |
| | Final | 62.57 | 1.29 | 31.72 |
| | Initial | 63.88 | 1.28 | 31.91 |
| | Final | 63.86 | 1.28 | 31.76 |
| | Final | 63.02 | 1.27 | 31.39 |
| 200 % Excess | Initial | 64.43 | 1.26 | 32.16 |
| | Final | 63.11 | 1.26 | 31.90 |
| | Final | 63.42 | 1.27 | 33.75 |
| | Final | 63.25 | 1.27 | 33.57 |
| | Final | 62.28 | 1.26 | 33.38 |
| 100 % Excess | Initial | 62.75 | 1.19 | 33.15 |
| | Final | 61.19 | 1.22 | 33.21 |
| | Final | 60.88 | 1.24 | 33.08 |
| | Initial | 63.85 | 1.28 | 33.32 |
| | Final | 62.35 | 1.26 | 33.46 |

*Table C.2. ICP results for tests performed in the presence of selenium*

| Test conditions | Sample ID | Cu (g/ℓ) | Fe (g/ℓ) | Ni (g/ℓ) | Se (mg/ℓ) |
|---|---|---|---|---|---|
| Se 20ppm | Initial | 63.30 | 1.19 | 33.19 | 28.08 |
| | Final | 61.32 | 1.23 | 33.08 | 26.66 |
| | Initial | 61.46 | 1.23 | 33.11 | 31.30 |
| | Final | 62.40 | 1.09 | 33.85 | 27.10 |
| | Final | 60.22 | 1.10 | 33.54 | 24.42 |
| | Final | 61.95 | 1.12 | 34.65 | 23.12 |
| Se 57ppm | Initial | 63.43 | 1.25 | 33.93 | 57.16 |
| | Final | 61.24 | 1.23 | 33.37 | 52.68 |
| | Final | 61.34 | 1.24 | 33.34 | 51.16 |
| | Final | 60.40 | 1.25 | 32.99 | 50.89 |
| Se 150ppm | Initial | 61.03 | 1.19 | 31.83 | 155.86 |
| | Final | 58.97 | 1.20 | 31.59 | 132.78 |
| | Final | 58.24 | 1.22 | 31.58 | 130.04 |

*Table C.3. ICP results for tests performed using standard electrolyte*

| Test conditions | Sample ID | Cu (g/ℓ) | Fe (g/ℓ) | Ni (g/ℓ) |
|---|---|---|---|---|
| Cu | Initial | 64.18 | 0.87 | 34.35 |
| | Final | 63.29 | 1.07 | 34.31 |
| | Final | 62.24 | 1.08 | 34.09 |
| | Final | 63.08 | 1.07 | 33.46 |
| | Final | 63.45 | 1.13 | 34.85 |

*Table C.4. Actual and assay electrodeposit weights obtained in the electrowinning tests*

| Conditions | Test number | Wt of holder | Wt of holder + Sample | Deposited metal actual (g) | Deposited metal by assay (g) |
|---|---|---|---|---|---|
| Cu +100% Excess TU | 1 | 2.89 | 3.02 | 0.126 | 0.233 |
| | 2 | 2.97 | 3.10 | 0.128 | 0.280 |
| | 3 | 2.97 | 3.13 | 0.158 | 0.225 |
| Cu + 200% Excess TU | 1 | 2.95 | 3.10 | 0.143 | 0.198 |
| | 2 | 2.94 | 3.07 | 0.128 | 0.152 |
| | 3 | 2.95 | 3.08 | 0.127 | 0.171 |
| Cu +320% Excess TU | 1 | 2.90 | 2.97 | 0.068 | 0.138 |
| | 2 | 2.91 | 2.98 | 0.073 | 0.129 |
| | 3 | 2.95 | 2.97 | 0.023 | 0.003 |
| Cu + 20 ppm Se | 1 | 2.90 | 3.09 | 0.187 | 0.248 |
| | 2 | 2.93 | 3.11 | 0.185 | 0.230 |
| | 3 | 2.98 | 3.17 | 0.190 | 0.135 |
| Cu + 57 ppm Se | 1 | 2.95 | 3.13 | 0.180 | 0.273 |
| | 2 | 2.94 | 3.13 | 0.186 | 0.314 |
| | 3 | 2.90 | 3.09 | 0.193 | 0.356 |
| Cu + 150 ppm Se | 1 | 2.94 | 3.20 | 0.254 | 0.258 |
| | 2 | 2.92 | 3.22 | 0.300 | 0.348 |
| Cu | 1 | 2.95 | 3.14 | 0.193 | 0.112 |
| | 2 | 2.95 | 3.13 | 0.179 | 0.243 |
| | 3 | 2.95 | 3.14 | 0.190 | 0.138 |
| | 4 | 2.95 | 3.09 | 0.141 | 0.284 |
| Cu + 10 ppm Tu | 1 | 2.95 | 3.13 | 0.175 | 0.146 |
| | 2 | 2.95 | 3.12 | 0.169 | 0.083 |

*Table C.5. Sample of cathodic current data during deposition in the presence of thiourea*

| Time (s) | No Tu I (mA) | 10 ppm Tu I (mA) | 100% Excess Tu I (mA) | 200% Excess Tu I (mA) | 320% Excess Tu I (mA) |
|---|---|---|---|---|---|
| 1 | 32.01 | 29.01 | 18.19 | 9.46 | 9.70 |
| 2 | 32.76 | 28.27 | 16.17 | 5.89 | 12.24 |
| 3 | 32.64 | 28.08 | 17.08 | 6.03 | 12.39 |
| 4 | 32.60 | 28.18 | 18.28 | 6.55 | 12.57 |
| 5 | 32.63 | 28.25 | 19.07 | 7.45 | 12.84 |
| 6 | 32.65 | 28.27 | 19.50 | 8.99 | 12.87 |
| 7 | 32.64 | 28.24 | 19.71 | 10.71 | 12.86 |
| 8 | 32.64 | 28.19 | 19.84 | 12.22 | 12.95 |
| 9 | 32.69 | 28.18 | 19.91 | 13.39 | 12.96 |
| 10 | 32.68 | 28.17 | 19.97 | 14.32 | 12.96 |
| 20 | 32.86 | 28.32 | 20.19 | 14.00 | 12.96 |
| 30 | 33.08 | 28.46 | 20.30 | 17.23 | 12.98 |
| 40 | 33.27 | 28.53 | 20.38 | 18.38 | 13.00 |
| 50 | 33.64 | 28.63 | 20.44 | 18.60 | 13.20 |
| 60 | 33.86 | 28.73 | 20.51 | 18.67 | 13.15 |
| 70 | 34.00 | 28.85 | 20.56 | 18.72 | 13.21 |
| 80 | 34.28 | 28.90 | 20.60 | 18.74 | 13.25 |
| 90 | 34.32 | 28.99 | 20.64 | 18.80 | 13.27 |
| 100 | 34.45 | 29.05 | 20.68 | 18.86 | 13.28 |
| 200 | 35.49 | 29.82 | 21.18 | 19.75 | 13.62 |
| 300 | 36.34 | 30.43 | 21.56 | 20.75 | 13.88 |
| 400 | 37.02 | 30.82 | 21.88 | 21.25 | 14.41 |
| 500 | 37.72 | 31.16 | 22.14 | 21.62 | 14.33 |
| 600 | 38.30 | 31.43 | 22.42 | 21.99 | 14.49 |
| 700 | 38.96 | 31.71 | 22.65 | 22.29 | 14.73 |
| 800 | 39.56 | 32.04 | 22.87 | 22.64 | 14.85 |
| 900 | 40.18 | 32.28 | 23.14 | 22.99 | 15.06 |
| 1000 | 40.76 | 32.54 | 23.35 | 23.27 | 15.21 |
| 2000 | 45.91 | 35.00 | 25.70 | 26.30 | 16.77 |
| 3000 | 50.14 | 37.31 | 28.01 | 28.93 | 18.26 |
| 4000 | 53.80 | 39.54 | 30.17 | 31.39 | 20.02 |
| 5000 | 57.14 | 42.69 | 32.25 | 33.53 | 21.83 |
| 6000 | 61.03 | 45.34 | 34.26 | 35.97 | 23.55 |
| 7000 | 64.23 | 47.66 | 36.35 | 38.56 | 25.62 |
| 8000 | 67.27 | 49.81 | 38.63 | 41.18 | 27.71 |
| 9000 | 70.01 | 51.70 | 44.65 | 43.28 | 29.28 |
| 10000 | 72.63 | 54.02 | 46.75 | 46.06 | 31.21 |
| 10800 | 74.61 | 56.26 | 47.45 | 47.39 | 32.44 |

*Table C.6. Sample of cathodic current data during deposition in the presence of selenium*

| Time (s) | No Se I (mA) | 20 ppm Se I (mA) | 57 ppm Se I (mA) | 150 ppm Se I (mA) |
|---|---|---|---|---|
| 1 | 32.01 | 35.88 | 37.42 | 48.89 |
| 2 | 32.76 | 37.93 | 34.64 | 50.55 |
| 3 | 32.64 | 35.24 | 33.83 | 47.06 |
| 4 | 32.60 | 30.59 | 33.72 | 41.29 |
| 5 | 32.63 | 30.03 | 33.70 | 40.87 |
| 6 | 32.65 | 30.23 | 33.73 | 40.88 |
| 7 | 32.64 | 30.38 | 33.75 | 40.96 |
| 8 | 32.64 | 30.44 | 33.77 | 40.97 |
| 9 | 32.69 | 30.44 | 33.83 | 41.03 |
| 10 | 32.68 | 30.37 | 33.84 | 41.05 |
| 20 | 32.86 | 30.30 | 34.17 | 41.27 |
| 30 | 33.08 | 31.10 | 34.33 | 41.54 |
| 40 | 33.27 | 31.29 | 34.49 | 41.73 |
| 50 | 33.64 | 31.55 | 34.79 | 41.93 |
| 60 | 33.86 | 31.83 | 34.95 | 42.08 |
| 70 | 34.00 | 32.08 | 35.09 | 42.25 |
| 80 | 34.28 | 32.22 | 35.25 | 42.48 |
| 90 | 34.32 | 32.41 | 35.40 | 42.64 |
| 100 | 34.45 | 32.66 | 35.49 | 42.79 |
| 200 | 35.49 | 34.21 | 36.51 | 44.14 |
| 300 | 36.34 | 35.21 | 37.27 | 45.31 |
| 400 | 37.02 | 34.04 | 37.96 | 46.29 |
| 500 | 37.72 | 36.71 | 38.53 | 47.23 |
| 600 | 38.30 | 37.29 | 39.12 | 48.09 |
| 700 | 38.96 | 37.84 | 39.58 | 48.94 |
| 800 | 39.56 | 38.40 | 40.08 | 49.79 |
| 900 | 40.18 | 38.92 | 40.52 | 50.58 |
| 1000 | 40.76 | 39.46 | 40.98 | 51.51 |
| 2000 | 45.91 | 44.35 | 44.97 | 60.68 |
| 3000 | 50.14 | 48.45 | 48.66 | 69.00 |
| 4000 | 53.80 | 51.79 | 52.00 | 76.39 |
| 5000 | 57.14 | 54.78 | 54.99 | 83.10 |
| 6000 | 61.03 | 57.52 | 57.73 | 90.06 |
| 7000 | 64.23 | 60.08 | 60.30 | 96.96 |
| 8000 | 67.27 | 62.50 | 62.68 | 102.90 |
| 9000 | 70.01 | 64.66 | 65.00 | 108.80 |
| 10000 | 72.63 | 66.85 | 67.12 | 114.80 |
| 10800 | 74.61 | 68.42 | 68.69 | 118.90 |

## Determination of current efficiency

- The current efficiency was calculated based on the total weight of sample deposited.
- The actual weight of sample deposited was the taken as a ratio of the theoretical weight of sample deposited to get the current efficiency.
- The theoretical weight of deposited was calculated using Equation C.1.

$$M_w = \frac{M_r \times I \times t}{n \times F} \qquad \text{C.1}$$

*Table C.7. Current efficiencies obtained during the electrowinning tests*

| Test conditions | Current (mA) | Theoretical Wt (g) | Actual Wt(g) | % Current Efficiency |
|---|---|---|---|---|
| No Tu | 56.55 | 0.201 | 0.193 | 96.06 |
| 10 ppm Se | 49.43 | 0.176 | 0.169 | 96.01 |
| 100% Tu | 37.80 | 0.134 | 0.126 | 93.88 |
| 200% Tu | 38.54 | 0.137 | 0.127 | 92.87 |
| 320% Tu | 23.40 | 0.083 | 0.073 | 87.46 |
| 20 ppm Se | 54.32 | 0.193 | 0.185 | 95.96 |
| 57 ppm Se | 55.06 | 0.196 | 0.186 | 94.78 |
| 150 ppm Se | 83.14 | 0.296 | 0.252 | 85.35 |

# SEM micrographs-Elemental maps

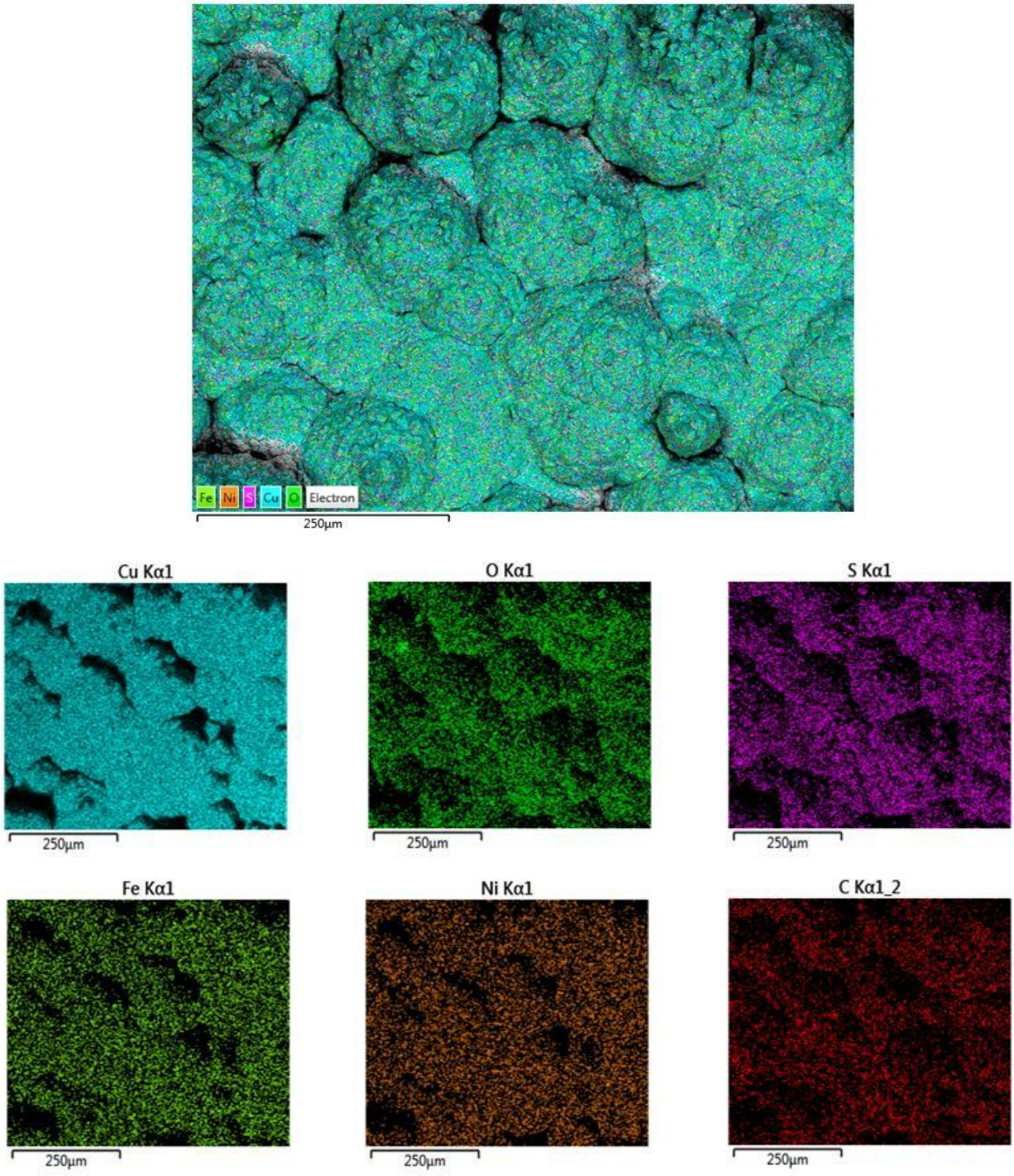


*Figure C.1 SEM image and elemental maps showing distribution of elements in an electrodeposit obtained from a standard electrolyte*

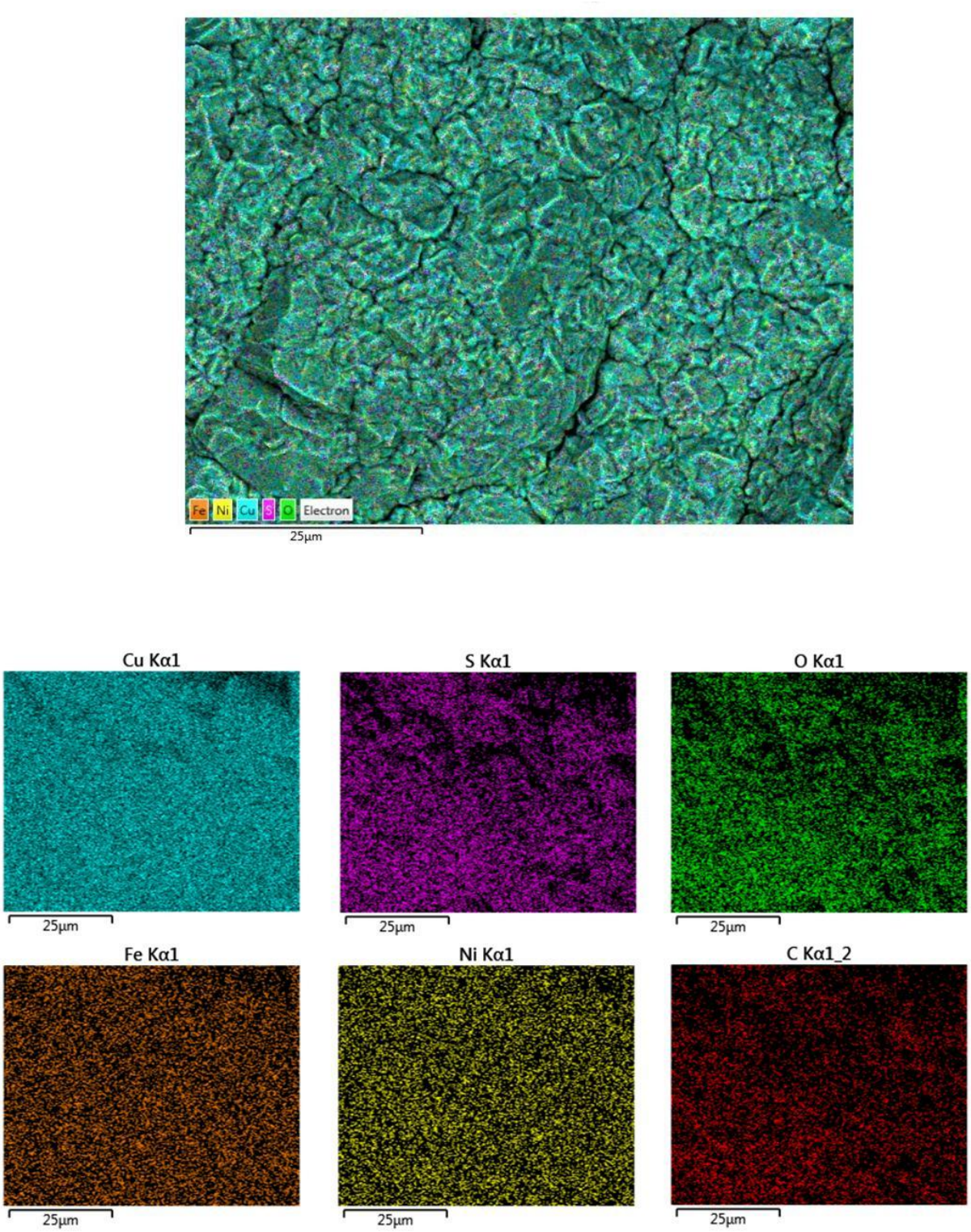


*Figure C.2 SEM image and elemental maps showing grain structure and distribution of elements in an electrodeposit obtained from a standard electrolyte*

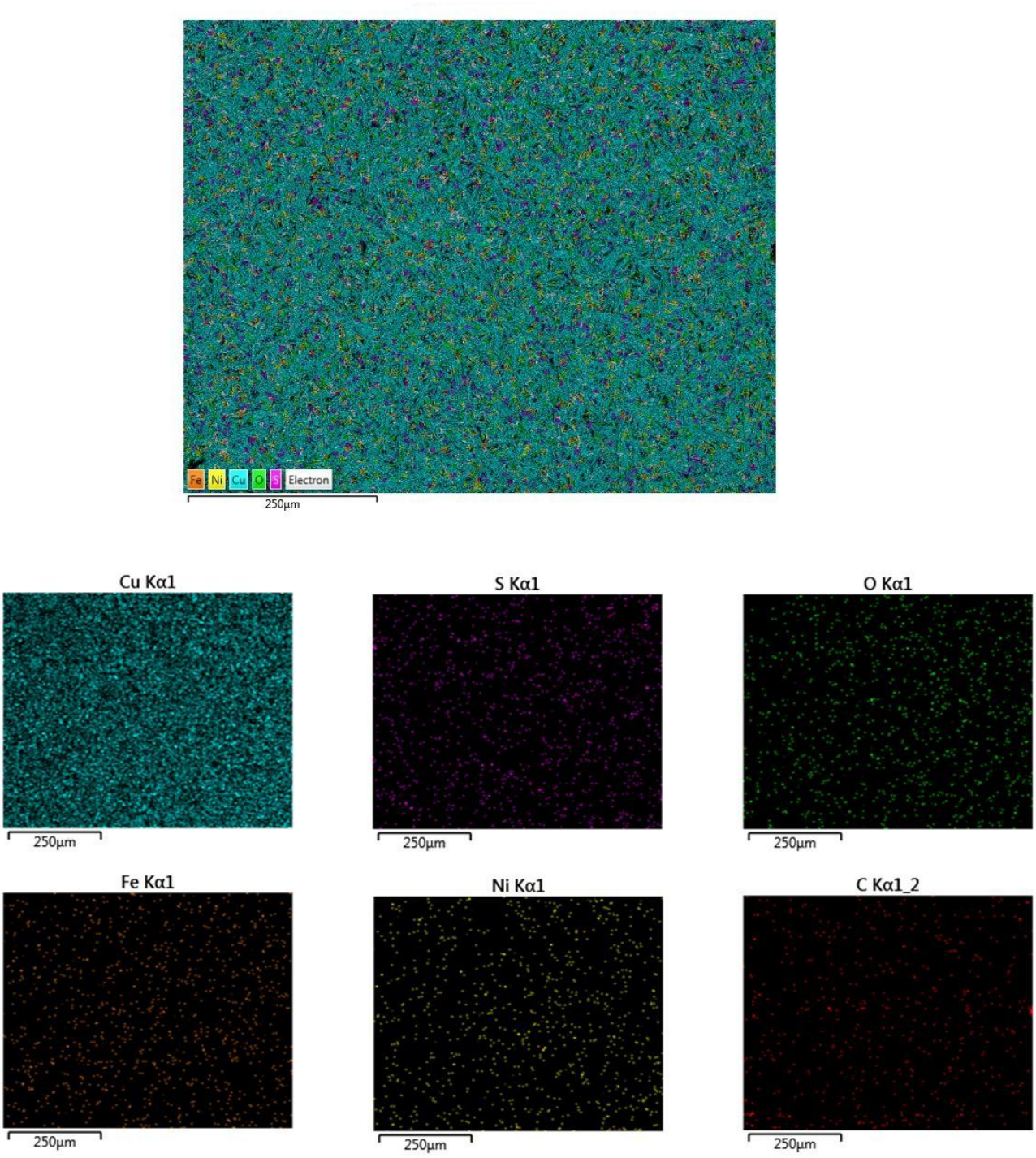


*Figure C.3 SEM image and elemental maps showing the distribution of elements in an electrodeposit obtained in the presence of 10 mg/ℓ thiourea*

.

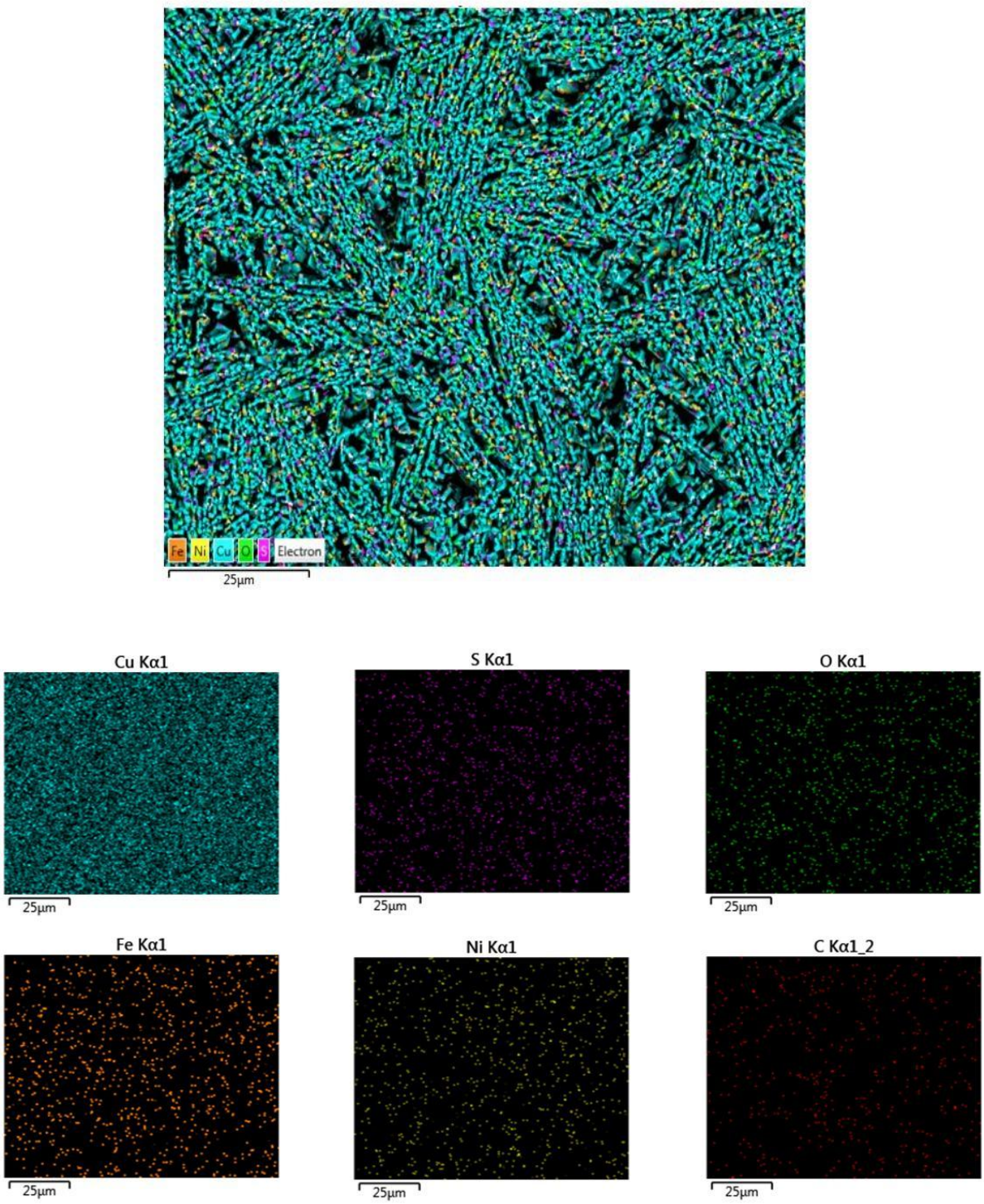


*Figure C.4 SEM image and elemental maps showing grain structure distribution of elements in an electrodeposit obtained in the presence of 10 mg/ℓ thiourea*

.

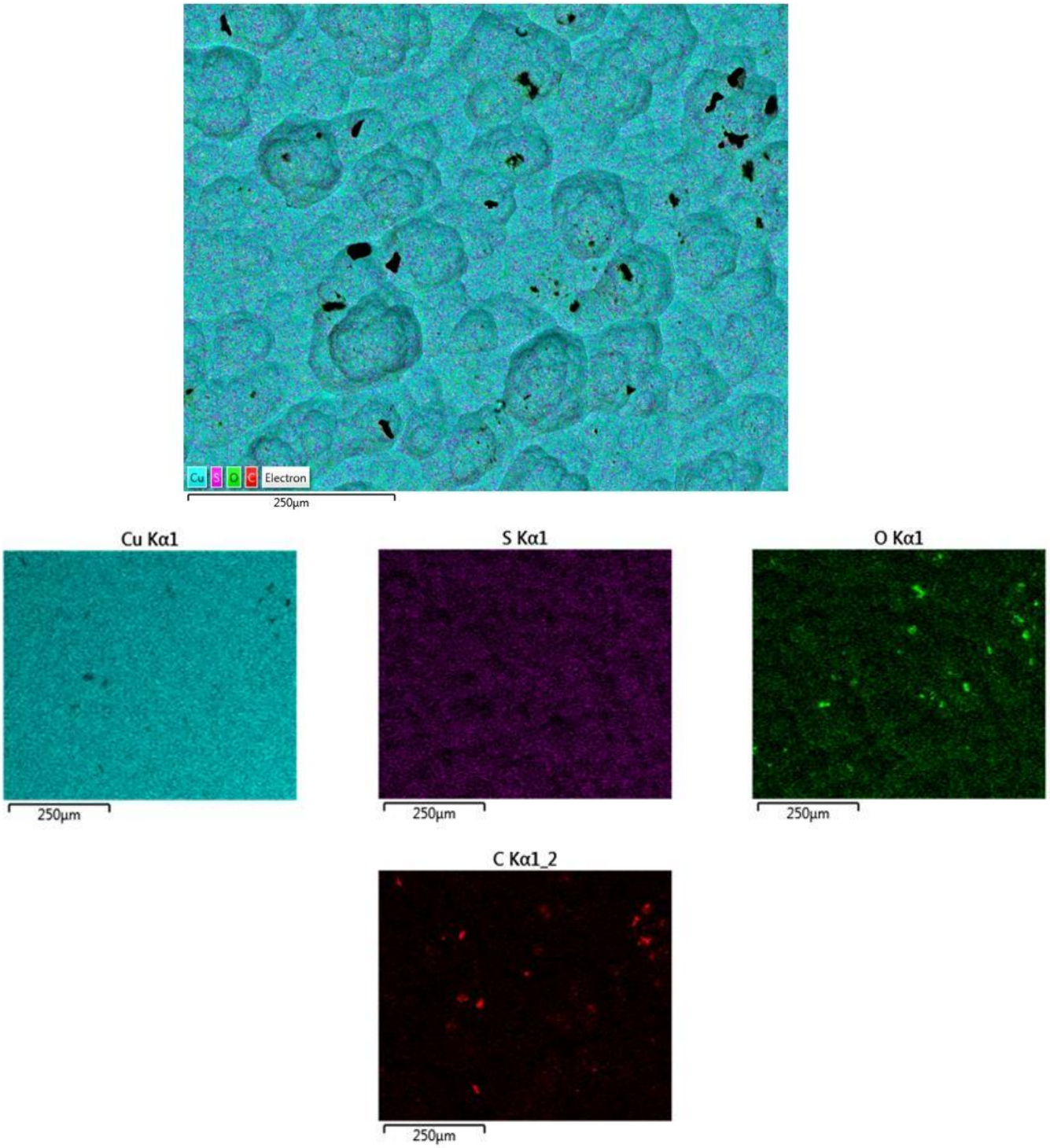


*Figure C.5.SEM image and elemental maps showing the distribution of elements in an electrodeposit obtained in the presence of 100% excess thiourea*